MORPHODYNAMICS OF RIVER DUNES

SUSPENDED SEDIMENT TRANSPORT ALONG MOBILE DUNES AND DUNE DEVELOPMENT TOWARDS UPPER STAGE PLANE BED

Suleyman Naqshband

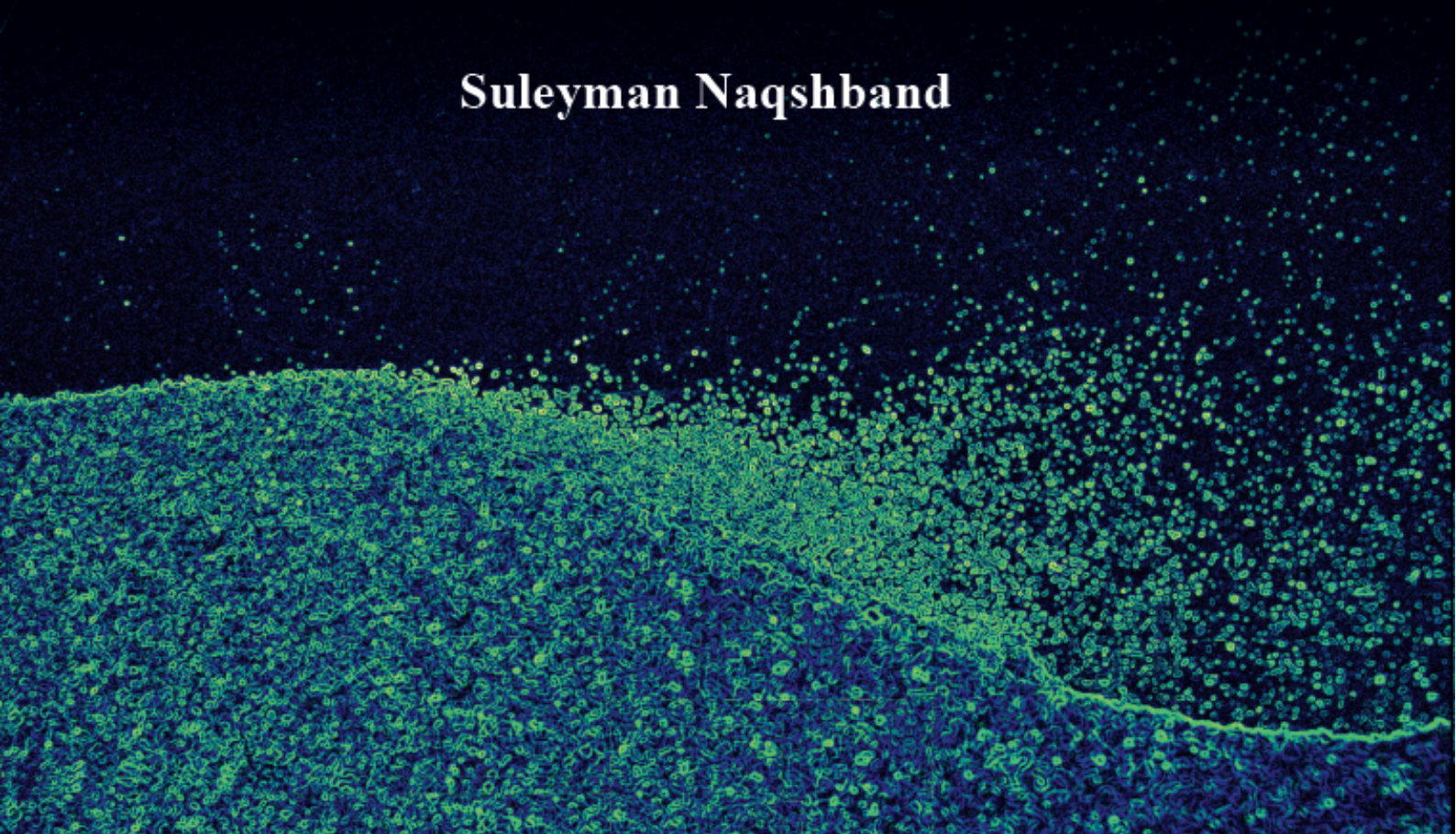

Promotion committee:

prof. dr. ir. G.P.M.R. Dewulf	University of Twente, chairman and secretary
prof. dr. S.J.M.H. Hulscher	University of Twente, promotor
dr. ir. J.S. Ribberink	University of Twente, co-promotor
prof. dr. ir. L.C. van Rijn	University of Utrecht
prof. dr. ir. W.S.J. Uijttewaal	University of Delft
prof. dr. ir. C.H. Venner	University of Twente
dr. ir. C.M. Dohmen-Janssen	University of Twente
dr. ir. D. Hurther	University of Grenoble, LEGI, CNRS
dr. ir. A. Crosato	UNESCO-IHE, Institute for Water Education

This study is part of the project named Bed-FormFlood, supported by the Dutch Technology Foundation STW, the applied science division of NWO and the technology program of the Ministry of Economic Affairs, the Netherlands.

Cover photo: Sediment transport over a mobile dune (by Suleyman Naqshband)

Printed by Gildeprint Drukkerijen, Enschede, The Netherlands

ISBN: 978-90-365-3813-8
DOI: 10.3990/1.9789036538138
URL: http://dx.doi.org/10.3990/1.9789036538138

MORPHODYNAMICS OF RIVER DUNES

SUSPENDED SEDIMENT TRANSPORT ALONG MOBILE DUNES AND DUNE DEVELOPMENT TOWARDS UPPER STAGE PLANE BED

PROEFSCHRIFT

ter verkrijging van
de graad van doctor aan de Universiteit Twente,
op gezag van de rector magnificus,
prof. dr. H. Brinksma,
volgens besluit van het College voor Promoties
in het openbaar te verdedigen
op donderdag 18 december 2014 om 14.45 uur

door

Suleyman Naqshband
geboren op 15 september 1985
te Kabul, Afghanistan

This thesis is approved by:

prof. dr. S.J.M.H. Hulscher	promotor
dr. ir. J.S. Ribberink	co-promotor

The inanimate, lifeless cloud that resembles carded cotton has of course no knowledge of us, when it comes to our aid, it is not because it takes pity on us. It cannot appear and disappear without receiving orders. Rather it acts in accordance with the orders of a most Powerful and Compassionate commander.

— Bediüzaman Said Nursî (1877-1960)
The Supreme Sign; Observations of a traveller questioning creation

CONTENTS

PREFACE

At last, I have arrived to the final part of this thesis which is writing the preface ☺!

Firstly, I would like to thank the One who has given me the eyes to see and to experience His creation with the aim of getting to know Him and to appreciate His art (including sand dunes :)), which is to state Alhamdulillah. May His blessings and peace be with the one who (Mohammad, His noble messenger) brought the key to the door of eternal happiness.

Dear Jan,
I am one of the lucky PhDs that has been supervised by you. Probably, I was your toughest PhD who – as I remember well – dropped by your office almost daily to just show you a "new" plot. You were always patient and enthusiastic which made it possible to achieve this. I learned a lot from you and you are a great mentor.

Dear Suzanne,
It all started with an email of you where you asked me to apply for this PhD position. I am truly thankful to you for giving me the opportunity and trust to work in such a nice group. Your input to my research has been of indispensable value.

This thesis would have never come so far without the support and help of Fenneke, Marjolein, Olav, Arjan and David. All of you have contributed to this work on a different but yet very important way. Many thanks to all of my colleagues of the WEM-department through these years. Ronald, Erik, Olav, Mustafa, Mehmet, Hatem, Andry, Hero, Jord, Joep, Anne, Bas, Rolien, Wouter, Freek, Lianne, Jolanthe, Juan, Rick, Geert, Wenlong, Abebe thank you all for the pleasant and joyful time.

Special thanks, appreciation and dua for the support of the abilar including my Hoca's Sedreddin Akan and Said Atici, Ahmed Samir, Abdul Aziz, Rahmatullah, Zia, Wahid, Helmi and all my ablalar and abilar in Imaan: *Allah razi olsun* :)!

Padar wa Modar,
Wat ik ook hier aan dank voor jullie schrijf zal nooit maar iets van jullie liefde en steun voor mij kunnen omschrijven. Daarom gebruik ik Zijn woorden:

Rabbi irhamhuma kama rabbayanee sagheeran
[Koran, 17 Al-Isra: 24]

Walid, Khatera, Zohal, Massih, Sahar, Dunya, & Ellaha (binnenkort ook familie ins ;)):
Ik hou van jullie!

Suleyman Naqshband
Enschede, 23 november 2014.

SUMMARY

Dunes are the most common bedforms present in nearly all fluvial channels. Dunes are generally asymmetric with gentle stoss side slopes and steep lee side slopes possessing intermittent or permanent flow separation zones where the water flow detaches the dune surface. They migrate in downstream direction and are almost out of phase with respect to water surface. Because of their dimensions, dunes are of central importance in predicting flow roughness and water levels. During floods in several rivers (e.g., the Elkhorn, Missouri, Niobrara, and Rio Grande), dunes are observed to grow rapidly as flow strength increases, undergoing an unstable transition regime, after which they are washed out in what is called upper stage plane bed. This morphological evolution of dunes to upper stage plane bed is the strongest bedform adjustment during time-varying flows and is associated with a significant change in hydraulic roughness and water levels.

The work presented in this thesis aimed to obtain a better understanding and quantitative data of the flow and sediment transport mechanisms controlling the dune morphology and dune transition to upper stage plane beds. This thesis investigated (I) the dominant flow and sediment transport processes that control dune morphology and dune transition to upper stage plane bed; (II) the relative contributions of bed load and suspended load sediment transport to dune morphology and dune transition to upper stage plane bed; (III) the relative contributions of the turbulent and the advective sediment fluxes to the total sediment fluxes along dunes and (IV) modelling of the transition of dune to upper stage plane bed with an idealized dune evolution model.

An extended literature study was carried out to identify the processes controlling the dune morphology and dune transition to upper stage plane beds (Chapter 2). A large number of dune dimension data sets was compiled and analyzed in this study – 414 experiments from flumes and the field – showing a significantly different evolution of dune height and dune length in flows with low Froude numbers (negligible free surface effects) and flows with high Froude numbers (large free surface effects). For high Froude numbers (0.32 – 0.84), relative dune heights are observed to grow only in the bed load dominant transport regime and start to decay for u_* / w_s (suspension number) exceeding 1. Dunes in this case are not observed for suspension numbers greater than 2.5. For low Froude numbers (0.05 – 0.32), relative dune heights continue to grow from the bed load to suspended load dominant transport regime. Dunes in this case are not observed for suspension numbers greater than 5. The study revealed that for reliable predictions of dune morphology and their evolution to upper stage plane beds, it is essential to address both free surface effects and sediment transport mode.

Detailed flume experiments were carried out at LWI of the Technical University of Braunschweig (Germany) to obtain quantitative knowledge on the behavior of the bed and the suspended load transport along mobile dunes (Chapter 3). Using the newly developed acoustic system (ACVP, developed by *Hurther et al*. [2011]), we were able – for the first time – to measure co-located, simultaneous, and high temporal and spatial resolution profiles of both two-component flow velocity and sediment concentration referenced to the exact position at dune bed. The data has illustrated that, due to the presence of a dense sediment layer close to the bed and migrating secondary bedforms over the stoss side of the dune towards the dune crest, the near-bed flow and sediment processes are significantly different from the near-bed flow and sediment dynamics measured over fixed dunes. The pattern of the total sediment transport distribution along dunes is dominated by the bed load transport. This implies that bed load transport is mainly responsible for the continuous erosion and deposition of sediment along the stoss side of the migrating dunes. The bed load distribution at the lee side of the dunes decays rapidly because of sediment avalanching on the dune slip face. The suspended load transport, on the other hand, is advected further downstream and is more gradually deposited on the lee side and in the trough of the dune. Whereas the bed load is entirely captured in the dune with zero transport at the flow reattachment point, a significant part of the suspended load (the bypass fraction) is advected to the downstream dune depending on the flow conditions. For the two flow conditions measured, the bypass fraction was about 10% for flow with $Fr = 0.41$ and 27% for flow with $Fr = 0.51$. This means that respectively 90% (for the $Fr = 0.41$ flow) and 73% (for the $Fr = 0.51$ flow) of the total sediment load that arrived at the dune crests contributed to the morphology

and migration of the dunes. Based on the insights obtained from these flume experiments, the part of the suspended load acting as the bypass fraction is expected to play an important role during the transition of dunes to upper stage plane bed where dunes are flattened and eventually washed out.

The total sediment fluxes along mobile dunes were – for the first time – quantified by deploying the ACVP (Chapter 4). The data revealed a similar behavior of the total mean streamwise sediment flux $\overline{cu}$ and the mean advective flux $\bar{c}\bar{u}$ along the dune profile. However, along the entire dune profile and mainly in the bed load layer, the absolute magnitudes of $\bar{c}\bar{u}$ are much larger compared to $\overline{cu}$. This overestimation is caused by the negative contribution of the mean turbulent flux $\overline{c'u'}$. Over the stoss side of the dune, $\overline{c'u'}$ reaches up to 40% of the total mean sediment flux, and over the lee side of the dune the contribution of $\overline{c'u'}$ to the total sediment flux is larger and reaches up to 50%. Therefore, indirect measurements of sediment fluxes along dunes (limited to $\bar{c}\bar{u}$) may overestimate the actual sediment fluxes ($\overline{cu}$) up to a factor 2.
Contour maps of the total mean vertical flux $\overline{cw}$ showed peaks on the stoss side of the dune. These peaks were found to be the result of turbulent bursts emanating from the flow detachment zone subject to strong shear instabilities and hitting the dune bed downstream of the flow reattachment point. The mean vertical turbulent flux $\overline{c'w'}$, along the entire dune bed and in the bed load layer, reaches nearly 30% of the total mean vertical flux $\overline{cw}$.

The dune evolution model of *Paarlberg et al.* [2009] was used to study the transition of dunes to upper stage plane bed (Chapter 5). This model was extended by including in the model the transport of bed sediment in suspension. The extended dune evolution model showed significant improvement in the prediction of equilibrium dune parameters (dune height, dune steepness, dune migration rate, dune lee side slope) both under bed load dominant and suspended load dominant transport regimes. However, the equilibrium dune length is still poorly predicted by the dune evolution model.
Where simulations with the original dune evolution model always resulted in a fixed dune lee side slope of 30° after a critical angle of 10° is exceeded, the dune lee side slope predicted with the extended dune evolution model entirely depends on the sediment transport rates. For the suspended load dominant experimental condition a lower lee side slope was predicted (23°) compared to the bed load dominant condition (26°). The chosen modeling approach allowed us to model the transition of dunes to upper stage plane bed which was not possible with the original dune evolution model.

The extended model predicted the change in the dune shapes as was observed in the flume experiments with decreasing dune heights and dune lee side slopes. Furthermore, the time needed to reach upper stage plane bed after increasing the flow discharge is quite well predicted by the extended model (90 minutes in the flume experiments and 80 minutes with the extended model).

SAMENVATTING

Op de rivierbodem vormen zich bodemvormen door interactie tussen stroming, sedimenttransport en morfologie. Rivierduinen zijn de meest waargenomen bodemvormen in zandige rivierbodems en hebben een asymmetrische vorm met een steile lijzijdehelling. Door deze steile lijzijde vertonen duinen gedeeltelijke of volledig ontwikkelde stromingsloslating. Rivierduinen bepalen voor een grote deel de stromingsweerstand in een rivier en zijn daarom van invloed op de waterstanden. Tijdens hoogwater groeien duinen onder invloed van toenemende aanvoer van sediment, maar ze kunnen echter bij hogere stroomsnelheden geheel weer afvlakken. Omdat er relatief weinig kennis is over het afvlakken van duinen kunnen bestaande modellen de stroming- en sedimentcondities voor het afvlakken van duinen niet voorspellen. Dit betekent dat ook de bodemruwheid en daarmee de waterstanden tijdens een hoogwater nog niet voldoende accuraat voorspeld kunnen worden.

Het doel van dit onderzoek is om het proces van duingroei en duinafvlakking beter te begrijpen en kwantitatieve data te verzamelen van de stroming- en sedimentcondities waarmee duinmorfologie en duinovergang naar vlak bed kunnen worden voorspeld. In dit proefschrift wordt ingegaan op (I) identificatie van dominante processen die de duinmorfologie en het afvlakken van duinen bepalen; (II) bijdrage van bodemtransport en suspensietransport aan duinmigratie en het afvlakken van duinen; (III) bijdrage van turbulente- en advective sedimentfluxen aan het totale sedimenttransport en (IV) modelleren van duinovergang naar vlak bed met een duinontwikkelingsmodel.

Om de processen te identificeren die het groeien en afvlakken van duinen bepalen, is een uitgebreide dataset samengesteld waarbij gebruik is gemaakt van data uit 414 experimenten in stroomgoten en in rivieren. De analyse van deze dataset laat zien dat duinontwikkeling en duinafvlakking voornamelijk wordt beïnvloed door het Froude getal (effect van vrij wateroppervlak) en de suspensieparameter u_* / w_s (effect van suspensietransport). Het blijkt dat duinen onder een relatief hoog Froude getal al beginnen af te vlakken wanneer het overgrote deel van het sedimenttransport nog als bodemtransport plaatsvindt. Voor lagere Froude getallen vindt duinafvlakking pas plaats wanneer vrijwel al het sedimenttransport in suspensie verloopt.

Bodemtransport en suspensietransport langs een mobiel duin zijn bestudeerd met de resultaten van een uitgebreide serie gootexperimenten. Hierbij is gebruik gemaakt van een recent ontwikkelde meetinstrument (ACVP) waarbij stroming- en sedimenteigenschappen simultaan en in dezelfde meetvolume gemeten kunnen worden. De resultaten van de gootexperimenten laten zien dat bodemtransport geheel bijdraagt aan de migratie van duinen terwijl suspensietransport – afhankelijk van de stroming condities – gedeeltelijk bijdraagt aan duinmigratie. Terwijl al het bodemtransport in de duin trog neervalt, wordt een deel van het suspensietransport over de duin trog naar de volgende (benedenstrooms) duin verplaatst. Dit deel van het suspensietransport wordt ook de bypass fractie genoemd. De resultaten van de gootexperimenten laten zien dat de bypass fractie toeneemt met toenemende stroming conditie. Deze bypass fractie zal een dominante rol spelen bij de overgang van duinen naar vlak bed. Verder kan uit de gootexperimenten geconcludeerd worden dat – voor de gemeten stroming condities – de duinlijzijdemorfologie voornamelijk bepaald wordt door het verloop (gradiënten) van bodemtransport langs de duin.

ACVP maakt het mogelijk om voor het eerst inzicht te krijgen in de grootte van de turbulente- en advective sedimenttransportfluxen langs een mobiel duin. Het blijkt dat de turbulente sedimenttransportfluxen een significant deel vormen van het totale sedimenttransport langs de gemeten duinen. Wanneer deze turbulente fluxen niet meegenomen worden in de berekening van de totale sedimenttransportfluxen, kunnen de voorspelde/berekende sedimenttransportfluxen een onnauwkeurigheid bevatten die kan oplopen tot een factor 2.

Om duinovergang naar vlak bed te kunnen voorspellen is in dit onderzoek een bestaand duinontwikkelingsmodel verder uitgebreid. De modelsimulaties laten zien dat – zoals ook in de gootexperimenten waargenomen – de duin lijzijdehelling afneemt met toenemende afvoer en sedimenttransport in suspensie. In tegenstelling tot het originele model dat alleen duingroei in het duinregime modelleert, laat het uitgebreide model ook duinafvlakking naar vlak bed zien. De mate maar ook de tijdschaal van de voorspeld duinafvlakking blijkt goed overeen te komen met de waarnemingen uit de gootexperimenten.

CHAPTER 1 – INTRODUCTION

1.1 RIVERS, RIVER BEDFORMS AND FLOOD MANAGEMENT

Alluvial rivers are of great importance geologically, biologically, historically and culturally. They provide transportation links between oceans and inland areas, and supply fresh water for drinking and irrigation. Despite the fact that less than 0.005 per cent of continental water is stored in rivers at any given time, rivers are vital carriers of water and nutrients to areas all around the earth [*Knighton*, 1998]. The character of a river is largely determined by the landscape through which it runs. In mountainous areas rivers display steep slopes with the river bed generally consisting of coarse sediments. In relatively flat areas such as the Netherlands, rivers are characterized as lowland rivers having mild slopes and wide floodplains with the river bed consisting of sand to fine gravel.

In rivers, depending on their topographic characteristics, complex interactions between flow and sediment transport give rise to various types of bedforms. With increasing flow intensity over a flat sand bed, the following sequence of bedforms develop in the lower flow regime: ripples, dunes superimposed with ripples and fully developed dunes. With higher flow intensities in the transitional regimes associated with high sediment transport, dunes are partly washed out and in the upper flow regime dunes totally disappear followed by anti-dunes, breaking waves, and chutes and pools [*Simons and Richardson*, 1966]. This morphological evolution of bedforms with increasing flow intensity is illustrated in Figure 1.1.

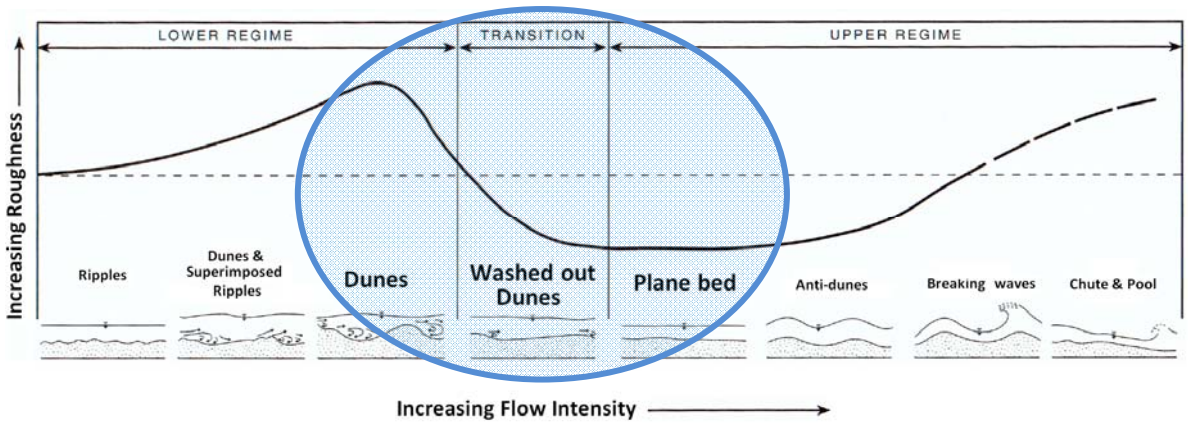

Figure 1.1 – Bedform and corresponding roughness evolution with increasing flow intensity observed during the flume experiments of *Simons and Richardson* [1966], figure after *Knighton* [1998].

The presence of bedforms in rivers cause flow resistance by generating mixing patterns that feed on energy from the mean flow, effectively slowing it down and causing higher water levels at a certain discharge. The magnitude of the bed roughness as experienced by the flow depends on the size and geometry of the bedform. Figure 1.1 shows the evolution of the hydraulic roughness corresponding to the evolution of the bedforms. In the lower flow regime, hydraulic roughness increases followed by a drastic decrease in the transition regime due to diminishing dune heights. In the upper flow regime, the hydraulic roughness initially remains unchanged but with increasing flow intensities unstable bedforms (breaking waves and, chute and pool) may occur on the river bed that will eventually result in an increase of the hydraulic roughness.

Dunes are the most common bedforms present in nearly all fluvial channels [*Best*, 2005a]. Dunes are generally asymmetric with gentle stoss side slopes and steep lee side slopes (Figure 1.2) possessing intermittent or permanent flow separation zones where the water flow detaches the dune surface. They migrate in downstream direction and are almost out of phase with respect to water surface.

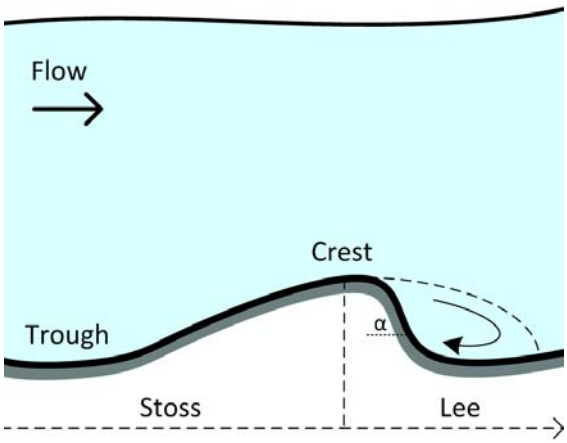

Figure 1.2 – Schematization of a river dune with a steep lee angle illustrating flow separation.

Particularly, in lowland rivers such as the river Rhine in the Netherlands, dunes are observed in all reaches of the river system. Figure 1.3 shows the spatial development of dunes at the Bovenrijn during the 1995 flood wave. During this flood, the dune heights were observed to increase drastically from 0.20 m up to 1.8 m. In addition, during floods in several rivers (e.g., the Elkhorn, Missouri, Niobrara, and Rio Grande), dunes are initially observed to grow rapidly as flow strength increases, followed by a transition regime that eventually resulted in washing out of the dunes towards upper stage plane bed [*Raslan*, 1994 and references therein, *Ashworth et al*., 2000; *Prent and Hickin*, 2001]. This morphological evolution of dunes to upper stage plane bed (USPB)

is the strongest bedform adjustment during time-varying flows and is associated with a significant change in hydraulic roughness and water levels [*Nelson et al.*, 2011]. This drastic change in hydraulic roughness during the dune transition to upper stage plane bed is also illustrated in Figure 1.1.

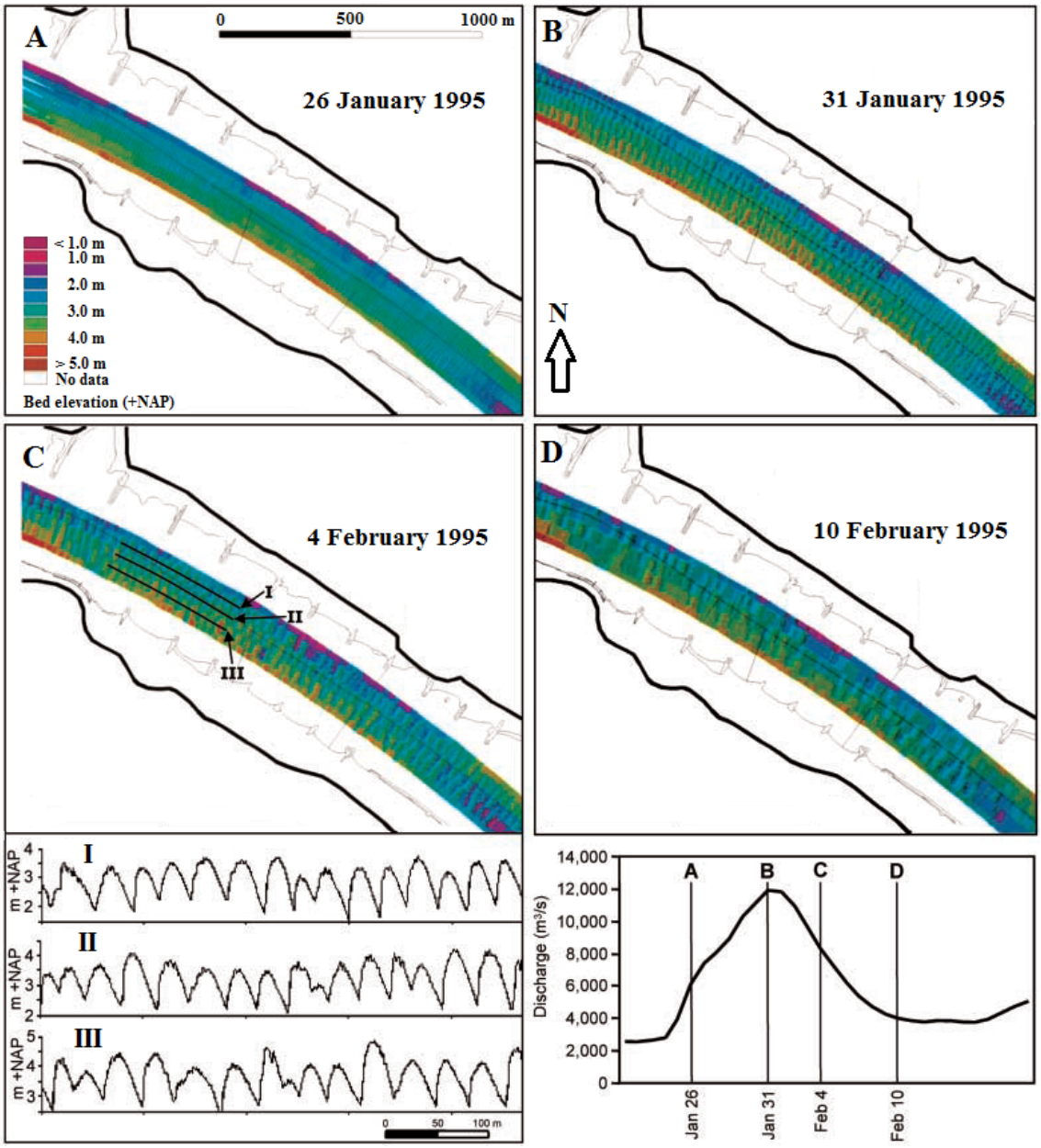

Figure 1.3 – Maps showing the spatial development of dunes in the Bovenrijn during the flood of 1995. (A) Bed elevation at the beginning of the flood, (B) at peak discharge, (C) after peak discharge and (D) at the end of the flood. Below (C), three profiles are plotted to show the differences in dune shape over the width of the river. m + NAP refers to an elevation in meters above the Dutch ordnance datum (after *Wilbers and Ten Brinke*, 2003).

In the Netherlands, river flood protection is established by law. The expected water levels corresponding to the design discharge are determined every five years [*Ministry of Transportation, Public Works and Water Management*, 2007]. The design discharge for the river Rhine is a discharge with a probability of occurrence of 1/1250 years and serves as guideline for the design of flood protection measures. Currently, the design discharge of the river Rhine is determined as 16,000 [m^3 s^{-1}] based on a statistical analysis of historical discharge data. However, due to climate change and global warming, the design discharge is expected to increase up to 18,000 [m^3 s^{-1}] over the next century [*Middelkoop and Buitenveld*, 1999]. This increase in the river discharge may have significant consequences for the riverbed morphology and thus for the water levels along the course of the river. The prediction of water levels corresponding to such extreme discharges is quite challenging as the behaviour of the fluvial system under these conditions is not yet fully understood [see also *Warmink*, 2011]. In particular, the water levels may increase due to increasing hydraulic roughness associated with rapid growth of dunes during high river discharge (Figure 1.3). On the other hand, due to high transport capability of the flow, dunes may also evolve towards upper stage plane beds. In this case, the water levels will decrease due to a decrease in the hydraulic roughness associated with the transition of dunes to upper stage plane beds (Figure 1.1).

To enable accurate predictions of water levels during extreme discharges, we need a bedform evolution model that can correctly predict the dune morphology and dune transition to upper stage plane bed. However, at present, there is no model available that – at operational time scales (time scale of a flood wave) – can describe the dune transition to upper stage plane bed. The main reason for this is the lack of knowledge of the exact flow and sediment transport processes that control this unstable transition. In the following section, different views are discussed on the processes that may contribute to the dynamic evolution of dunes and their transition to upper stage plane beds.

1.2 CONTROVERSY IN PROCESSES CONTROLLING DUNE TRANSITION TO UPPER STAGE PLANE BED

Dune evolution and transition to upper stage plane bed are repeatedly linked in literature to high suspended sediment transport of bed material [*Smith and McLean*, 1977; *Bridge and Best*, 1988; *Nnadi and Wilson*, 1995; *Best*, 2005a and references therein]. It was suggested by *Fredsøe* [1979] that, as the flow strength increases, a larger portion of bed material is transported in suspension; consequently, the ratio of suspended load to bed load increases with increasing flow strength and a smaller part of the sediment avalanches at the dune front as bed load. Furthermore, due to suppression of turbulence

by high near-bed sediment concentration, especially in the flow separation zone, sediment picked up from the dune crest settles in the dune trough, resulting in flatter dunes [*Bridge and Best*, 1988]. *Fredsøe* [1981] used stability analysis to examine the roles of bed load and suspended load on dune morphology. From his analysis he concluded that an increasing ratio of suspended load to bed load leads to decreasing dune heights. This was also concluded by field observations of *Kostaschuk* [2005] and *Kostaschuk and Best* [2005].

In contrast to the literature outlined above, a number of studies have also shown that in some natural channels the height and steepness of the dunes increase with increasing transport in suspension [*Roden*, 1998; *Amsler and Schreider*, 1999; *Amsler et al*., 2003], suggesting that suspended sediment transport may not be the only variable influencing bed form flattening. For instance, *Ditchfield and Best* [1992] showed that bed form amalgamation (smaller dunes superimposed on stoss side of large dunes) lead to local flattening of the dune crest and may therefore play an important role during the dune transition to upper stage plane beds. Additionally, laboratory experiments indicate that at certain clay concentrations the dune morphology may be significantly modified dependent on the clay concentration, clay type and applied shear rate. Flume experiments by *Wan and Wang* [1994] showed how the stability field of dunes is influenced by clay concentration, with dunes becoming increasingly replaced by upper stage plane beds at higher volumetric clay concentrations [see also *Best*, 2005a]. Furthermore, free surface effects (increasing Froude number) are repeatedly linked to the evolution of dunes to upper stage plane bed with upper stage plane bed occurring at Froude numbers in the vicinity of 1 [*Kennedy*, 1963, *Engelund*, 1970; *Colombini and Stocchino*, 2008].

Although it is likely that suspended sediment transport contributes to the transition of dunes to upper stage plane beds, it is not yet exactly known how suspended load contributes to dune morphology and evolution of dunes, and how this compares to bed load. In particular, we have no insight into the contribution of suspended load to sediment erosion on the stoss side of the dune and deposition on the lee side of the dune while the dune is migrating. In addition to this, due to the turbulent nature of the flow associated with dunes, turbulent sediment fluxes may play an important role in dune morphology and dune transition to upper stage plane bed. Mainly due to inherent limitations of the instruments available for the simultaneous and co-located measurement of both flow velocity and sediment concentration, the exact distribution of (turbulent) sediment fluxes along the dune bed and their contribution to dune morphology and dune evolution are not yet quantified.

1.3 RESEARCH OBJECTIVE

In the present study, we aim to obtain a better understanding and detailed quantitative data of the flow and sediment transport mechanisms controlling the dune morphology and dune transition to upper stage plane beds. These insights will enable us to efficiently model dune morphology and evolution for a better prediction of water levels during floods.

1.4 RESEARCH QUESTIONS

To reach the research objective, the following research questions are identified:

Q1. What are the dominant flow and sediment transport processes that control dune morphology and dune transition to upper stage plane bed?

Q2. What are the relative contributions of bed load and suspended load sediment transport to dune morphology and dune transition to upper stage plane bed?

Q3. What are the relative contributions of the turbulent and the advective sediment fluxes to the total sediment fluxes along dunes?

Q4. To what extent can the transition of dune to upper stage plane bed be reproduced with an idealized dune evolution model?

1.5 RESEARCH APPROACH

This study started with an extensive literature study that resulted in an overview of existing bedform data sets in both flume and in the field. These data sets – 10 in the flume and 9 in the field – were compiled and analysed to determine the dominant flow and sediment transport processes controlling dune morphology and dune transition to upper stage plane bed (**Q1**).

Once these processes were identified, detailed flume experiments were carried out to obtain a better insight in the contribution of these processes to dune morphology and dune transition to upper stage plane beds. A newly developed acoustic system, the Acoustic Concentration and Velocity Profiler (ACVP) developed by *Hurther et al*. [2011], allows us – for the first time – to measure co-located, simultaneous, and high temporal and spatial resolution profiles of both two-component flow velocity and sediment concentration referenced to the exact position at dune bed. By deploying the

ACVP in the present study, we obtain quantitative knowledge of the flow and sediment transport distribution along mobile sand dunes. In particular, sediment flux measurements along mobile dunes were obtained to quantify the relative contributions of bed load and suspended load sediment transport to dune morphology and dune transition to upper stage plane bed (**Q2**). Due to the turbulent flow associated with dune geometry, turbulent sediment fluxes may play an important role in dune dynamics. Decomposing the measured fluxes along dunes in turbulent and advective components allowed to quantify the relative contributions of the turbulent and the advective sediment fluxes to the total sediment fluxes along dunes (**Q3**).

For flood management purposes and in particular for Flood Early-Warning Systems (FEWS), there is need for a bedform evolution model that can efficiently predict (low computational time) the river bed regime and the exact bedform dimensions over the course of a full flood wave including the transition of dunes to upper stage plane bed. However, at present, there is no model available that – at operational time scales (time scale of a flood wave) – can describe the dune transition to upper stage plane bed.
Paarlberg et al. [2009] successfully developed a dune evolution model that is able to predict dune development from small initial disturbances towards fully developed dunes in the lower flow regime. The model's computational time was drastically reduced by using a parameterization of the flow separation zone instead of solving the full hydrodynamic and sediment equations in this turbulent region. Although the dune evolution model is shown to give good predictions of the dune dimensions in the dune regime, the model is not able to predict the transition of dunes to upper stage plane bed in the higher flow regime. The main reason for this is probably the use of an equilibrium bed load transport model and not including the transport of the bed sediment in suspension. To study to what extent dune transition to upper stage plane bed can be reproduced with an idealized model, the dune evolution model of *Paarlberg et al.* [2009] was used and extended by including in the model the transport of bed sediment in suspension (**Q4**). Furthermore, additional flume experiments were carried out to understand the morphological behavior of dunes for a wide range of flow conditions and to investigate the time scales related to the transition of dunes to upper stage plane bed. This data were used to validate the extended dune evolution model. An overview of the research approach is presented in Figure 1.4.

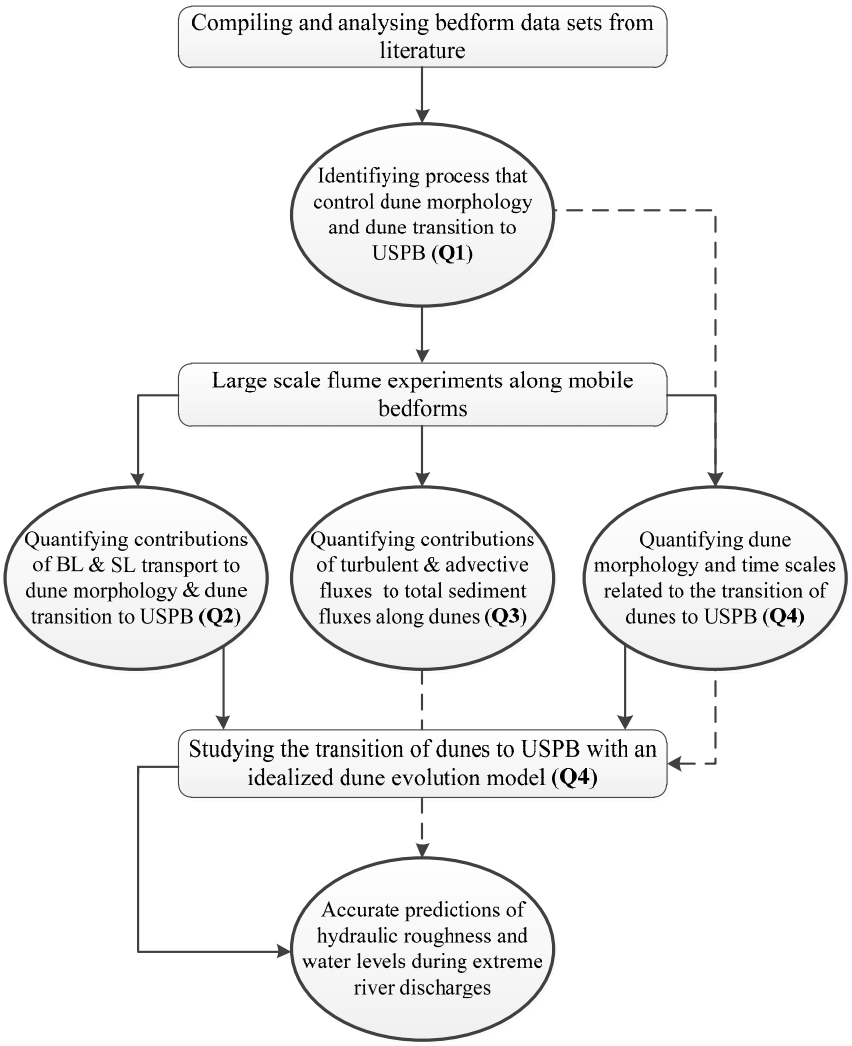

Figure 1.4 – Overview of the research approach

1.6 THESIS OUTLINE

Chapter 2 gives an overview of bedform data sets that are collected and analysed for the identification of different flow and sediment transport processes controlling dune morphology and dune transition to upper stage plane bed (**Q1**). Based on these data, a new method is presented that can be used to determine dune heights, dune lengths and bedform regime for predefined flow and sediment parameters.

Chapter 3 describes new detailed measurements of bed load and suspended load sediment transport along migrating dunes that are obtained by deploying the ACVP. The conducted flume experiments are outlined in detail and the relative contributions of bed load and suspended load sediment transport to dune morphology and dune transition to upper stage plane bed are discussed (**Q2**).

Chapter 4 shows a Reynolds decomposition of the measured total sediment fluxes along mobile dunes. This allows the quantification of the turbulent and the advective sediment fluxes along dunes (**Q3**).

Chapter 5 discusses the morphological evolution of dunes and their transition to upper stage plane beds based on the results of new flume experiments and by using an idealised dune evolution model that is extended with suspended sediment transport processes (**Q4**).

Chapter 6 discusses how this work (may) contributes to a better understanding of dune morphodynamics and dune evolution to upper stage plane bed. Furthermore, some reflection is made about the applied research approach and methodology.

Chapter 7 gives an overview of the main conclusions derived from this work together with challenges and possible directions for future research.

CHAPTER 2 – THE ROLE OF SUSPENDED SEDIMENT TRANSPORT AND FREE SURFACE EFFECT IN DUNE TRANSITION TO UPPER STAGE PLANE BED*

ABSTRACT

Dunes are common bed forms in sand bed rivers and are of central interest in water management purposes. Due to flow separation and associated energy dissipation, dunes form the main source of hydraulic roughness. A large number of dune dimension data sets was compiled and analyzed in this study – 414 experiments from flumes and the field – showing a significantly different evolution of dune height and length in flows with low Froude numbers (negligible free surface effects) and flows with high Froude numbers (large free surface effects). For high Froude numbers (0.32 – 0.84), relative dune heights are observed to grow only in the bed load dominant transport regime and start to decay for u_* / w_s (suspension number) exceeding 1. Dunes in this case are not observed for suspension numbers greater than 2.5. For low Froude numbers (0.05 – 0.32), relative dune heights continue to grow from the bed load to suspended load dominant transport regime. Dunes in this case are not observed for suspension numbers greater than 5. It was concluded that for reliable predictions of dune morphology and their evolution to upper stage plane bed, it is essential to address both free surface effects and sediment transport mode.

* This chapter has been published as: Naqshband, S., Ribberink, J., & S.J.M.H. Hulscher. (2014). Using both free surface effect and sediment transport mode parameters in defining the morphology of river dunes and their evolution to upper stage plane bed. *Journal of Hydraulic Engineering*, 140(6), 1-6, DOI: 10.1061/(ASCE)HY.0733-9429.0000873.

2.1 INTRODUCTION

During floods in several rivers (e.g., the Elkhorn, Missouri, Niobrara, and Rio Grande), dunes are observed to grow rapidly as flow strength increases, undergoing an unstable transition regime, after which they are washed out in what is called upper stage plane bed (USPB). This morphological evolution of dunes to upper stage plane bed (D-USPB) is the strongest bedform adjustment during time-varying flows and is associated with a significant change in hydraulic roughness and water levels [*Nelson et al*., 2011].
In addition to flow and sediment parameters, hydraulic roughness due to the presence of bed forms is directly related to bedform height Δ and length λ [*Yalin*, 1964; *Van Rijn*, 1984b; *Karim*, 1999; *Van der Mark*, 2009]. Therefore, during time-varying flow, reliable predictions of bedform regimes (e.g., dune regime, dune transitional regime, and USPB) and bedform dimensions are of great importance in determining hydraulic roughness and water levels for flood management purposes [*Best*, 2005a].

The first step in understanding the occurrence of bedform regimes was to apply the theory of potential flow together with two-dimensional (2D) and three-dimensional (3D) linear stability analysis [*Kennedy,* 1963; *Reynolds,* 1965; *Engelund,* 1970; *Fredsøe,* 1974a; *Colombini and Stocchino,* 2008; *Colombini and Stocchino,* 2012]. The sediment transport mode in these studies, which is related to the suspension number, was assumed to be either bed load or bed and suspended load. The suspension number represents the relative importance of suspended load to bed load and is further defined in a following section. From these theoretical studies, it was concluded that with increasing free surface effects (increasing Froude numbers), the bedform regime evolved from dune to USPB, with USPB occurring at Froude numbers in the vicinity of 1. The Froude number, as defined in equation (2.1), is the ratio of the average flow velocity u to the wave propagation speed in shallow water, where g = the gravitational acceleration constant and h = the average flow depth.

$$Fr = \frac{u}{\sqrt{gh}} \tag{2.1}$$

Although stability analysis serves to demonstrate the significance of bulk flow parameters in bedform mechanics – notably the Froude number – it does not provide information on the dimensions of bed forms or understanding of the detailed physics of bed deformation [*Coleman and Fenton*, 2000].

In addition to theoretical works, over the past century, a large number of experiments have been conducted to characterize the bedform regimes with the so-called bedform stability diagrams [*Liu*, 1957; *Simons and Richardson*, 1966; *Van Rijn*, 1984b; *Van den Berg and Van Gelder*, 1989; *Southard and Boguchwal*, 1990]. These diagrams show the occurrence of different bedform regimes as a function of sediment transport capability of the flow (e.g., the Shields parameter) but are independent of the Froude number (free surface effects). Furthermore, as the bedform stability diagrams are almost entirely based on flume data, care must be taken while using them under field conditions in natural flows with relatively low Froude numbers. Applying three different bedform stability diagrams, *Kostaschuk and Villard* [1996] showed that USPB were predicted in the Fraser River, where data showed the presence of dunes.

Along with the free surface effects, dune evolution and transition to USPB are repeatedly linked in literature to high suspended sediment transport of bed material [*Smith and McLean*, 1977; *Bridge and Best*, 1988; *Amsler and Schreider*, 1999; *Best*, 2005a and references therein]. It was suggested by *Fredsøe* [1979] that, as the flow strength increases, a larger portion of bed load is transported in suspension; consequently, a smaller part of the sediment load avalanches at the dune front as bed load. Furthermore, due to suppression of turbulence by high near-bed sediment concentration, especially in the flow separation zone, sediment picked up from the dune crest settles in the dune trough [*Bridge and Best*, 1988], resulting in flatter dunes.

From the aforementioned literature, it may be concluded that dune morphology and evolution to USPB are mainly controlled by two processes: free surface effects and high suspended sediment transport rates of bed material. In addition, the recent study of *Nelson et al.* [2011] showed that these two processes determine the response of bed forms to flow variability. However, for the prediction of the dimension of dunes during the D-USPB regime, predominantly empirical relations based on a limited number of mainly flume data sets with relatively high Froude numbers can be found in the literature [*Yalin*, 1964; *Allen*, 1978; *Ranga Ruju and Soni*, 1976; *Van Rijn*, 1984b; *Julien and Klaassen*, 1995; *Karim*, 1995]. These predictors relate dune dimensions to sediment transport capability of the flow and do not explicitly consider free surface effects or high suspended sediment transport of bed material. As a result, these predictors may not be suitable for the prediction of dune dimensions and the occurrence of USPB under relatively low Froude numbers in large rivers [Figures 6 and 7 in *Julien and Klaassen*, 1995].

The aim of this chapter is to investigate the importance of free surface effects and sediment transport mode on the morphological evolution of dunes to USPB. The study focuses on the evolution of dune height and length for a large range of Froude numbers and sediment transport rates.

2.2 METHOD

To examine the influence of sediment transport mode and free surface effect in determining dune dimensions in the D-USPB regime, a large number of bedform data from flumes and rivers was compiled and analyzed, as presented in Table 2.1. The 10 flume data sets are listed in the first part of Table 2.1, and the 9 field data sets are shown in the second part. Based on several criteria for the classification of dunes reported by Table 1 in *Venditti et al*. [2005], a total of 414 experiments – 187 flume experiments and 227 field experiments – were selected, which is quite unique compared to the number of experiments used by former authors while deriving empirical dune dimension predictors. *Van Rijn's* [1984b] predictor is based on 84 flume and 22 field experiments, while *Karim* [1995] used 71 flume and 21 field experiments for his dune height predictor in the D-USPB regime. The analysis in this study focuses on dunes where ripples are excluded from the data sets, as ripples scale with the grain size where dunes scale with the water depth [*Yalin*, 1964]. Furthermore, dune data were selected such that a wide range of Froude numbers was well-represented and the flow regime was hydraulically rough. In addition to dune dimension data sets in the dune and dune transitional regimes (Table 2.1), seven data sets from the literature on the occurrence of USPB in flumes and in the field were analyzed, as shown in Table 2.2, containing a total number of 72 data points.

Table 2.1 – Summary of the selected dune data sets from flumes and field experiments with range of different parameters.

Data sets	*# of Exp.*	$\bar{u}$ *(m/s)*	*h (m)*	$S * 10^{-3}$ *(-)*	D_{50} *(mm)*	*F (-)*	u_*/w_s *(-)*	Δ *(m)*	λ *(m)*
Delft Hydraulics Lab (1979)	24	0.39-0.86	0.09-0.59	0.30-6.90	0.79	0.21-0.83	0.51-0.71	0.03-0.15	0.65-1.98
Driegen (1986)	36	0.42-0.79	0.09-0.59	0.68-6.9	0.78	0.26-0.83	0.42-1.00	0.05-1.04	1.01-1.51
Guy et al. (1966)[a]	38	0.55-1.17	0.10-0.34	1.0-3.90	0.19-0.93	0.34-0.84	0.48-2.74	0.01-0.14	0.79-6.24
Iseya (1984)[b]	11	0.58-0.93	0.23-0.40	0.78-2.45	1.20	0.34-0.47	0.32-0.73	0.02-0.18	0.80-3.42
Stein (1965)[a]	17	0.51-1.12	0.12-0.31	1.68-3.87	0.39	0.31-0.71	1.18-1.65	0.05-0.10	1.37-3.26
Termes (1986)	7	0.60-1.34	0.17-0.35	2.70-2.97	0.39	0.47-0.78	1.18-1.70	0.06-0.14	1.56-4.76
Tuijnder (2010)	6	0.47-0.58	0.15-0.26	1.50-2.60	0.80	0.33-0.44	0.52-0.72	0.07-0.10	1.37-1.49
Van Enckevoort & Van der Slikke (1996)[b]	40	0.66-0.93	0.36-0.45	0.11-0.19	0.24	0.32-0.49	0.69-0.85	0.12-0.22	2.90-8.20
Venditti et al. (2005)	5	0.36-0.50	0.152	0.55-1.2	0.50	0.30-0.41	0.38-0.57	0.02-0.05	0.30-1.17
Williams (1970)[a]	13	0.45-0.63	0.09-0.22	0.80-2.10	1.35	0.36-0.58	0.21-0.43	0.01-0.05	0.73-1.89
Abdel-Fattah (1997)[b] – Nile River	17	0.31-0.88	2.28-5.72	0.004	0.24-0.54	0.05-0.15	0.18-0.47	0.14-2.17	4.30-68.5
Dinehart (1992)[b] – North Fork Toutle River	39	2.26-2.66	1.49-2.23	4.35	22.1-36.0	0.56-0.68	0.31-0.47	0.12-0.30	5.50-48.5
Gabel (1993)[b] – Calamus River	18	0.61-0.77	0.34-0.61	0.68-1.10	0.31-0.41	0.29-0.34	0.94-1.41	0.10-0.19	2.02-4.05
Julien (1992) – Bergsche Maas River	24	1.30-1.70	6.20-10.5	0.125	0.18-0.52	0.13-0.19	1.33-4.95	0.40-2.50	8.0-50.0
Julien (1992) – Jamuna River	33	1.30-1.50	8.20-19.5	0.07	0.20	0.09-0.17	3.19-4.92	0.80-5.10	15.0-251
Julien (1992) – Parana River	13	1.00-1.50	22.0-26.0	0.05	0.37	0.07-0.10	1.98-2.15	3.0-7.50	100-450
Neill (1969) – Red Deer River	30	0.58-1.37	0.91-3.66	0.074	0.34	0.19-0.23	0.50-1.00	0.31-1.83	3.1-21.3
Shen (1978)[a] – Missouri River	21	1.37-1.76	2.77-4.94	0.13-0.16	0.19-0.27	0.24-0.32	2.30-2.93	0.58-2.07	58.0-174
Ten Brinke et al. (1999)[b] – Rhine River	22	1.43-1.93	9.44-12.6	0.008-0.014	2.50	0.14-0.18	0.12-0.19	0.47-1.32	10.4-36.2

[a]References and additional experimental details can be found in *Brownlie* [1982].
[b]References and additional experimental details can be found in *Wilbers* [2004].

Table 2.2 – Summary of the USPB data sets from flume and field experiments with range of different parameters.

Data sets	*# of Exp.*	$\bar{u}$ *(m/s)*	*h (m)*	$S * 10^{-3}$ *(-)*	D_{50} *(mm)*	*T (°C)*	*F (-)*	u_*/w_s *(-)*
Guy et al. (1966)[a]	20	0.87-1.62	0.09-0.24	1.12-4.86	0.19-0.54	7.90-28.4	0.69-1.1	0.88-2.05
Bechman & Furness (1962)[a] – Elkhorn River	22	1.31-2.15	1.28-2.04	0.31-0.48	0.23	7.0-24.0	0.33-0.49	2.13-3.24
Colby & Hembree (1955)[a] – Niobrara River	14	0.96-1.70	0.40-0.59	1.33-1.71	0.22-0.32	1.1-21.1	0.46-0.54	1.93-3.03
Mahmood (1979)[a] – Pakistani Canals	3	0.62-0.65	2.23-2.232	0.07-0.09	0.11-0.13	23.0-24.0	0.13-0.14	3.01-3.61
Nordin (1964)[a] – Rio Grande River	11	0.90-2.38	0.39-1.25	0.55-0.84	0.17-0.29	11.0-27.0	0.41-0.68	1.57-2.93
Shen et al. (1978)[a] – Missouri River	1	1.67	2.77	0.16	0.22	5.0	0.32	2.79
Simons (1957)[a] – American Canals	1	0.59	1.83	0.84	0.10	23.2	0.14	4.54

[a]References and additional experimental details can be found in *Brownlie* [1982].

A well-known parameter used in the literature to represent the relative importance of suspended sediment load to bed load is the ratio of bed shear velocity u_* and particle fall velocity w_s (also referred to as the suspension number), first stated by *Bagnold* [1966] and later verified experimentally by *Van Rijn* [1984a]. Although the exact boundaries for the distinction between bed load and suspended load dominant transport regimes are not well-defined, sediment is transported mainly as bed load for $u_* / w_s < 1$, and transport of sediment in suspension becomes dominant for suspension numbers greater than 1.25 [*Van Rijn*, 1993].

The bed shear velocity in field experiments is calculated from equation (2.2), where g = the gravitational acceleration constant; h = the average flow depth; and S = the energy slope.

$$u_* = \sqrt{ghS} \tag{2.2}$$

For bed shear velocity in flume experiments, hydraulic radius R is used instead of h, where the method of *Vanoni and Brooks* [1957] is applied to correct for the influence of side-wall roughness. The particle fall velocity w_s is given in equation (2.3) after *Soulsby* [1997], where ν = the kinematic viscosity.

$$w_s = \frac{\nu}{D_{50}}\left[\left(10.36^2 + 1.049 D_*^3\right)^{1/2} - 10.36\right] \tag{2.3}$$

$$D_* = \left[\frac{g\left(s-1\right)}{\nu^2}\right]^{1/3} D_{50} \tag{2.4}$$

Where the water temperature was not reported by the authors, a temperature of 15°C was assumed. Furthermore, s = the specific gravity of sand used in the experiments; and D_{50} = the median grain size.

Free surface effects become important when the ratio of surface undulation $d\eta$ to bed undulation dH increases. The surface undulation is related to the mean amplitude of the surface waves, and bed undulation is related to the mean distance from the trough to the crest of the bed forms. From Bernoulli's law applied on open channel flows, as shown in equation (2.5), one can see that this ratio increases with the magnitude of the Froude number [*French*, 1985].

$$\frac{d\eta}{dH} = \frac{1}{1 - Fr^2} \tag{2.5}$$

For relatively low Froude numbers ($Fr < 0.3$), surface undulations are less than 10% of bed undulations and therefore have no significant impact on the bed. For larger Froude numbers, this percentage increases strongly, and free surface effects become important [*Fredsøe*, 1974b; *Niemann et al.*, 2011]. Following this, the dune data sets were divided into two classes of Froude numbers: low Froude numbers (0.05 – 0.32), resulting in small free surface undulations of less than approximately 10% of bed undulations; and high Froude numbers (0.32 – 0.84), resulting in large free surface undulations (up to three times the bed undulations) and therefore having a significant impact on the bed.

2.3 RESULTS

2.3.1 DUNE HEIGHT EVOLUTION

The height of the dunes during their evolution from dune regime to dune transitional regime and USPB was first considered. Figure 2.1 shows the relative dune heights Δ/h with increasing values of the suspension number. Two different behaviors of relative dune height evolution are observed corresponding to the two classes of Froude numbers defined previously.

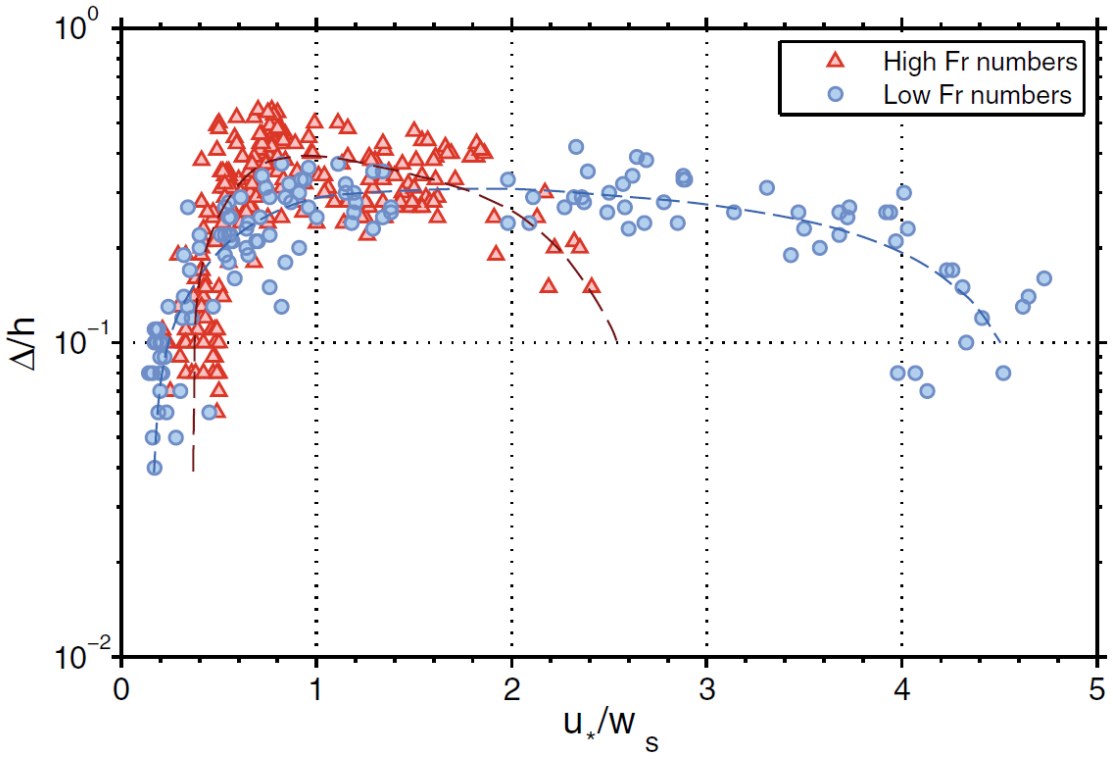

Figure 2.1 – Relative dune heights versus suspension number for 414 dune data points listed in Table 2.1. Two classes of Froude (*Fr*) numbers are distinguished based on the ratio of free surface to bed undulation: Low Froude numbers (0.05-0.32) and high Froude numbers (0.32-0.84).

For high Froude numbers (0.32 – 0.84) and large free surface undulations, which are mainly flows in flume experiments, Δ/h starts to increase rapidly toward a maximum with increasing magnitude of the suspension number. This growth is associated with sediment transport predominantly consisting of bed load as $u_* / w_s < 1$; sediment load avalanches at the dune front as bed load contributing to growth of the dunes. With an increasing amount of sediment transport in suspension, Δ/h starts to decay. A larger portion of sediment load is transported in suspension; consequently, a smaller part of the sediment load avalanches at the dune front as bed load [*Fredsøe*, 1979]. For these high Froude numbers (high free surface effects), USPB are expected to occur for suspension numbers in the vicinity of 2.5.

For low Froude numbers (0.05 – 0.32) and small free surface undulations, which are mainly flows in field experiments, Δ/h starts to increase more gradually toward a maximum with increasing magnitude of the suspension number. Relative dune heights in this case reach a maximum that is significantly lower than maximum heights reached under large free surface undulations (high Froude numbers). For the range of suspension numbers between 0.6 and 1.0, where maximum values of Δ/h are reached for both low and high Froude numbers, the average value of Δ/h is 0.38 for high Froude numbers and 0.26 for low Froude numbers. Furthermore, where relative dune heights Δ/h under large free surface undulations are observed to decay immediately after reaching their maximum heights, maximum Δ/h under small free surface undulations (low Froude numbers) persist for a large range of suspension numbers. For these low Froude numbers, USPB are expected to occur for suspension numbers in the vicinity of 5.

This morphological transition of dunes to USPB as a function of the Froude and suspension numbers is confirmed by the 72 USPB data points shown in Table 2.2 and plotted in Figure 2.2 together with 414 dune data points. Figure 2.2 displays the transition from dune regime (circles) to USPB regime (squares) for a range of Froude and suspension numbers. In contrast to the theoretical studies discussed previously, the data show the occurrence of USPB for a large range of Froude numbers depending on the sediment transport mode. The transition from dunes to USPB occurs for different combinations of the Froude and suspension numbers. For higher Froude numbers, USPB are reached for smaller values of suspension numbers. For relatively low Froude numbers, USPB can be reached only if transport of suspended sediment is dominant over transport of bed load. Furthermore, it can be concluded that using either the Froude number or the suspension number is not sufficient in describing the dune transition to USPB and that both parameters should be considered while deriving dune height predictors.

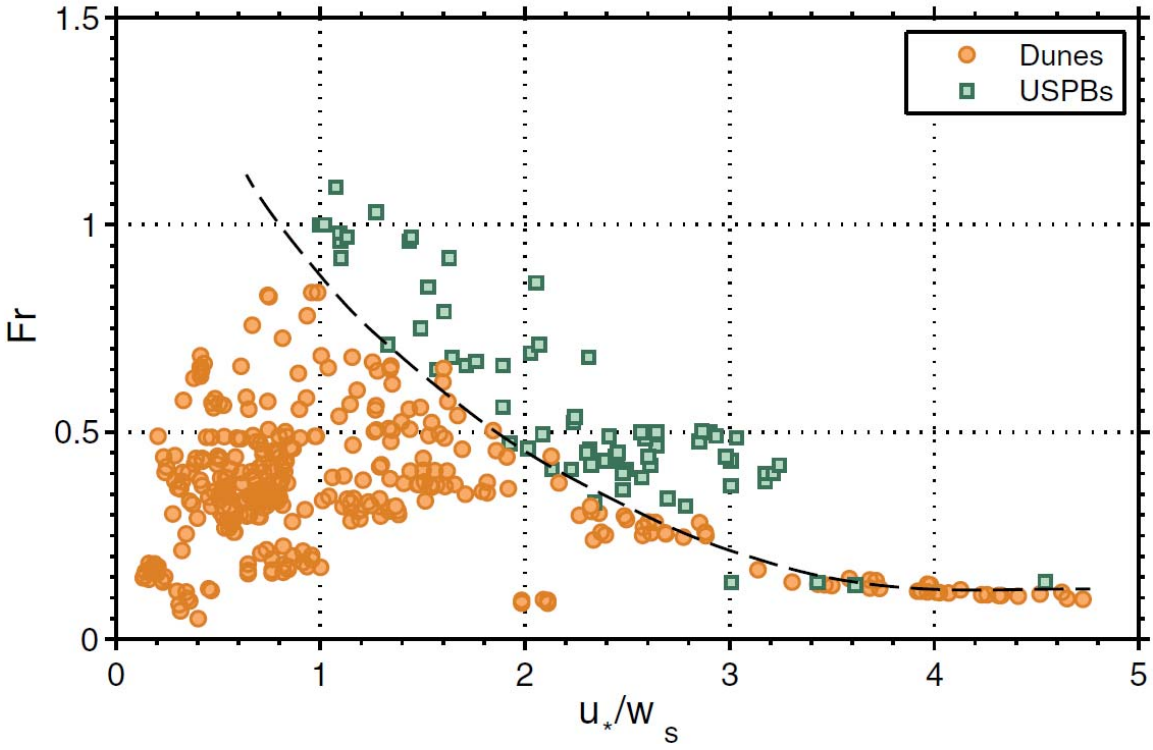

Figure 2.2 – Transition from dune regime (data from Table 2.1) to USPB regime (data from Table 2.2) for different Froude numbers and suspension numbers. For relatively high Froude numbers USPB are reached for smaller values of suspension numbers compared to low Froude numbers.

2.3.2 DUNE LENGTH EVOLUTION

For the two classes of Froude numbers, Figure 2.3 shows the relative dune lengths λ/h with increasing values of the suspension number. Despite the large scatter in the dune length data, λ/h is generally larger for flows with large free surface undulations (high Froude numbers) compared to flows with small free surface undulations (low Froude numbers). The average value of λ/h is 8.3 for high Froude numbers, and the average value of λ/h is 3.4 for low Froude numbers. Averaged over all flume and field data plotted in Figure 2.3, $\lambda/h = 6.8$ is found, which is comparable to the values found in the literature. Furthermore, with an increasing suspension number, there is a weak increasing trend in the relative dune lengths for both flows.

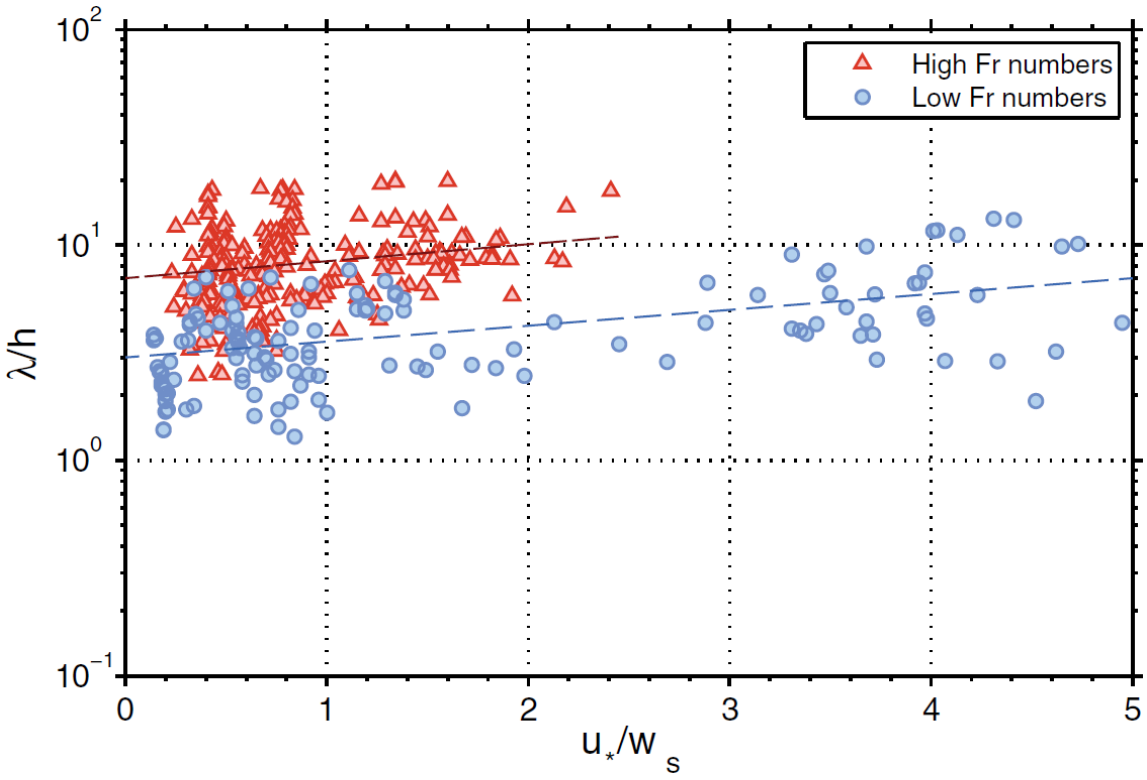

Figure 2.3 – Relative dune lengths versus suspension number for 414 dune data points listed in Table 2.1. Two classes of Froude (*Fr*) numbers are distinguished based on the ratio of free surface to bed undulation: Low Froude numbers (0.05-0.32) and high Froude numbers (0.32-0.84).

2.4 Discussion and Conclusions

Analysis of a large number of bedform data from flumes and rivers showed that sediment transport mode and free surface effects are two crucial processes in determining dune heights and lengths during the evolution of dunes to USPB. The occurrence of USPB is linked to the Froude and suspension numbers. It can be found in the literature that bedform amalgamation or the presence of a certain clay concentration may also lead to local flattening of the dune crest. *Ditchfield and Best* [1992] showed that amalgamation of two dunes, migrating with different speeds, leads to the formation of a new dune having a height lower than the sum of the two dune heights before amalgamation. The experiments of *Wan and Wang* [1994] showed the influence of clay concentration on the bedform stability diagrams, with dunes being increasingly replaced by USPB at higher volumetric clay concentrations. Because the addition of clay can change the sediment transport mode by lowering the fall velocity of sand particles, this phenomenon is related to the work described in this study.

Due to large variations in dune lengths, existing relations for the relative dune length λ/h available in the literature assume a constant value independent of the Froude and suspension numbers. Based on mainly dune data from flumes (high Froude numbers), *Van Rijn* [1984b] found that $\lambda/h = 7.3$. *Julien and Klaassen* [1995] corrected this value to $\lambda/h = 6.5$ using primarily dune data from the field (low Froude numbers), and *Yalin* [1972] theoretically determined the relation $\lambda/h = 2\pi$ for the relative dune length. Despite the large scatter in the dune length data, the relative dune length is not constant and depends on the magnitude of the Froude and suspension numbers.

Furthermore, records of dune morphology in rivers have shown the coexistence of dunes of different length scales due to either non-uniform and unsteady character of the flow (hysteresis effects) or the developing internal boundary layer on the stoss side of large dunes [*Best*, 2005a and references therein]. These records show a range of different dune lengths for the same flow and sediment conditions. Using these dune lengths as input for the calculation of hydraulic roughness and water levels may result in computed values with a larger range of uncertainty. Therefore, care must be taken while applying dune height and length predictors for engineering purposes.

In contrast to the existing bedform regime diagrams, where the dune and USPB regimes are not clearly distinguished [*Van den Berg and Van Gelder*, 1989; *Southard and Boguchwal*, 1990], this study shows that by using the Froude and suspension numbers, these regimes are very well-separated. The results of this study can be used to investigate the bedform regime and make a first estimation of the hydraulic roughness corresponding to this regime. In addition, using the data presented in this chapter, dune height and length predictors can be derived that take both the free surface effects and sediment transport mode into account.

The main conclusions of our analysis are presented below:

1. Morphological evolution of river dunes to USPB is more readily and accurately identified by observing the magnitude of both the Froude and suspension numbers. Therefore, dune dimension predictors, which are mainly derived from experimental data in flows with high Froude numbers (large free surface effects), are generally not suitable for application in rivers where Froude numbers are usually lower and free surface effects are negligible.

2. For flows with high Froude numbers, the transition of dunes to USPB occurs for smaller values of the suspension number than in flows with low Froude numbers.

3. Relative dune heights under high Froude numbers reach a maximum that is larger than maximum heights reached under low Froude numbers.

4. Relative dune lengths are generally larger in flows with high Froude numbers and tend to increase with increasing values of the suspension number.

CHAPTER 3 – CONTRIBUTIONS OF BED LOAD AND SUSPENDED LOAD TRANSPORT TO DUNE MORPHOLOGY AND DUNE TRANSITION TO UPPER STAGE PLANE BED*

ABSTRACT

Dunes dominate the bed of sand rivers and are of central importance in predicting flow roughness and water levels. The present study has focused on the details of flow and sediment dynamics along migrating sand dunes in equilibrium. Using a recently developed acoustic system (ACVP: Acoustic Concentration and Velocity Profiler), new insights are obtained in the behavior of the bed and the suspended load transport along mobile dunes. Our data have illustrated that, due to the presence of a dense sediment layer close to the bed and migrating secondary bedforms over the stoss side of the dune towards the dune crest, the near-bed flow and sediment processes are significantly different from the near-bed flow and sediment dynamics measured over fixed dunes. It was observed that the shape of the total sediment transport distribution along dunes is mainly dominated by the bed load transport although the bed load and the suspended load transport are of the same order of magnitude. This means that it was especially the bed load transport that is responsible for the continuous erosion and deposition of sediment along the migrating dunes. Whereas the bed load is entirely captured in the dune with zero transport at the flow reattachment point, a significant part of the suspended load is advected to the downstream dune depending on the flow conditions. For the two flow conditions measured, the bypass fraction was about 10% for flow with a Froude number (*Fr*) of 0.41 and 27% for flow with Froude number of 0.51. This means that respectively 90% (for the *Fr = 0.41* flow) and 73% (for the *Fr = 0.51* flow) of the total sediment load that arrived at the dune crests contributed to the migration of the dunes.

* This chapter has been published as: Naqshband, S., Ribberink, J., Hurther, D. & S.J.M.H. Hulscher. (2014). Bed load and suspended load contributions to migrating sand dunes in equilibrium. *Journal of Geophysical Research – Earth Surface*, 119, 1043-1063, DOI: 10.1002/2013JF003043.

3.1 INTRODUCTION

Sand dunes are rhythmic features resulting from the interaction between flow and sediment transport and form the main source of hydraulic roughness of the river bed. Dunes can reach heights up to one third of the water depth and therefore dominate the entire flow field. Both the mean and the turbulent flow structures and consequently the sediment pick-up and deposition are strongly influenced by dunes. Particularly during floods, dunes are observed to grow rapidly resulting in significant changes of the hydraulic roughness and water levels.

Sediment in rivers is transported as bed-material load and wash load. Wash load is fine sediment that is transported in permanent suspension and does not usually contribute to the morphological development of dunes. Bed-material load consists of sediment that originates on the bed and is sub-divided into bed load and suspended bed-material load. Bed load moves close to the bed in traction and saltation and suspended bed-material load (hereafter referred to as 'suspended load' for brevity) is transported above the bed in intermittent suspension. Sediment transport that contributes to the migration of dunes is often assumed to be bed load [e.g., *Carling et al.,* 2000; *Jerolmack and Mohrig,* 2005; *Kostaschuk et al.,* 2009; and references therein], although several researchers have demonstrated that a significant fraction of the total sediment transport in sand bed rivers may consist of suspended load [e.g., *Smith and McLean,* 1977*; Kostaschuk and Villard,* 1996*; Kostaschuk,* 2005*; Nittrouer et al.,* 2008]. In addition, a large number of numerical and experimental studies have illustrated that suspended load is crucial in changing the dune form. *Smith and McLean* [1977] found that, in the Columbia River, asymmetric dunes with flow separation occurred when bed load was the dominant transport mechanism while symmetric dunes without flow separation zone (low-angle dunes) developed when most sand is transported in suspension. They suggested that the steep lee sides of asymmetric dunes are maintained by avalanching of bed load down the lee slope, whereas the much lower angle lee sides of symmetric dunes result from deposition of sand from suspension in the lee side and trough between dunes [*Best and Kostaschuk,* 2002]. This was also concluded from the field measurements performed by *Kostaschuk and Villard* [1996], *Kostaschuk* [2000] and *Amsler et al.,* [2003]. Field data from the Rio Paraná in Argentina, collected by *Kostaschuk* et al. [2009], showed that about 17% of the suspended load transported over the dune crest was deposited on the lee side slope of the dune before it reached the trough.

Stability analysis carried out by *Fredsøe* [1981] on the role of sediment transport on dune morphology illustrated that an increase in bed load transport will lead to an

increase in the dune height while an increase in suspended load transport will result in a decrease of the dune height. *Amsler and Schreider* [1999] found that with an increasing ratio of suspended load to bed load, dune heights were reduced during floods in the Rio Paraná. *Kostaschuk* [2005] and, *Kostaschuk and Best* [2005] concluded from field and numerical studies that deposition of suspended sediment in the trough and on the lee side slope of dunes results in a reduction of dune height and lowering of lee slope angle. Suspended sediment transport is also found to contribute to the transition of dunes to upper stage plane beds [e.g., *Best,* 2005a, and references therein]. In a recent study *Naqshband et al.* [2014] illustrated that the transition from dunes to upper stage plane beds can only occur if sufficient sediment is transported into suspension depending on the magnitude of the bed shear stress and the Froude number.

Although it is likely that suspended sediment transport contributes to the migration of dunes [*Kostaschuk et al.,* 2009], it is not yet exactly known how suspended load contributes to dune morphology and migration and how this compares to bed load. In particular, we have no insight into the contribution of suspended load to sediment erosion on the stoss side of the dune and deposition on the lee side of the dune while the dune is migrating. The fraction of the total sediment transport that is not captured in the dune trough and therefore does not contribute to the migration of dunes (bypass fraction) is also not yet properly quantified. As highlighted by *Parsons and Best* [2013], sediment transport and the exact nature of lee side deposition processes are key to predicting dune migration. *Coleman and Nikora* [2011] attributed this gap of knowledge partly to the fact that most of the experimental studies associated with dunes have focused on flow and sediment dynamics above fixed beds [e.g., *Cellino and Graf*, 2000; *Best and Kostaschuk,* 2002; *Kleinhans*, 2004; *Best*, 2005a,b; *Venditti*, 2007]. The advantage of utilizing fixed bedforms is that they allow detailed flow measurements without the complications of both a migrating and changing bedform and the difficulties of flow measurement in the presence of sediment transport over a fully mobile bed [*Best and Kostaschuk,* 2002].

Another reason why the contributions of bed load and suspended load to dune migration have not yet been fully determined is that there are inherent limitations of the instruments available for the simultaneous measurement of both flow velocity and sediment concentration, mainly in the near-bed region. Experimental studies conducted with mobile dunes focusing on the direct measurement of sediment fluxes, both in the flume as in the field, have therefore been limited to the simultaneous measurement of flow velocity and sediment concentration above a considerable distance from the migrating dune bed [e.g., *Parsons et al.,* 2005; *Wren et al.,* 2007; *Coleman et al.,* 2008;

Wren and Kuhnle, 2008; *Kostaschuk et al.,* 2009; *Shugar et al.,* 2010]. Consequently, only a fraction of the suspended load is measured while the bed load cannot be determined at all. Furthermore, for determining sediment fluxes, usually two different instruments are deployed to measure the flow velocity and sediment concentration and they do not measure at the same point in the flow. As a result, the measured sediment flux cannot be referenced to an exact location along the dune bed. *Wren and Kuhnle* [2008] used a Laser Doppler Velocimeter (LDA) and an acoustic backscatter system (BSS) to measure coupled flow and sediment motion over mobile sand dunes. To determine the suspended sediment transport and deposition over a mobile dune, *Kostaschuk et al.* [2009] deployed an acoustic Doppler current profiler (aDcp) for flow velocity measurements while suspended sediment concentration was measured with an in-situ laser diffraction transmissometer (LISST-100C). By calibrating the acoustic backscatter signal of the aDcp using different instruments, *Kostaschuk et al.* [2009] also obtained concentration measurements which abled them – to an extent – to measure sediment fluxes with the aDcp (see also *Shugar et al.* [2010]). In addition, using two different systems for the measurement of flow velocity and sediment concentration limits the sediment flux studies to flow scales larger than the separation distance between the two instruments. In particular, turbulence processes, which are the most important mechanisms of sediment entrainment and transport, cannot be addressed directly [*Hurther et al.,* 2011].

A newly developed acoustic system, the Acoustic Concentration and Velocity Profiler (ACVP) developed by *Hurther et al.* [2011], now allows us to measure co-located, simultaneous, and high temporal and spatial resolution profiles of both two-component flow velocity and sediment concentration referenced to the exact position at the bed. The ACVP also measures both in the bed load layer and in the suspended load layer over the entire water column (see section 3.2.1 for more details on the ACVP). Recently, the ACVP has been successfully applied under waves [*Hurther and Thorne,* 2011; *Ruessink et al.,* 2011]. By deploying the ACVP in the present study, we obtain quantitative knowledge of the flow and sediment transport distribution along mobile, equilibrium sand dunes. In particular, we measure the contributions of both bed load and suspended load to dune morphology and migration.

3.2 FLUME EXPERIMENTS

3.2.1 EXPERIMENTAL SET-UP AND INSTRUMENTATION

The experiments were conducted in the Hydraulics Laboratory of the Leichtweiss institute of the Technical University of Braunschweig, Germany. The flume has a width of 0.5 m and a length of 30 m, where the effective measuring length for dune morphology was approximately 8 m (Figure 3.1). Flow discharge to the flume was delivered from a constant head-tank approximately 5 m above the flume level. Stacked tubes were used to direct the flow into the flume. Using an Inductive Discharge Measurement device (IDM), the desired discharge was set with an accuracy of 1%. The flume slope and the weir at the end of the flume were adjustable, which made it possible to achieve equilibrium flow conditions at a predefined discharge and water depth. The sediment at the end of the flume was caught by a funnel and transported back to the upstream end of the flume after the completion of each experiment. At the effective measurement section of the flume, the bed and water levels were measured continuously using echo sounders that were mounted on a semi-automatic measurement carriage. The water level was measured at the center of the flow, where the bed level measurements were taken at three parallel transects across the flume width. The accuracy of the bed level measurements was determined by repeatedly measuring a fixed bed profile. The vertical standard deviation was less than 1 mm, where the horizontal standard deviation was approximately 3 mm. In the horizontal direction the accuracy of the echo sounders is determined by the area of the acoustic footprint at the bed, which was a few centimeters in diameter [*Tuijnder et al.,* 2009]. This makes the echo sounders suitable for studying large-scale features of the dunes, but the grain scale processes cannot be resolved.

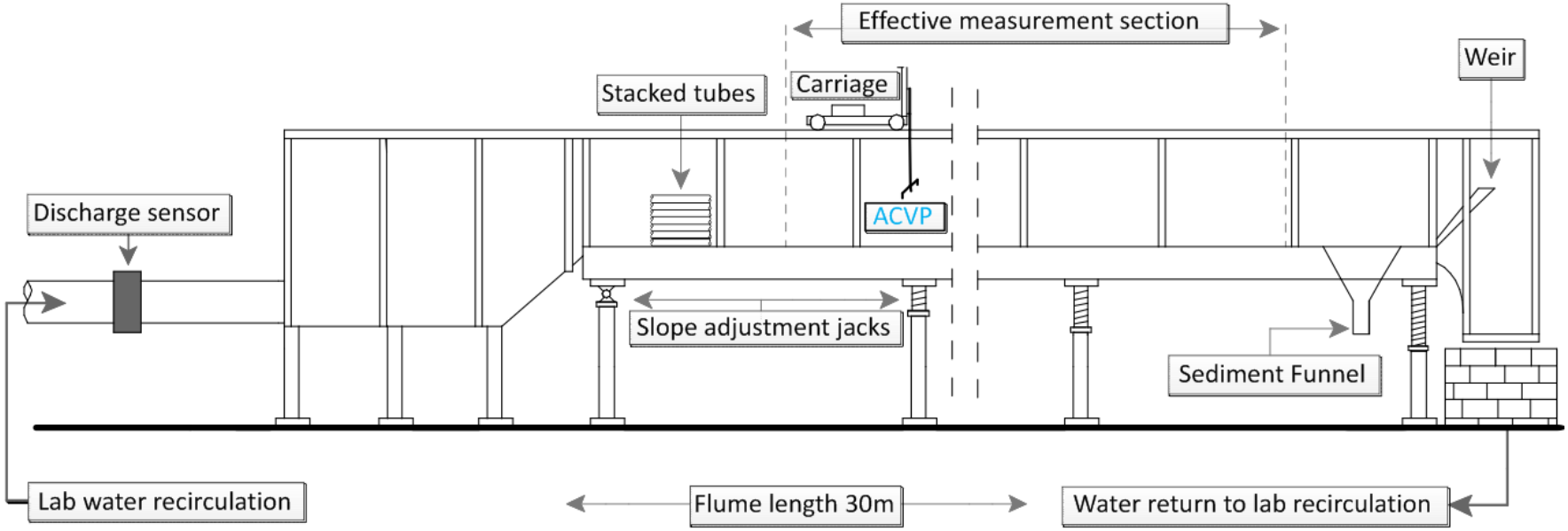

Figure 3.1 – Side view of the flume used, adapted from *Tuijnder et al*. [2009]. Water flow is from left to right and is supplied to the flume from a constant head-tank. Equilibrium flow conditions are reached by adjusting the flume slope and the weir at end of the flume.

To study the contributions of bed load and suspended load to dune migration, sediment fluxes are measured over the entire flow depth using the ACVP developed by *Hurther et al*. [2011]. The ACVP (Figure 3.2) combines an Acoustic Doppler Velocity Profiler (ADVP) [*Hurther and Lemmin*, 2001] with an Acoustic Backscatter System (ABS) *[Thorne and Hanes*, 2002] in a single measuring tool enabling the direct measurement of sediment fluxes in the suspension layer and in the bed load layer.

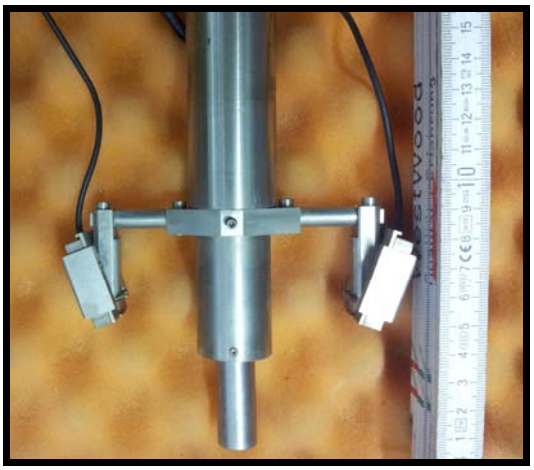

Figure 3.2 – Front view of the Acoustic Concentration and Velocity Profiler (ACVP) configuration with one piezoelectric transmitter (middle) and two side receivers.

The major advantage of this single system is that it provides bed referenced, simultaneous, co-located profile measurements of two-component flow velocity and sediment concentration at high temporal (25 Hz) and spatial resolution (3 mm). Sediment concentration profiles are determined by applying the dual-frequency inversion method to the ACVP backscattered signal. Compared to the well-known implicit iterative [*Thorne et al*., 1993] and the explicit inversions [*Lee and Hanes*, 1995], this technique offers the unique advantage of being unaffected by the non-linear sediment attenuation effect across highly concentrated flow regions [*Hurther et al*., 2011]. The sand bed interface and the interface between the suspended load and the bed load are determined by identifying, in the backscattered signal profile, the non-moving bed echo characterized by its immobility and the echo from the suspended sediment concentration, respectively. These two near-bed echoes can be separated when the acoustic intensity profile is derived from the demodulated Doppler signals since the acoustic scatters constituting the non-moving sand bed produce a constant voltage with negligible signal variance (for more details on the acoustic interface detection methods, see *Hurther and Thorne,* 2011, and *Hurther et al.,* 2011).

This results in the time evolution of the non-moving sand bed, the overlaying high sediment concentration layer (the bed load layer) and the suspended load layer including both the two-component flow velocity and the sediment concentration data in these three zones. Whether the region in between the two interfaces corresponds to the physical bed load layer is difficult to validate. This is mainly due to different definitions used for the thickness of the bed load layer in literature. In addition, due to instrumental limitations, no data could be collected to trace sediment movement or sediment paths in this layer and to determine whether the sediment in this layer was transported while remaining primarily in contact with the immobile bed. However, using the interface detection method, the bed load layer that was identified within several millimeters from the non-moving sand bed is the same order of magnitude of the bed load layer thickness reported by several researchers [see, e.g., *Van Rijn*, 1984, and references therein]. A more physical definition for the thickness of the high near-bed sediment concentration layer, termed the sheet-flow layer, is given by *Dohmen-Janssen et al.* [2001] as the distance between the non-moving bed and the level where the time-averaged concentration reaches a value of 8% volume concentration (212 kg m^{-3}). However, sheet-flow conditions are typically reached for Shields parameter θ between 0.8 to 3 depending on the sediment grain size [*Camenen et al.,* 2006] where values of θ in the current study varied between 0.31 to 0.69 (see Table 3.1). Therefore, the sheet-flow layer definition of *Dohmen-Janssen et al.* [2001] is not applicable in the current study.

3.2.2 EXPERIMENTAL PROCEDURE

A sand layer approximately 25 cm thick was installed over the entire length of the flume and flattened at the beginning of each experiment (Figure 3.3). For each experiment, the water discharge and water depth were predefined (see section 3.2.3). The flume was slowly filled with water from both the downstream and upstream end of the flume to make sure the bed was not disturbed. Subsequently, the predefined discharge was set and the required water depth was obtained by adjusting the flume slope and the weir level at the downstream end of the flume. The sand bed and water levels were measured continuously over the entire effective measurement section of the flume using echo sensors fixed on the carriage (Figure 3.1). Every 2 to 3 minutes, the carriage made a scan of the entire flume in the streamwise direction at three parallel transects across the flume width. The stored data was processed and analyzed directly after each bed scan to monitor the water and bed level development in the flume. The weir level was adjusted when the water depths in the flume significantly (more than 10%) differed from the predefined water depth as a result of developing bedforms. Starting from plane beds, ripples appeared instantaneously as the flow was introduced in the flume. Dunes

subsequently developed and finally a steady-state condition was obtained where the dunes migrated through the flume with a constant speed and without significantly changing form. This dynamic equilibrium was found by analyzing dune height and length statistics from the measured bed profiles using the bedform tracking tool of *Van der Mark et al.* [2008]. Average and standard deviations of dune height and length were determined over the effective measurement section of the flume (section 3.2.3).

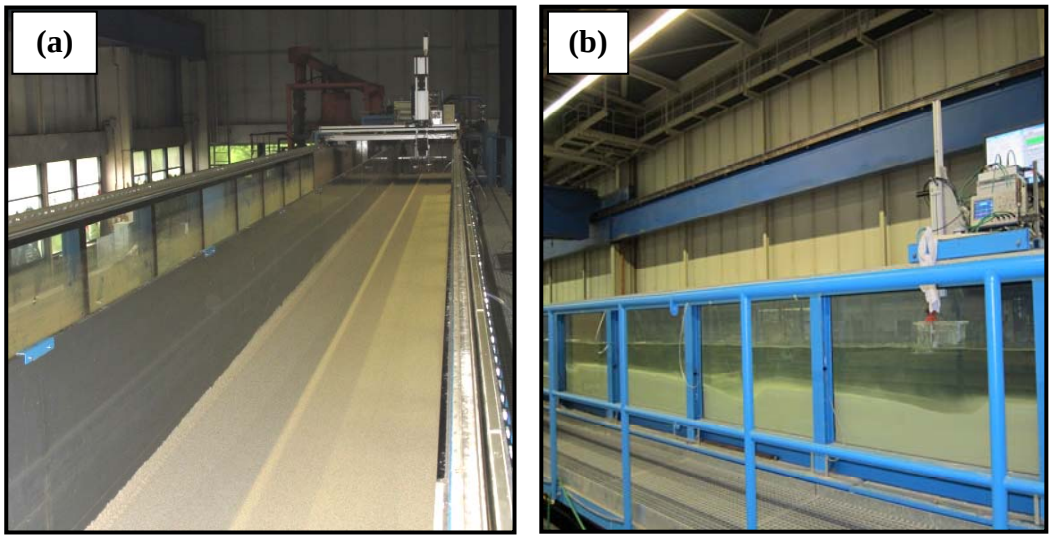

Figure 3.3 – Flattened sand bed, before the start of the experiment (a), and developed dune field at the end of the experiment (b).

The measurements of flow velocity and sediment concentration with the ACVP started as soon as equilibrium flow condition was obtained and the dunes were observed to be in the dynamic equilibrium. The carriage with the ACVP was placed at a fixed position along the flume and the dunes migrated underneath the carriage with a constant speed. One dune length was typically covered within one hour of ACVP measurement. As the sediment transport through the flume was not recirculated back to the upstream end of the flume, an erosion wave was generated at the upstream end of the flume. Generally, three dune lengths were covered by the ACVP measurements before the dynamic equilibrium in the effective measurement section of the flume was disturbed by this migrating erosion wave. An averaging period of 10 seconds was chosen for the ACVP measurements so that bed displacement within this period was small compared to the dune length. This results in a maximum bed displacement of 0.7 to 1.3 cm for a dune length of 2.25 m (EXP1) and 4.35 m (EXP2), respectively (Table 3.1). In addition, this averaging period of 10 seconds was chosen to encompass both the short-term turbulent events (small burst and sweeps) and relatively long-term turbulent events (larger, energy-carrying structures: vortices and eddies).

The ACVP should be submerged totally in the flow. As the water depth in the experiments was limited (25 cm), this would reduce the measurement height above the bed significantly. In addition, due to its dimensions, the ACVP would act as an obstacle and effect the flow and the bed. To avoid this, a partly enclosed PVC box was constructed and filled with water to produce negative pressure in the box. The ACVP was fixed in this box and located just below the water surface enabling the measurement of flow velocity and sediment concentration over almost the entire water depth (Figure 3.4).

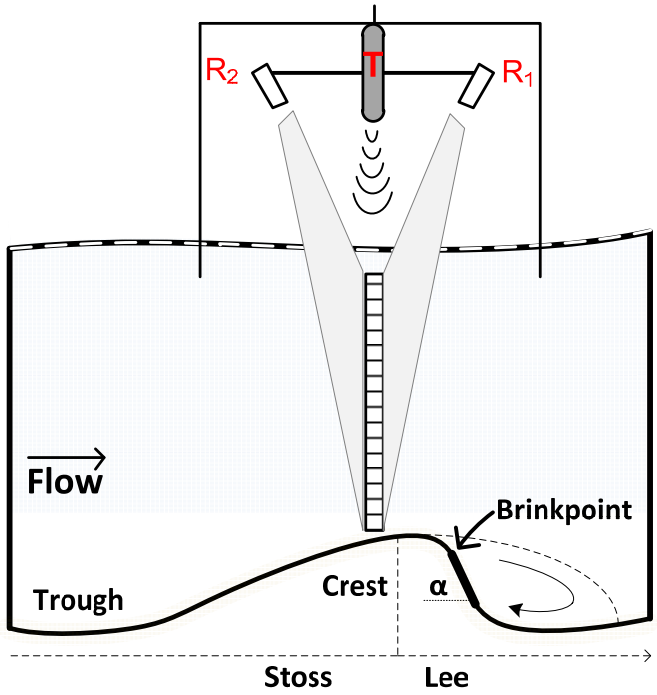

Figure 3.4 – Acoustic Concentration and Velocity Profiler (ACVP) fixed in a PVC box filled with water (not to scale) and positioned just below the water surface. T, R1, and R2 are the piezoelectrical transmitter, the downstream side receiver, and the upstream side receiver, respectively.

After the completion of each experiment, the discharge through the flume was stopped and the sediment accumulated at the end of the flume was returned to the upstream end of the flume. The bed was flattened and the same procedure outlined above was repeated, capturing at least 10 different dunes with the ACVP for two different flow conditions (Table 3.1).

3.2.3 FLOW, SEDIMENT AND BED CONDITIONS

To study bed and suspended load contributions to migrating dunes, two different experiments were conducted under equilibrium flow conditions. Table 3.1 gives an overview of the flow, sediment and bed conditions for both experiments.

Parameter[a,b]	**EXP1**	**EXP2**
Discharge Q, $m^3\ s^{-1}$	0.08	0.10
Flume slope $S \times 10^{-3}$	1.0	2.20
Water depth h, m	0.25	0.25
Mean bulk velocity U, $m\ s^{-1}$	0.64	0.80
Froude number Fr	0.41	0.51
Hydraulic radius R_b , m	0.15	0.15
Bed shear stress τ_b, Pa	1.47	3.24
Bed shear velocity u_*, $m\ s^{-1}$	0.038	0.057
Shields parameter θ	0.31	0.69
$D_{10} \times 10^{-3}$, m	0.21	0.21
$D_{50} \times 10^{-3}$, m	0.29	0.29
$D_{90} \times 10^{-3}$, m	0.40	0.40
Equilibrium dune length λ_e, m	2.25	4.35
Equilibrium dune height Δ_e, m	0.082	0.072
Equilibrium dune steepness Δ_e/λ_e	0.036	0.018
Time to equilibrium T_e, min	150	90
Equilibrium migration speed $C_e \times 10^{-4}$, $m\ s^{-1}$	7.0	13.0

Table 3.1 – Flow, sediment and bed conditions for the two experiments.

[a]The bed shear stress is corrected for the influence of side-wall roughness using the method of *Vanoni and Brooks* [1957] for the calculation of the hydraulic radius R_b

[b]Flume width B equals 0.50 meter. The following expressions are used for different parameters: $U = Q/(hB)$, $Fr = U/\sqrt{(gh)}$, $\tau_b = \rho_w g R_b S$, $u_* = \sqrt{(\tau_b/\rho_w)}$, $\theta = \tau_b/(\rho_s - \rho_w)gD_{50}$ with ρ_s *the sand and* ρ_w *the water density, respectively.*

The experiments were carried out with two different flow strengths where the water depth was kept constant. A discharge of 0.08 $m^3\ s^{-1}$ was used for the low flow strength experiment (EXP1) where a discharge of 0.10 $m^3\ s^{-1}$ was used for the high flow strength experiment (EXP2). The bed shear stress τ_b was calculated using the hydraulic radius R_b where the method of *Vanoni and Brooks* [1957] is used to correct for the influence of side-wall roughness. Applying the bedform stability diagram of Van den Berg and Van Gelder [1993], uniform sand with D_{50} of 0.29 mm was used to obtain 2D dunes in the flume.

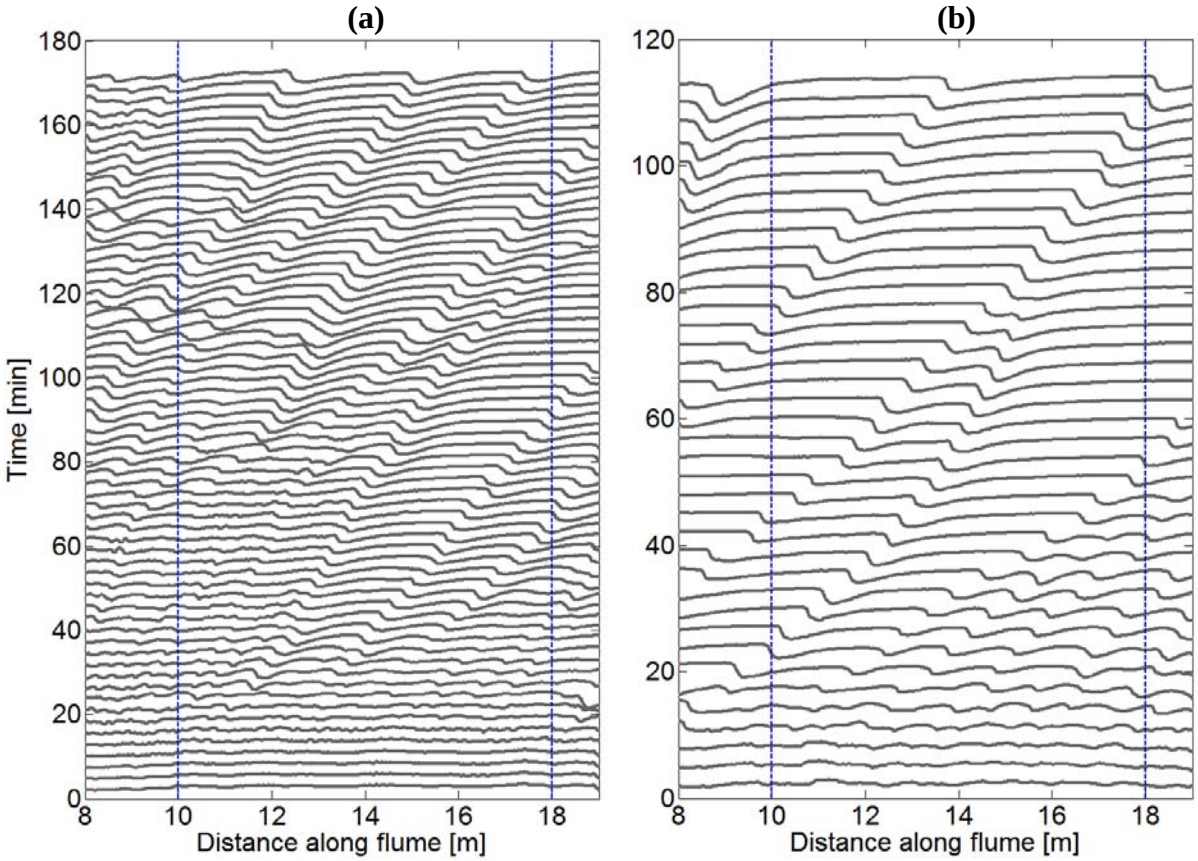

Figure 3.5 – Bed evolution in time along the flume with blue dotted lines indicating the effective measuring section of the flume, EXP1 (a) and EXP2 (b).

Figure 3.5 displays the bed evolution in time along the effective measuring section of the flume. The time T_e needed to reach dune dynamic equilibrium was determined by considering the average and standard deviations of dune height and length over the effective measuring section of the flume (x = 10 to 18 m, Figure 3.6). For EXP1, approximately after 2.5 hours, the standard deviations for both average dune height and length decreased significantly and remained constant. For EXP2 dune equilibrium was reached after approximately 1.5 hours because the greater flow strength results into larger sediment transport capability of the flow (higher bed shear stress τ_b, see Table 3.1) and the steady-state condition is reached faster. This is also reflected in the equilibrium migration speed of dunes C_e for EXP2 which is almost two times larger than for EXP1. Furthermore, for both experiments equilibrium dune heights Δ_e are quite similar (Table 3.1), while – despite the similar water depths h for both experiments – equilibrium dune lengths λ_e for EXP2 are twice the dune lengths reached under EXP1. Although it is generally accepted that the dune length is a function of the water depth [e.g., $\lambda/h = 7.3$, see *Van Rijn*, 1984], *Naqshband et al.* [2014] showed that relative dune length (λ/h) increases with increasing amount of sediment into suspension.

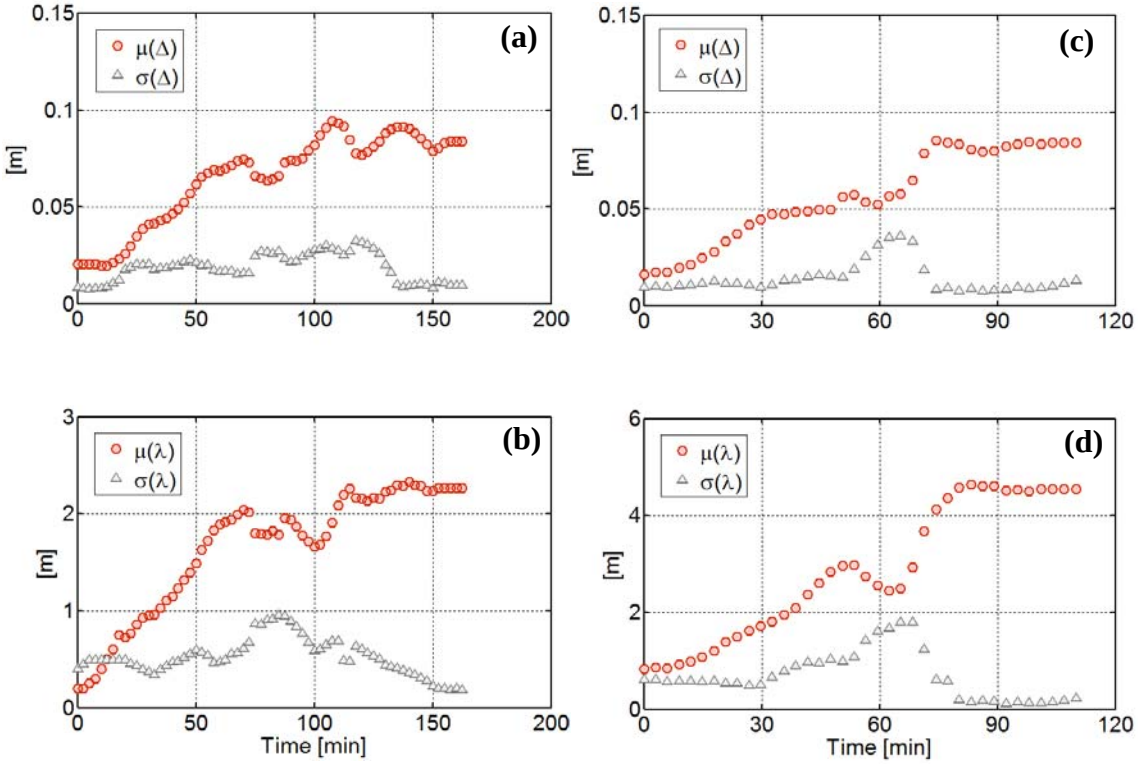

Figure 3.6 – Average μ and standard deviation σ for the dune height Δ for EXP1 (a) and EXP2 (c). Average μ and standard deviation σ for the dune length λ for EXP1 (b) and EXP2 (d)

The ACVP data examined in this study correspond to the period of time needed for the migration of at least one entire dune length beneath the ACVP. As the dune migration speed in equilibrium C_e is nearly constant, multiplying the measured time by the migration speed converts time to streamwise distance x along the dune. Furthermore, the horizontal x and vertical z axes are made dimensionless using the measured dune length and height, respectively.

3.3 FLOW STRUCTURE

The mean flow structure over migrating dunes was examined by velocity and turbulence relations generally used to describe flow fields over bedforms. This includes the mean streamwise and vertical velocities, mean streamwise and vertical turbulent intensities, and Reynolds shear stresses. The mean streamwise $\overline{u}$ and vertical $\overline{w}$ flow velocities are defined in equation (3.1). The instantaneous flow velocities are denoted by u_i and w_i and n is the total number of measurements within the averaging period of time. With a measuring frequency of 25 Hz and an averaging period of 10 seconds, n = 250.

$$\overline{u} = \frac{1}{n}\sum_{i=1}^{n} u_i \qquad \text{and} \qquad \overline{w} = \frac{1}{n}\sum_{i=1}^{n} w_i \tag{3.1}$$

The mean streamwise I_u and vertical I_w turbulent intensities are defined in equation (3.2) with $u' = u_i - \overline{u}$ as the streamwise and $w' = w_i - \overline{w}$ as the vertical velocity fluctuation.

$$I_u = \left[\frac{1}{n}\sum_{i=1}^{n}\left(u'\right)^2\right]^{\frac{1}{2}} \qquad \text{and} \qquad I_w = \left[\frac{1}{n}\sum_{i=1}^{n}\left(w'\right)^2\right]^{\frac{1}{2}} \tag{3.2}$$

The Reynolds shear stress τ_{uw} is calculated from equation (3.3) with ρ_w the fluid density.

$$\overline{u'w'} = \frac{1}{n}\sum_{i=1}^{n}\left(u_i - \overline{u}\right)\left(w_i - \overline{w}\right) \qquad \text{and} \qquad \tau_{uw} = -\rho_w \overline{u'w'} \tag{3.3}$$

3.3.1 MEAN FLOW FIELD

Figure 3.7 shows the contour maps and selected profiles of the mean streamwise flow velocity $\overline{u}$ along dunes for the low flow strength experiment with a dune length of 2.25 m (EXP1) and for the high flow strength experiment with a dune length of 4.35 m (EXP2). The arrows represent the time-averaged velocity vector field $\boldsymbol{V}(\overline{u}, \overline{w})$ overlaid onto the contour maps. The mean position of the dune bed is shown by the solid black line and the flow is from left to right. Irregularities in the dune topography, in both experiments, indicate the presence of small, mobile secondary bedforms that migrate on the stoss side of the main dune towards its crest. In our experiments, these secondary bedforms reached heights of several centimeters and they clearly display a flow recirculation area at their lee sides that can have local effects on the near-bed flow and sediment dynamics.

Several time-averaged flow features over dunes are observed in Figure 3.7 that have been described in other studies [e.g., *Raudkivi*, 1966; *Parsons et al.,* 2005; *Venditti,* 2007; *Coleman et al.,* 2008; *Grigoriadis et al.,* 2009; *Shugar et al.,* 2010; *Bradley et al.,* 2013]. This includes (1) a zone of lee side flow reversal or deceleration; (2) flow acceleration due to convergence on the stoss side of the dune towards the dune crest with largest mean streamwise velocities at the crest area; (3) flow deceleration due to expansion in the wake region with negative velocities in the flow separation zone; (4) an outer, near-surface region with higher velocities overlying the flow separation zone; and (5) development of an internal boundary layer starting on the stoss side of the dune towards the dune crest. Furthermore, the mean distance from the separation point to the flow reattachment point (indicated with open circles in Figure 3.7a and Figure 3.7c), the flow separation length, is found to be 5 to 6 times the equilibrium dune height Δ_e, which

is in good agreement with values reported in previous studies [e.g., *Paarlberg et al.,* 2007, and references therein]. The exact location of the flow reattachment point at the bed is the boundary between the negative and the positive mean streamwise flow velocities. The flow reattachment point is located at 0.1 to 0.2 times Δ_e which is higher than the minimum dune trough level.

In addition to topographic forcing effects, the near-bed mean streamwise flow velocity above mobile dunes also seems to be affected by the presence of a dense mobile sediment layer close to the bed. As a result, the near-bed mean streamwise velocity above mobile beds deviates from the logarithmic profile often observed above plane or fixed dune beds. *Sumer et al.* [1996] measured a small, nearly constant mean streamwise velocity in the high sediment concentration layer near the bed and found that the velocity outside this layer follows the logarithmic law. This behavior of the mean streamwise flow velocity close to the bed, as shown in Figure 3.7, is also observed in the current experiments. The sediment concentration plots in section 3.4.1 (Figure 3.12) confirm the presence of high sediment concentration in this near-bed layer where the mean streamwise velocity profile deviates from the logarithmic law. Furthermore, the mean streamwise velocities close to the bed are also affected by the presence of secondary bedforms. The experimental study of *Carling et al.* [2000] showed that secondary bedforms had a significant effect on the near-bed flow, inducing low velocities near the bed and accelerated flow above the height of the secondary bedforms. As a result, the mean streamwise velocity profiles also deviated from the logarithmic velocity profiles displaying small, nearly constant velocities in the vicinity of the bed and much larger velocities towards the water surface (see Figure 12 in *Carling et al.* [2000]).

The contour maps and selected profiles of the mean vertical flow velocities $\overline{w}$ along dunes for both experiments are shown in Figure 3.8. The clockwise flow rotation formed in the flow separation zone is clearly observed. Negative (directed towards the bed) mean vertical velocities are localized in the trough region downstream of the dune crest. Due to topographic forcing effects, positive (directed towards the water surface) mean vertical velocities are present almost along the entire dune surface with largest values occurring at the midstoss side of the dunes between $x/\lambda = 0.2$ and $x/\lambda = 0.6$. Although the flow strength is larger for EXP2 than EXP1, due to a much smaller dune steepness (Δ_e/λ_e) for EXP2 (Table 3.1), the mean vertical velocities for this experiment are generally smaller compared to EXP1.

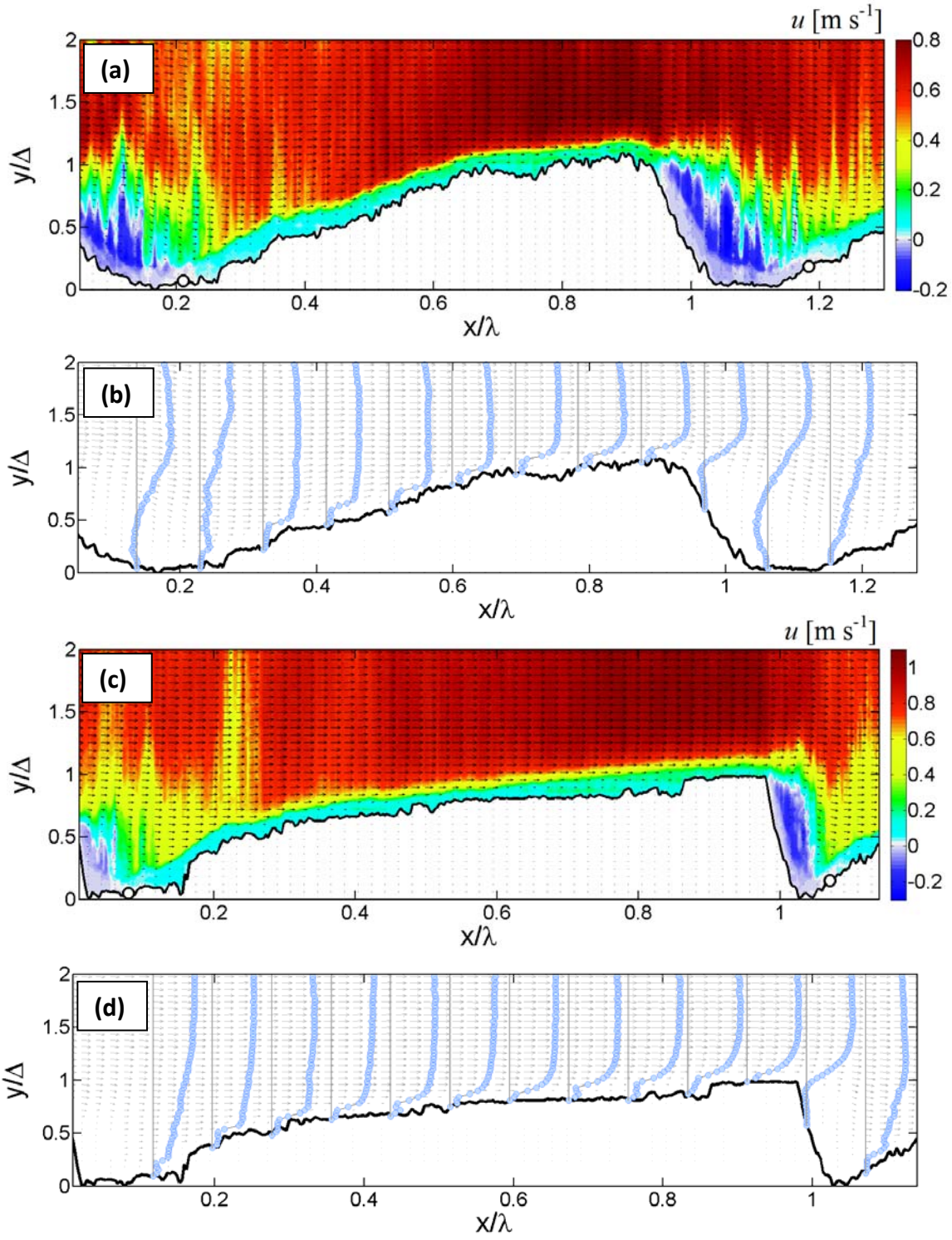

Figure 3.7 – Contour maps and selected profiles of the mean streamwise flow velocity $\overline{u}$ [m s^{-1}] for EXP1 (a and b) and EXP2 (c and d). The arrows represent the mean velocity vector field $V(\overline{u}, \overline{w})$ and the solid line shows the dune profile with open circles indicating the flow reattachment point. Flow direction is from left to right. Vertical, solid lines along the dune bed indicate the location of the velocity profiles origin with negative velocities to the left and positive velocity to the right of this line. The distance between two vertical lines scales with $\overline{u}$ = 1.25 m s^{-1}.

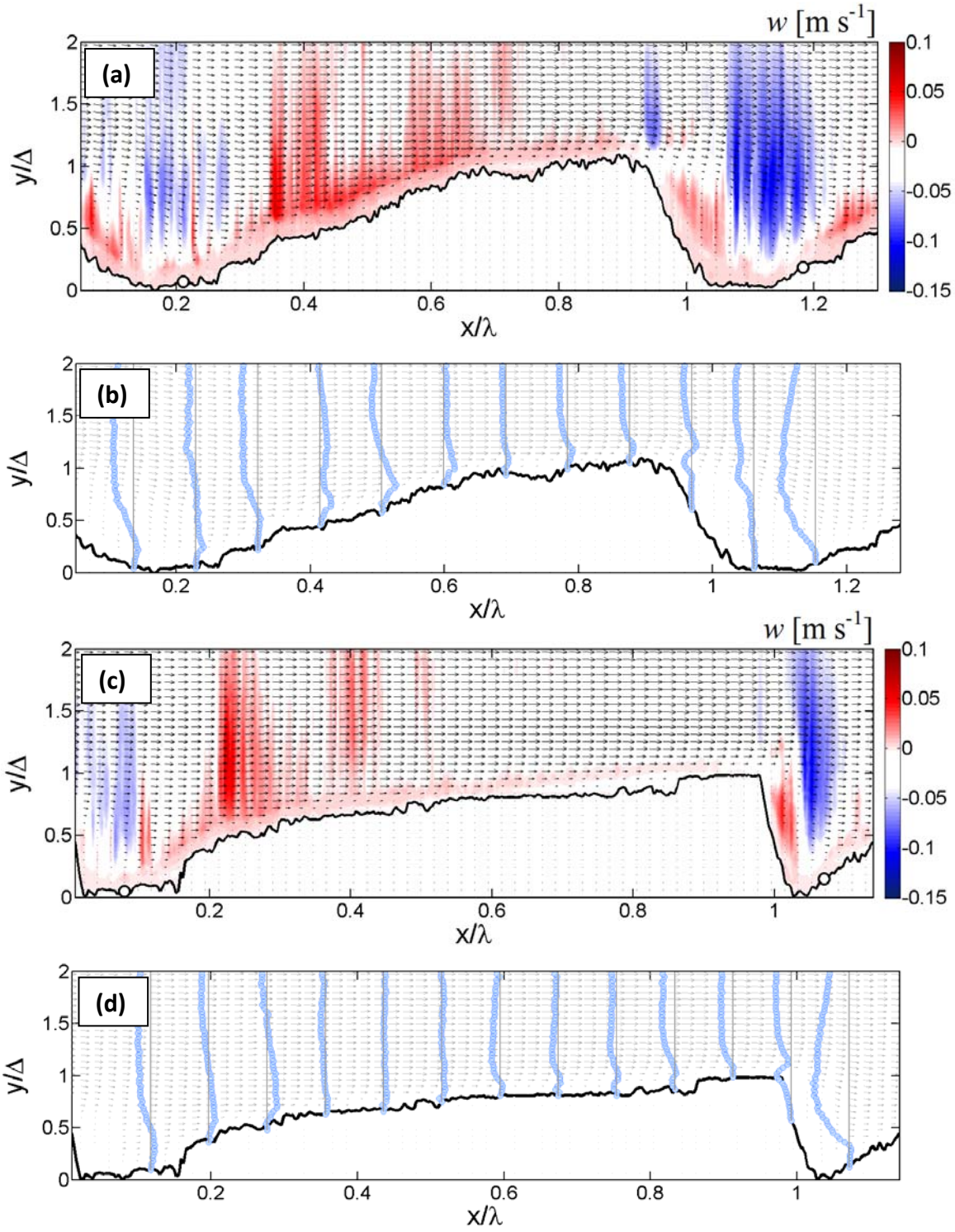

Figure 3.8 – Contour maps and selected profiles of the mean vertical flow velocity $\overline{w}$ [m s^{-1}] along dunes for EXP1 (a and b) and EXP2 (c and d). The arrows represent the mean velocity vector field $V(\overline{u}, \overline{w})$. Vertical, solid lines along the dune bed indicate the location of the velocity profiles origin with negative velocities to the left and positive velocity to the right of this line. The distance between two vertical lines scales with $\overline{w}$ = 0.5 m s^{-1}.

3.3.2 MEAN TURBULENT FIELD

The mean streamwise I_u and vertical I_w turbulent intensities for both experiments are shown in Figure 3.9 and Figure 3.10, respectively. Similar behavior of mean turbulent intensity is observed for both experiments. The contour maps show zones of high turbulence intensity behind the dune lee side and in the trough region of the dunes with maximum values occurring within and just downstream of the flow separation zone. Where high values of the mean streamwise turbulent intensities I_u are localized in the trough area of the dune, high values of vertical turbulent intensities I_w are advected towards the water surface over the midstoss side of the dune. Selected profiles of I_u (Figure 3.9b and Figure 3.9d) and I_w (Figure 3.10b and Figure 3.10d) show, behind the dune crest, peaks that illustrate the development of a wake structure and a separating shear layer. Over the entire stoss side of both dunes, I_u shows little variation and is more or less constant towards the water surface. The I_w over the stoss side of the dunes, on the other hand, is observed to increase with increasing distance from the bed. Similar to the behavior of the near-bed mean streamwise velocity profiles along the dune stoss side (see Figure 3.7), I_u and I_w profiles seem to be affected by near-bed flow and sediment processes (large sediment concentration and secondary bedforms). The magnitudes of I_u and I_w are constant and nearly zero near the bed while an increase is observed at higher distances from the bed.

Figure 3.11 shows the contour maps and selected profiles of the Reynolds shear stresses τ_{uw} along dunes. Close to the dune bed, τ_{uw} values are small and negative while positive values are observed elsewhere along the dune. Maximum values of τ_{uw} occur at, and just downstream of the reattachment zone along the separating shear layer. Towards the water surface, τ_{uw} values decrease strongly over the flow separation zone of the dunes while less variation is observed in τ_{uw} values over the stoss side of the dunes. The near-bed behavior of mean and turbulent flow evolution over mobile dunes observed in this study is significantly different from the near-bed flow evolution over fixed dunes reported in the literature. This is probably due to the presence of a dense sediment layer close to the bed and due to the effects of migrating secondary bedforms. In particular, the small and nearly constant mean streamwise flow velocity close to the bed is not observed over fixed dune measurements. In addition, the small and negative values of the Reynolds shear stresses observed close to the bed are not identified along fixed dunes. Further above the dune bed, the patterns of mean and turbulent flow evolution are consistent with observations from previous experimental and numerical studies over fixed and mobile dunes [e.g., *Bennett and Best,* 1995; *Cellino and Graf,* 2000; *Grigoriadis et al.,* 2009; *Omidyeganeh and Piomelli*, 2011; and references therein].

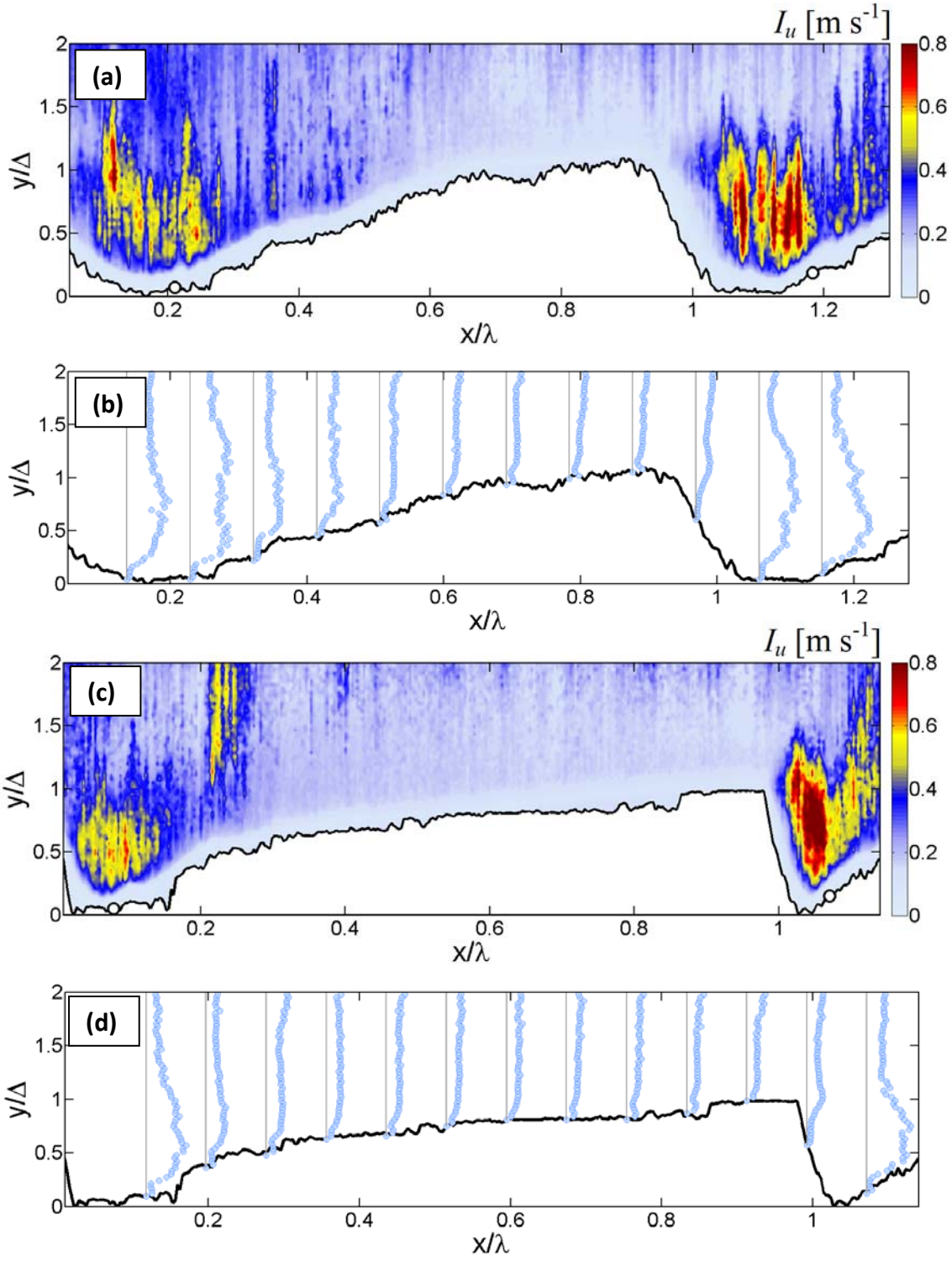

Figure 3.9 – Contour maps and selected profiles of the mean streamwise turbulent intensity I_u [m s^{-1}] along dunes for EXP1 (a and b) and EXP2 (c and d). Vertical, solid lines along the dune bed indicate the location of the profiles origin and the distance between two vertical lines scales with I_u = 0.8 m s^{-1}.

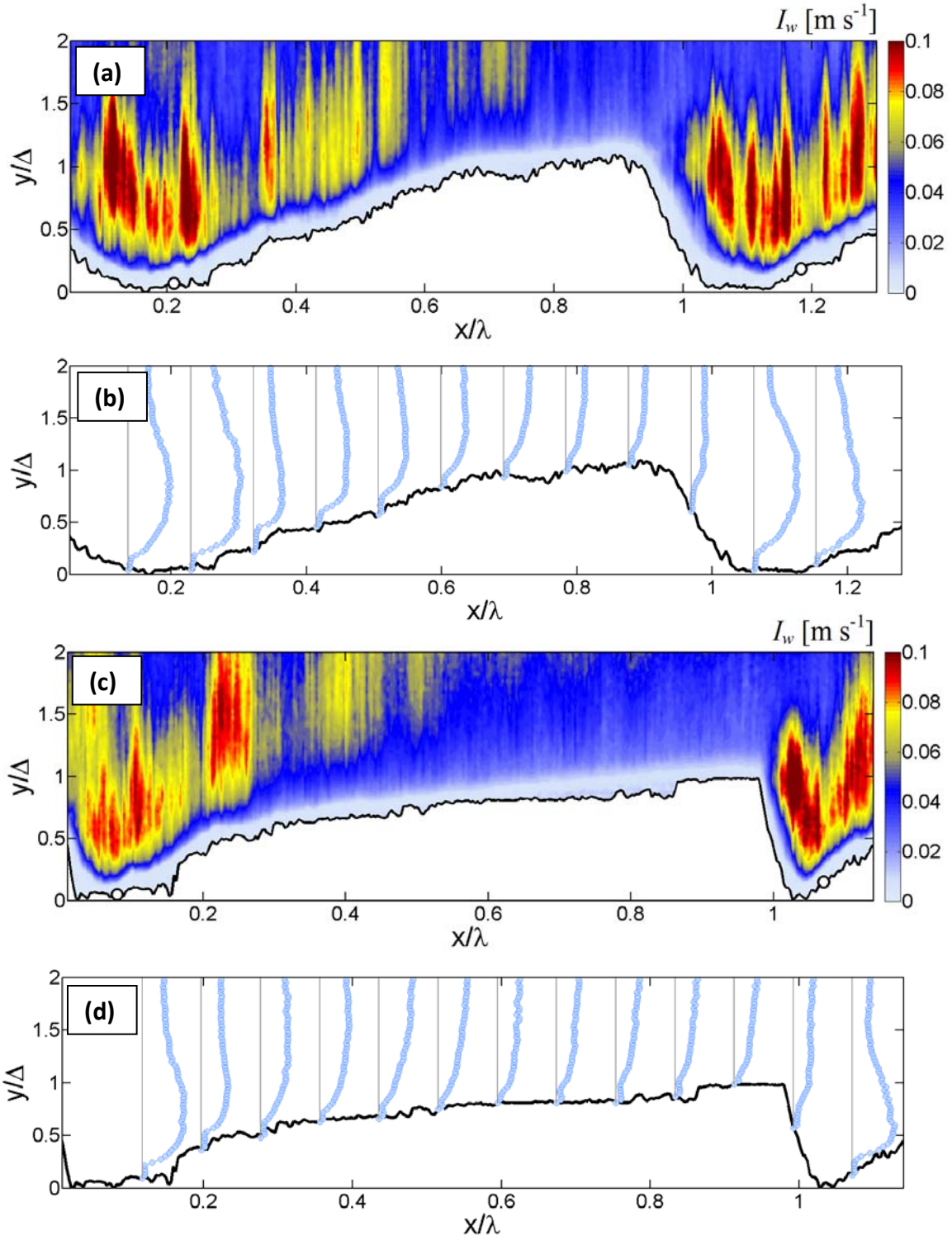

Figure 3.10 – Contour maps and selected profiles of the mean vertical turbulent intensity I_w [m s^{-1}] along dunes for EXP1 (a and b) and EXP2 (c and d). Vertical, solid lines along the dune bed indicate the location of the profiles origin and the distance between two vertical lines scales with I_w = 0.1 m s^{-1}.

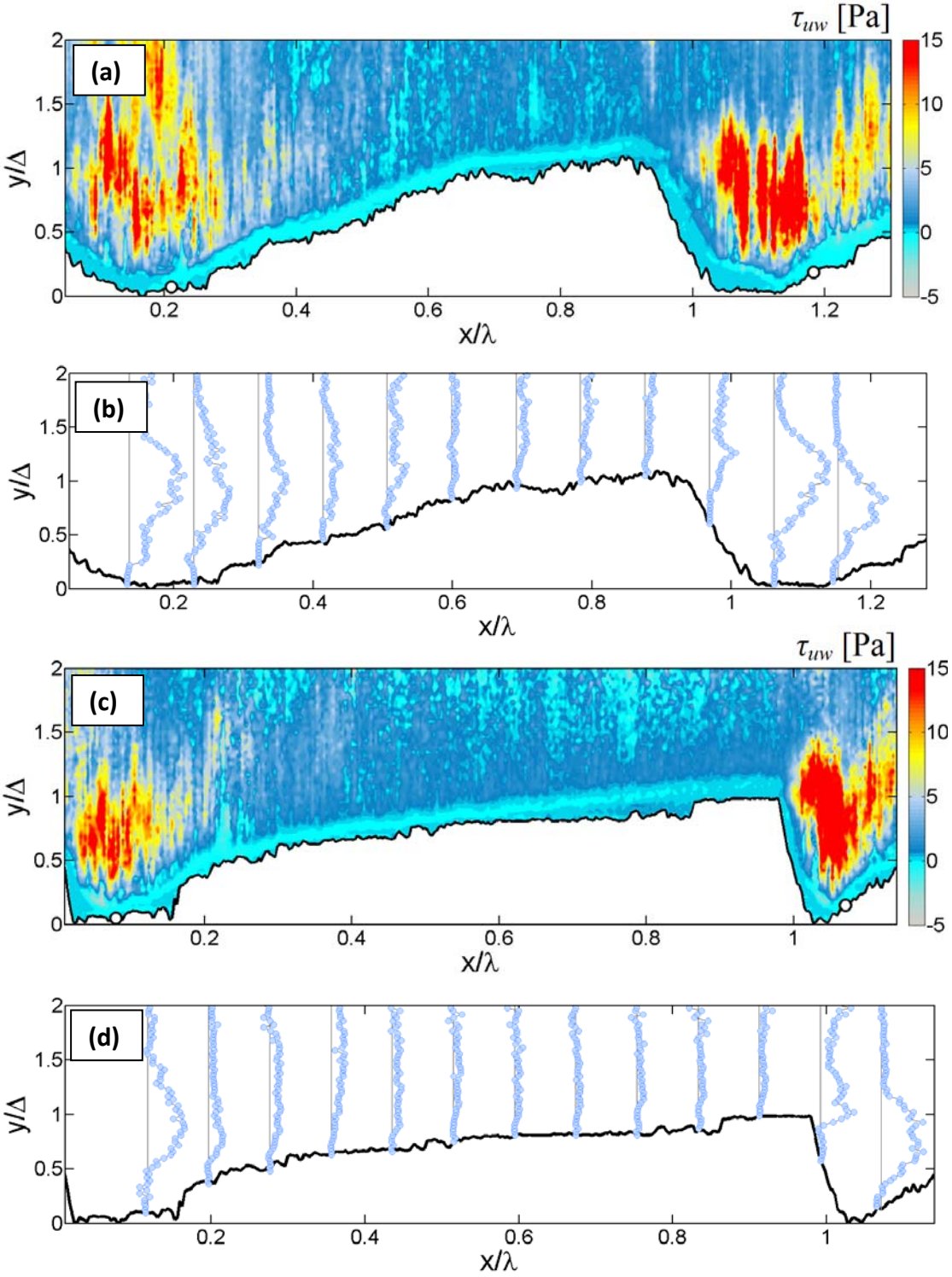

Figure 3.11 – Contour maps and selected profiles of the Reynolds shear stress τ_{uw} [Pa] along dunes for EXP1 (a and b) and EXP2 (c and d). Vertical, solid lines along the dune bed indicate the location of the profiles origin and the distance between two vertical lines scales with τ_{uw} = 15 Pa.

3.4 SEDIMENT TRANSPORT PROCESSES

3.4.1 MEAN SEDIMENT CONCENTRATION

Contour maps and selected profiles of the mean sediment concentration $log_{10}(c)$ [kg m^{-3}] along dunes for both experiments are shown in Figure 3.12. The black, dotted line represents the interface between the suspended load and the bed load layer determined by the acoustic interface detection method [*Hurther and Thorne,* 2011; *Hurther et al.,* 2011]. This interface clearly represents a concentration threshold. Typically, the concentration threshold varies between 40-60 [kg m^{-3}] which is much smaller than 212 [kg m^{-3}] used as sheet-flow layer threshold by *Dohmen-Janssen et al.* [2001]. The sediment concentration at the bed equals the bulk density $\rho_s(1-\varepsilon) = 1590$ [kg m^{-3}], where $\rho_s=2650$ [kg m^{-3}] is the sand density and $\varepsilon=0.4$ [-] is the sand porosity. The highest sediment concentration is found within the bed load layer whereas much smaller concentrations (up to one order of magnitude) are observed in the suspension layer. Similar large sediment concentration gradients above river dunes were found by *Shugar et al.* [2010], and Kostaschuk and Villard [1999] where a 10-fold decrease was found in the mean sediment concentration – relative to near-bed concentration – throughout the water column. *Johns et al.* [1990] also reported a similar concentration gradient over tidal dunes.

Typically, sediment concentration decreases with increasing distance from the bed over the entire dune and becomes very small near the water surface. The concentration profiles (Figure 3.12b and Figure 3.12d) along the dunes demonstrate that this decrease of sediment concentration towards the water surface occurs more gradually over the trough and the lee side of the dune compared to the crest and the stoss side of the dune. Due to flow deceleration and associated turbulence generation in the trough region of the dune, sediment is picked up and transported to higher distances from the bed compared to the dune crest where flow is accelerated. In addition, the magnitude and intensity of suspension peaks are largest in the trough region and decay towards the crest where turbulent energy is much lower (see Figure 3.9, Figure 3.10 and Figure 3.11). Using phase coherence wavelet analysis, *Shugar et al.* [2010] showed that streamwise flow deceleration in the dune trough is linked to the vertical flux of fluid towards the water surface in the form of large turbulent fluid ejections. They showed that regions of high suspended sediment concentration are strongly correlated with such events.

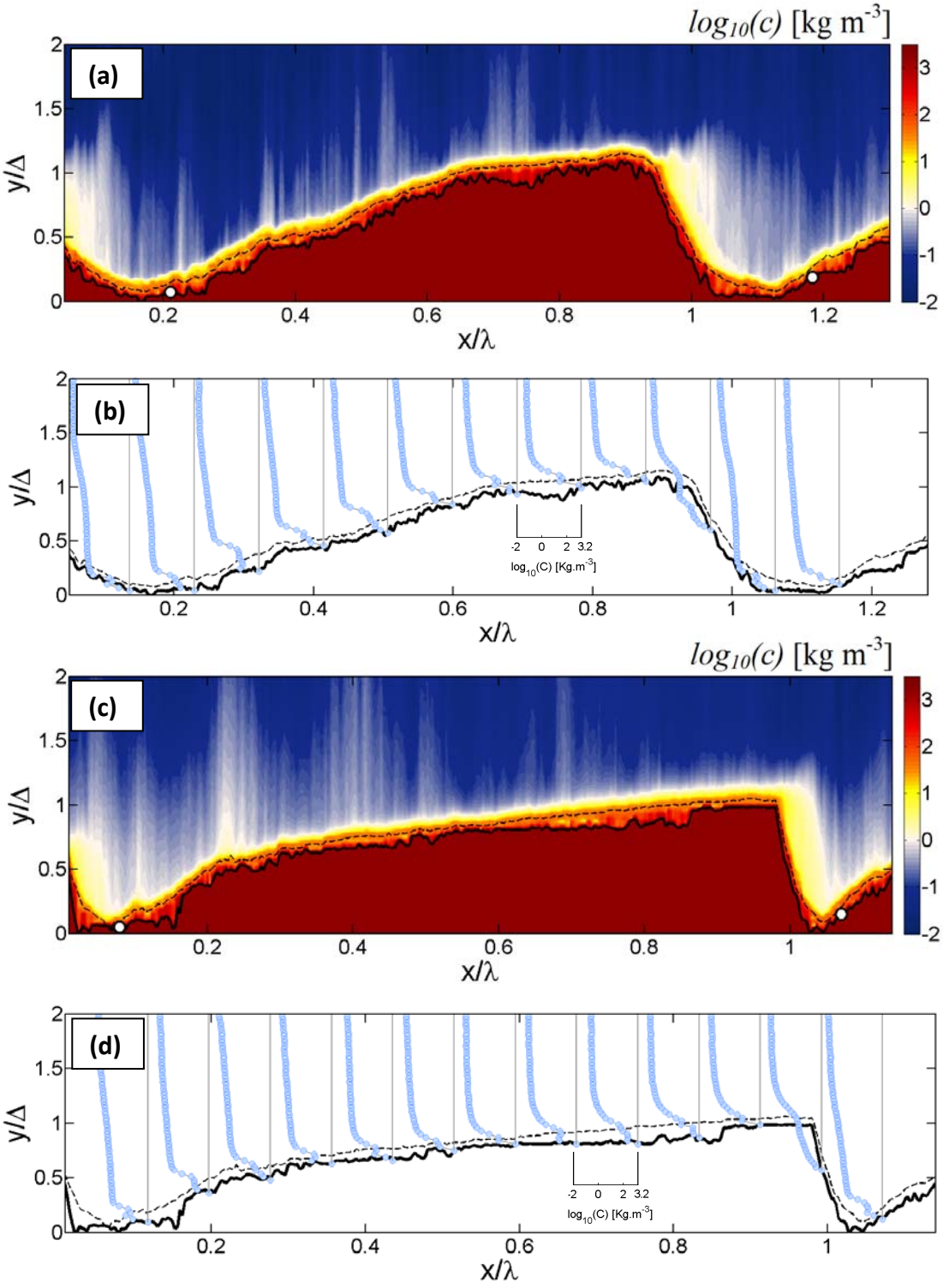

Figure 3.12 – Contour maps and selected profiles of the mean sediment concentration *log10(c)* [kg m^{-3}] along dunes for EXP1 (a and b) and EXP2 (c and d). The black, dotted line is the interface between the suspended load and the near-bed load layer determined by acoustic interface detection method. Vertical, solid lines along the dune bed indicate the location of the mean concentration profiles origin.

In the trough region of the dunes, the profiles of mean sediment concentration (Figure 3.12b and Figure 3.12d) display a 'bulging' shape which is in agreement with the theory of flow separation effects on the suspended sediment distribution [e.g. *Zyserman and Fredsøe*, 1994; *Carling et al.,* 2000]. Close to the bed and mainly within the bed load layer, the concentration profiles display a linear decreasing trend with increasing distance from the bed.

The patterns of mean sediment concentration discussed above are consistent for both experiments. Due to larger flow strength and thus larger bed shear stresses (see Table 3.1), sediment concentration is generally higher for EXP2. For EXP2, the high sediment concentration persists over a larger distance downstream from the dune crest and the vertical decrease of sediment concentration towards the water surface occurs more gradually. The intensity and the number of suspension peaks were also greater for this experiment.

3.4.2 MEAN SEDIMENT FLUXES

The contour maps and selected profiles of the mean streamwise sediment flux $\overline{cu}$ for both experiments are shown in Figure 3.13. The fluxes are largest close to the bed and decrease with distance towards the water surface. On the stoss side of the dune in the bed load layer, $\overline{cu}$ is positive and increases towards the dune crest due to flow acceleration and the associated increase in the bed shear stresses. At a further distance from the bed and above the dune trough, $\overline{cu}$ displays local peaks that decay towards the dune stoss side. These peaks are related to the turbulence generation due to the developing shear layer. On the lee side of the dune and mainly in the flow separation region close to the bed, sediment is transported in the opposite direction towards the dune crest while at higher distance from the bed a positive sediment flux is observed. Although most of the sediment that is transported over the stoss side of the dune remains in the same dune by deposition on the lee side and in the trough of the dune thus contributing to dune migration, a significant amount of sediment in suspension is advected towards the following dune (positive transport rates downstream of the flow reattachment points indicated in Figure 3.13). This fraction of the sediment that is not captured into the dune forms, also termed the bypass fraction, is important for the prediction of dune migration and dune behavior [*Mohrig and Smith,* 1996].

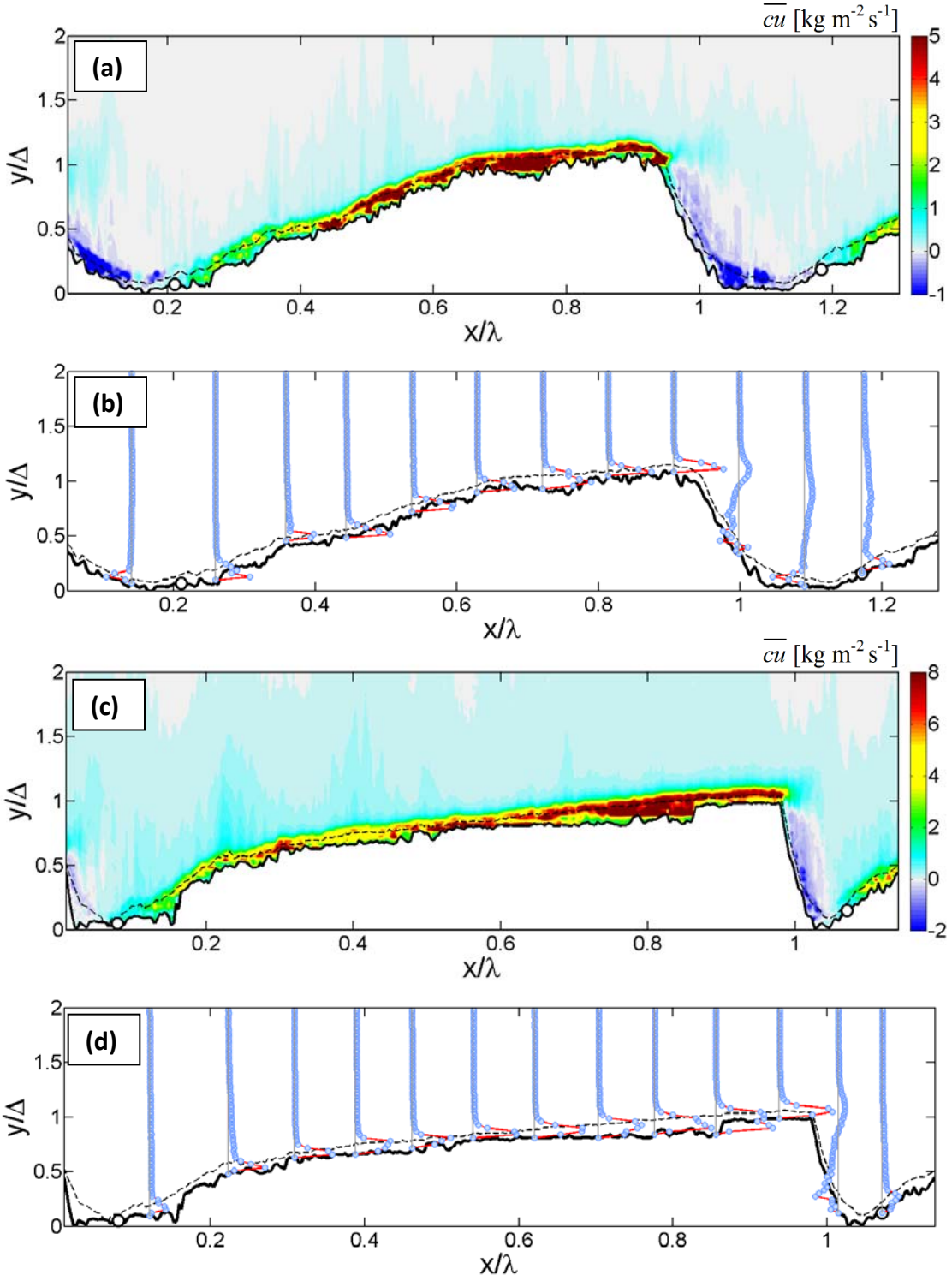

Figure 3.13 – Contour maps and selected profiles of the mean streamwise $\overline{cu}$ sediment fluxes [kg m^{-2} s^{-1}] along dunes for EXP1(a and b) and EXP2 (c and d). Vertical, solid lines along the dune bed indicate the location of the profiles origin and the distance between two vertical lines scales with $\overline{cu}$ = 8 [kg m^{-2} s^{-1}]. The open circles in the dune bed indicate the flow reattachment points.

Contour maps and profiles of the mean vertical sediment flux $\overline{cw}$ (Figure 3.14) show that the largest values are close to the bed and that they drastically decrease with increasing distance from the bed. Positive (upward) sediment fluxes are observed over the entire dune with large peaks on the stoss side of the dune downstream of the flow reattachment point, reflecting the pick-up of sediment. These peaks result from the shear layer vortices that impact the dune bed, generating turbulent sediment bursts that are absent elsewhere. Negative (downward) sediment fluxes are observed on the stoss side of the dune and over the dune crest in the dune lee side, with the largest values over the dune crest and dune lee side reflecting sediment deposition in these locations. In addition, in the dune trough close to the bed, upward vertical fluxes are coupled with small downward fluxes further from the bed, illustrating the turbulent behavior of the flow in the flow separation zone. Although sediment is deposited over the entire dune profile, the dune is migrating and thus the effect of the mean streamwise sediment fluxes $\overline{cu}$ are much larger than the effect of the mean vertical sediment fluxes $\overline{cw}$. This is reflected in the values of $\overline{cu}$ being an order of magnitude larger than $\overline{cw}$ (Figure 3.13 and Figure 3.14).

3.4.3 MEAN BED AND SUSPENDED LOAD TRANSPORT

Sediment transport rate T [kg m^{-1} s^{-1}] is calculated from the integration of the streamwise flux profiles over depth z.

$$T = \int_{z=a}^{z=b} \overline{cu}\, dz \tag{3.4}$$

For the total load transport T_{tot}, the integration boundaries a and b are the non-moving bed and the water surface, respectively. For the bed load transport T_{bed} the boundaries a and b are the non-moving bed and the interface between bed and suspended load transport determined from the acoustic interface detection method, respectively. For the suspended load transport T_{susp}, the integration boundaries are the interface position and the water surface. The total, the suspended and the bed load transport distribution along migrating dunes for both experiments are shown in Figure 3.15.

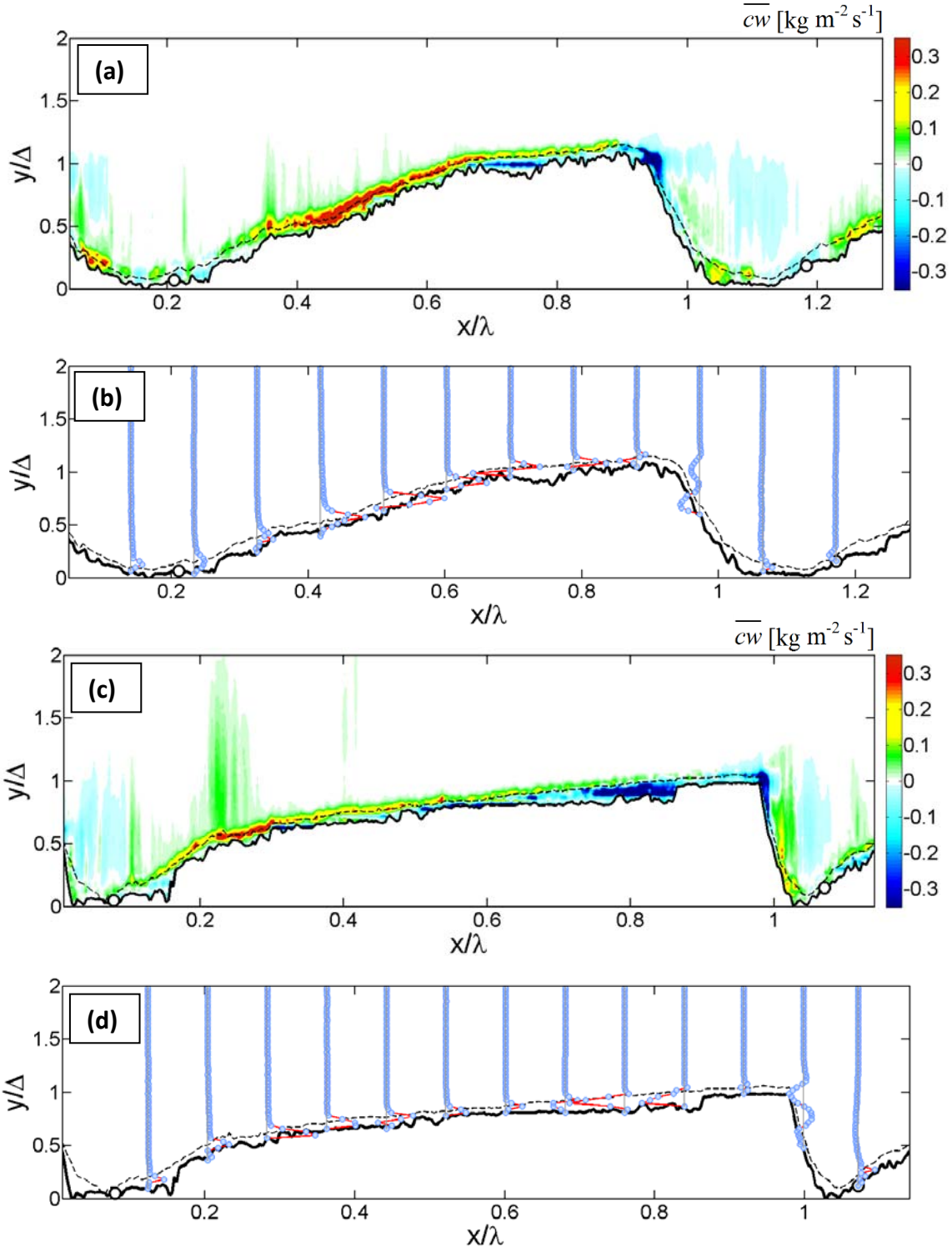

Figure 3.14 – Contour maps and selected profiles of the mean vertical $\overline{cw}$ sediment fluxes [kg m^{-2} s^{-1}] along dunes for EXP1 (a and b) and EXP2 (c and d). Vertical, solid lines along the dune bed indicate the location of the profiles origin and the distance between vertical lines scales with $\overline{cw}$ = 0.35 [kg m^{-2} s^{-1}].

For migrating dunes in equilibrium, the measured total sediment transport (Figure 3.15a and Figure 3.15d) follows more or less the dune shape with increasing transport towards the dune crest, deposition at the lee and trough side of the dune, and negative sediment transport within the flow reattachment zone. Although the bed and the suspended load transport are of the same order of magnitude, the shape of the total sediment transport distribution along dunes is dominated by the bed load transport (Figure 3.15b and Figure 3.15e). Where the bed load transport displays a small, positive gradient over the entire stoss side of the dune towards the dune crest, the suspended load transport (Figure 3.15c and Figure 3.15f) mainly increases over a small distance on the stoss side of the dune and remains nearly constant towards the dune crest. This means that the bed load transport is more effective in dune migration, that is erosion on the stoss side and deposition on the lee side of the dune. The high variability observed in the bed load transport is caused by the irregularities in the bed due to secondary bedforms on the stoss side of the dune that are migrating towards the dune crest (see also *Carling et al.* [2000], and references therein).

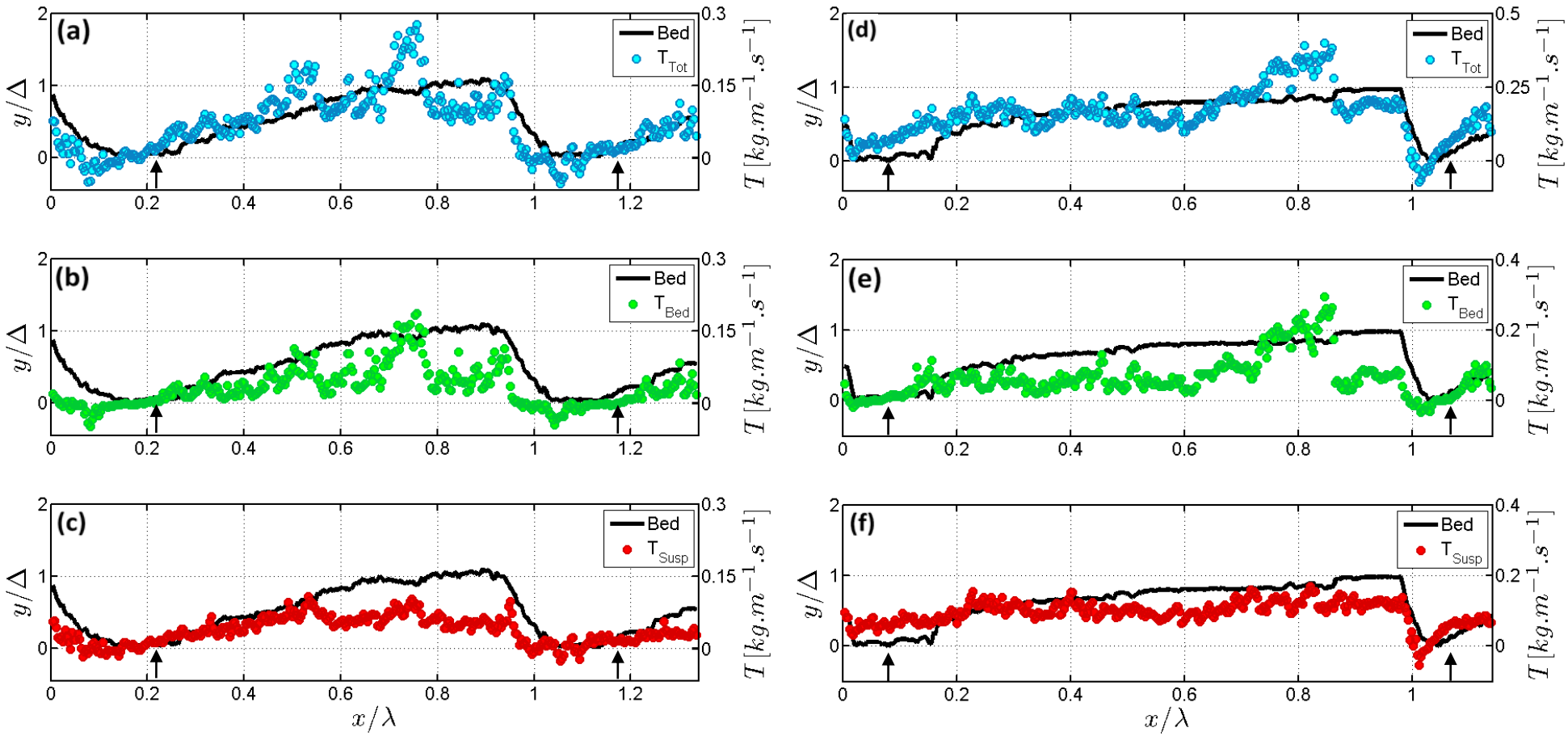

Figure 3.15 – Total T_{tot}, bed T_{bed} and suspended T_{susp} load transport distribution along dunes for EXP1 (a, b, c) and EXP2 (d, e, f). The vertical arrows indicate the position of the flow reattachment points.

Figure 3.16 shows the bed and the suspended load transport distribution in the trough of the dunes. The dashed, vertical lines indicate the brinkpoint position and the position of the flow reattachment point. Whereas the dune crest is the highest point at the dune, the dune brinkpoint is where bed load avalanching begins and produces a straight lee face depositional slope. The sediment avalanching process is clearly observed from the immediate decay of the bed load transport while approaching the dune lee side. The suspended load is advected a little further downstream and is more gradually deposited on the lee side and in the trough of the dune. At the flow reattachment points the total sediment transport is positive (see arrows in Figure 3.15) and equal to the transport of suspended sediment as the bed load transport is practically zero at these locations. This part of the suspended load is neither deposited on the dune lee side nor in the dune trough and therefore does not contribute to dune migration. The bypass fraction is thus the suspended load transport at the flow reattachment point relative to the total sediment transport (bed load + suspended load) arriving at the dune crest. For EXP1 the bypass fraction is about 10% and for EXP2 the bypass fraction is about 27%. This increase in the bypass fraction can be explained by the relative increase in the mean streamwise flow velocity from EXP1 to EXP2. If compared to the suspended sediment transport arriving at the dune crest, for EXP1 the bypass fraction is 16% and for EXP2 39%. This clearly shows that a substantial part of the suspended load transport is not captured in the dune form and thus does not contribute to dune migration, whereas the entire bed load transport arriving at the dune crest avalanches on the dune lee side and takes part in dune migration. Contrary to *Mohrig and Smith* [1996] who use the horizontal lee side distance (slip face distance) for the calculation of the bypass fraction, assuming that all the sediment that is deposited at further distance downstream than the horizontal slip face distance does not contribute to dune migration, we argue that sediment particles with greater excursion lengths than the slip face distance but smaller excursion lengths than the flow separation length still contribute to dune migration as these particles are transported towards the dune lee side (negative transport rates in the dune trough, see Figure 3.16). Therefore, under same flow conditions, the bypass fraction calculated using the model of *Mohrig and Smith* [1996] will result in an overestimation of the actual sediment fraction that is not contributing to dune migration, compared to our results. However, it should be noticed that the dunes observed in the field have much smaller lee side slopes (low-angle dunes) that results in a zone of highly intermittent or non-existent flow reversal [e.g., *Best*, 2005a; *Shugar et al.,* 2010; *Bradley et al.,* 2013]. Therefore, sediment particles with greater excursion lengths than the slip face distance might not be transported back towards the dune lee side and thus not contribute to dune migration.

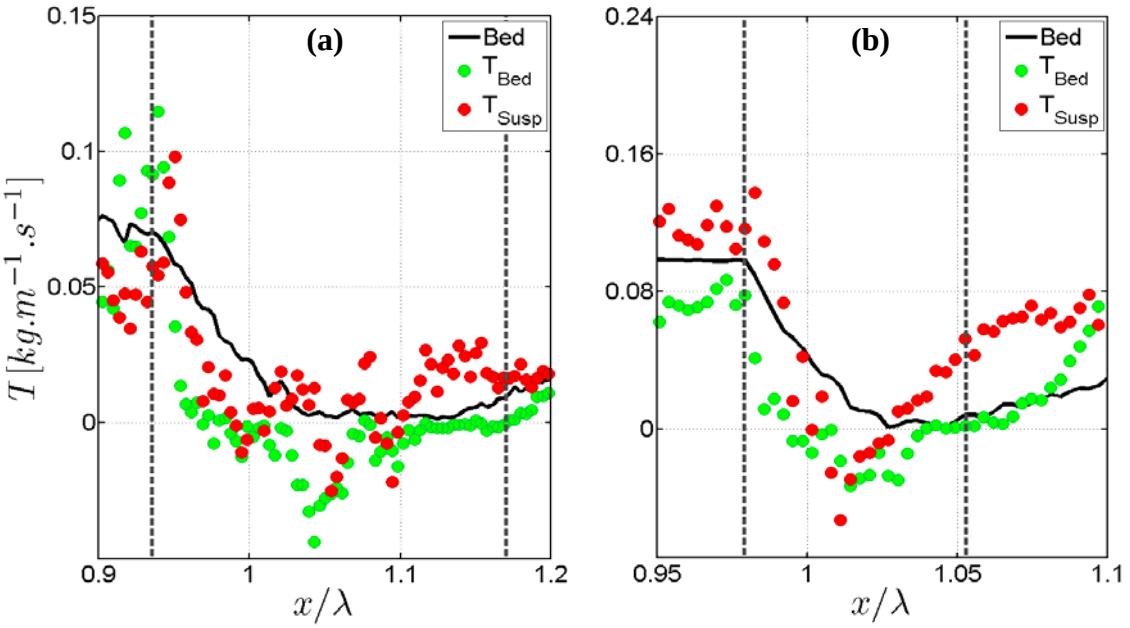

Figure 3.16 – Enlarged lee side of the dunes for EXP1 (a) and EXP2 (b) showing the bed and the suspended load transport distribution. The black solid line is the dune bed where the dashed lines indicate the brinkpoint position (left) and the flow reattachment point (right).

3.5 DISCUSSION AND RECOMMENDATIONS

The present study has focused on the details of flow and sediment dynamics along mobile, migrating sand dunes in equilibrium. In particular, the distribution of sediment transport along dunes and the contributions of both bed and suspended load to dune morphology and migration were investigated. Measurements were carried out using the ACVP during a series of mobile bed experiments. The experiments illustrated that, due to the presence of a dense sediment layer close to the bed and migrating secondary bedforms over the stoss side of the dune towards the dune crest, the near-bed flow and sediment processes are significantly different from the near-bed flow and sediment dynamics measured over fixed dunes.

Application of an interface detection method revealed the distribution of the bed load and the suspended load transport along migrating dunes. It was observed that the bed load was entirely captured in the dune with zero transport at the flow reattachment point, while a significant part of the suspended load was advected to the downstream dune depending on the flow conditions. The bypassed suspended sediment probably plays an important role during the transition of dunes to upper stage plane beds where dunes are flattened and eventually washed out [e.g., *Naqshband et al.,* 2014]. Therefore, further research is needed on the quantification of this fraction during the dune transitional stages under non-equilibrium flow conditions.

The bypass fraction can be compared to the following sediment transport balance. The mass of sand (per unit channel width) transported by the flow over an entire dune length M_{flow}, calculated from Figure 3.15a and Figure 3.15d using equation (3.5), is 215.9 [kg m^{-1}] for EXP1 and 504.8 [kg m^{-1}] for EXP2. The integration boundaries *a* and *b* in this equation are the non-moving bed and the water surface, respectively. The dune period is represented by the ratio of dune length λ_e to dune migration speed C_e.

$$M_{flow} = \frac{\lambda_e}{C_e} \int_{z=a}^{z=b} \overline{cu}\, dz \tag{3.5}$$

The sand mass M_{flow} is compared to the sand mass derived from the dune shape measurement M_{shape} using equation (3.6). Here, *z(x)* is the non-moving bed height along the streamwise dune position with *z=0* at the dune trough, ρ_s*=2650* [kg m^{-3}] is the sand density and ε*=0.4* [-] is the sand porosity (see Figure 3.15a and Figure 3.15d).

$$M_{shape} = \rho_s \left(1-\varepsilon\right) \int_{x=0}^{x=\lambda_e} z\left(x\right) dx \tag{3.6}$$

For EXP1, M_{shape} equals to 185.5 [kg m^{-1}] and for EXP2, M_{shape} is 377.3 [kg m^{-1}]. The difference between the two calculated sand masses (M_{flow} and M_{shape}) is 16% for EXP1 and 34% for EXP2 which is in good agreement with the bypass fractions calculated from the relative difference in sediment transport at the flow reattachment point and at the dune crest (see section 3.4.3).

Another aspect of measuring sediment fluxes that is not treated in this study, is the relative importance of turbulent fluxes to the total sediment fluxes along migrating dunes. Using two separate instruments for the measurement of flow velocity and sediment concentration limits sediment flux studies to flow scales larger than the separation distance between the two instruments. In addition, the measured sediment fluxes cannot be referenced to an exact location along the dune bed. The ACVP, on the other hand, provides direct flux measurements referenced to the exact location at the bed. As a result, both the mean and the turbulent part of sediment fluxes are addressed. The turbulent part of sediment fluxes might be dominant in the flow separation zones where turbulence is generated. This aspect will be addressed in future work.

Other important direction for future research is linking the results of this study to complex numerical models that describe the development and migration of dunes [e.g., *Nabi et al.,* 2010]. In particular, the near-bed flow behavior above migrating dunes observed in this study should be well reproduced by numerical models. In addition, the new insights obtained in this research on the distribution of bed load and suspended load can be used as reference for modeling sediment transport. However, it should be noticed that the results of this study are strongly related to 2D dune topography in a laboratory flume. Future research is needed to investigate whether these findings are consistent for field conditions with a strong 3D dune topography.

3.6 CONCLUSIONS

The present study has provided new insights in the flow and sediment dynamics over migrating dunes in equilibrium. The main findings of this study are summarized below:

1. A dense sediment layer close to the bed and migrating secondary bedforms over the stoss side of the dune towards the dune crest result in near-bed flow and sediment processes that are significantly different from the near-bed flow and sediment dynamics measured over fixed dunes. In particular, the near-bed mean streamwise velocity above mobile beds deviates from the logarithmic profile often observed above plane or fixed dune beds. The near-bed concentration profiles above mobile beds also deviate from the near-bed concentration profiles observed above fixed dunes, displaying a linear decreasing trend with increasing distance from the bed.

2. The pattern of the total sediment transport distribution along dunes is dominated by the bed load transport although the bed load and the suspended load transport are of the same order of magnitude. This implies that bed load transport is responsible for the continuous erosion and deposition of sediment along the migrating dunes.

3. The bed load distribution at the lee side of the dunes decays rapidly because of sediment avalanching on the dune slip face. The suspended load transport, on the other hand, is advected further downstream and is more gradually deposited on the lee side and in the trough of the dune.

4. Whereas the bed load is entirely captured in the dune with zero transport at the flow reattachment point, a significant part of the suspended load is advected to the downstream dune depending on the flow conditions. For the two flow conditions measured, the bypass fraction was about 10% for flow with $Fr = 0.41$ and 27% for flow with $Fr = 0.51$. This means that respectively 90% (for the $Fr = 0.41$ flow) and 73% (for the $Fr = 0.51$ flow) of the total sediment load that arrived at the dune crests contributed to the migration of the dunes.

CHAPTER 4 – CONTRIBUTIONS OF TURBULENT AND ADVECTIVE SEDIMENT FLUXES TO THE TOTAL SEDIMENT FLUXES ALONG DUNES*

ABSTRACT

In this chapter, we present direct measurements of sediment fluxes along migrating sand dunes in equilibrium. Using a novel acoustic flow instrumentation recently developed within the European project Hydralab 4-WISE, we are able to investigate the contribution of turbulent bed and suspended sediment fluxes to the total sediment fluxes along the entire dune profile, and over the full flow depth. Our measurements showed that, over the stoss side of the dune and in the bed load layer, the turbulent mean streamwise flux $\overline{c'u'}$ is negative and reaches up to 40% of the total mean streamwise flux $\overline{cu}$. Over the lee side of the dune, where turbulent intensities are highest, the contribution of $\overline{c'u'}$ to $\overline{cu}$ is larger and reaches up to 50%. The mean vertical turbulent flux $\overline{c'w'}$, along the entire dune bed and in the bed load layer, reaches nearly 30% of the total mean vertical flux $\overline{cw}$.

* This chapter is based on a paper that is currently in press as: Naqshband, S., Ribberink, J., Hurther, D., Barraud, P.A. & S.J.M.H. Hulscher (in press). Experimental evidence for turbulent sediment flux constituting a large portion of total sediment flux along migrating sand dunes. *Geophysical Research Letters,* DOI: 10.1002/2014GL062322.

4.1 INTRODUCTION

Dunes are rhythmic features observed at a variety of spatial-temporal scales and are of central importance for many water management purposes. River dunes result from the interaction between flow and sediment transport and exert a significant influence on the nature of turbulent flow, which in turn controls the processes of sediment transport, sediment pick-up, and deposition [*Best*, 1996]. Quantification of the morphology and behavior of dunes necessarily require the consideration of complex interaction mechanisms between turbulent flow, dune form and sediment transport [*Parsons and Best*, 2013].

Dune related studies in the past have mainly focused on the measurement of the mean advective sediment flux distribution along dune beds while the turbulent sediment flux components have received much less attention. Although due the turbulent nature of the flow associated with dunes, it is likely that turbulent sediment fluxes may have a significant contribution to the total sediment fluxes, their exact distribution along the dune bed and their contribution to dune migration are poorly understood mainly due to the difficulties of measuring them quantitively. This gap of knowledge is partly attributed to the fact that a majority of the experimental studies associated with dunes have focused on flow and sediment dynamics above fixed beds [e.g., *Van Mierlo and de Ruiter*, 1988; *Lyn*, 1993; *Nelson et al.*, 2003; *McLean et al.*, 1999; Cellino *and Graf*, 2000; *Best and Kostaschuk,* 2002; *Maddux et al.*, 2003; *Kleinhans*, 2004; *Best*, 2005a,b; *Venditti*, 2007].

Another important reason why the contribution of turbulent sediment fluxes to the total sediment fluxes have not been fully determined is that there are inherent limitations of the flow instruments for providing the simultaneous and co-located measurement of both multi-component flow velocity and sediment concentration, mainly in the near-bed region [see *Naqshband et al.,* 2014b and references therein]. Therefore, a majority of sediment transport studies above mobile dune beds have been limited to the indirect measurements of sediment fluxes deploying two separate instruments to measure the flow velocity and sediment concentration at different positions in the flow [e.g., *Parsons et al.,* 2005; *McLean et al.,* 2008; *Wren et al.,* 2007; *Coleman et al.,* 2008; *Wren and Kuhnle*, 2008; *Kostaschuk et al.,* 2009; *Shugar et al.,* 2010]. As a result, the sediment flux studies are limited to turbulent flow scales larger than the separation distance between the two instruments which is usually greater than the largest turbulent flow scales. In particular, smaller scale turbulence processes, which are important mechanisms of sediment entrainment and transport, cannot be addressed directly.

By using an Acoustic Doppler Velocimeter (ADV), *Nikora and Goring* [2002] quantified several statistical quantities from point-wise measurements of sediment concentration fluctuations and turbulent sediment fluxes along a flat channel bed. More recently, *Sassi et al.* [2013] succeeded to obtain turbulent sediment fluxes in the tidal River Mahakam by measuring turbulent flow and sediment quantities simultaneously in the same sampling volume. For this purpose they used coupled Acoustic Doppler Current Profilers (ADCPs) [see also *Kostaschuk et al.,* 2009; *Shugar et al.* 2010]. Because the ADCPs use separate diverging acoustic beam working in a multi-monostatic configuration, it is impossible to determine co-located turbulent flow and sediment quantities. This technical aspect is particularly limiting for measurements close to the bed where the separation distance between the different (monostatic) beams can reach several meters. This hinders the use of ADCP technology to fully resolve the flow velocity in the lee side separation/deceleration zone of the dune due to the strong spatial non-uniformity of the flow in this nearbed region [e.g., *Kostaschuk et al.,* 2004; *Parsons et al.,* 2005; *Shugar et al.,* 2010].

A newly developed acoustic system, the Acoustic Concentration and Velocity Profiler (ACVP) developed by *Hurther et al.* [2011], allows us to measure simultaneous and co-located vertical profiles of 1D2C flow velocity (u,w) and sediment concentration (c) referenced to the acoustically measured position of the flow bed. The spatio-temporal resolution of the ACVP technology is sufficiently high to resolve small turbulent flow scales as previously shown by *Mignot et al.* [2009] and *Hurther and Thorne* [2011]. From the high rate profiling of the streamwise u and the vertical w velocity components and the co-located sediment concentration c, the direct measurements of the total mean sediment fluxes $\overline{cu}$ and $\overline{cw}$ are obtained (see equations 4.1 and 4.2). Applying a Reynolds decomposition to all measured variables, the mean advective (or current related) fluxes $\bar{c}\bar{u}$ and $\bar{c}\bar{w}$, and the mean turbulent fluxes $\overline{c'u'}$ and $\overline{c'w'}$ can be evaluated in the streamwise and vertical directions, respectively.

$$\overline{cu} = \bar{c}\bar{u} + \overline{c'u'} \tag{4.1}$$

$$\overline{cw} = \bar{c}\bar{w} + \overline{c'w'} \tag{4.2}$$

Another novelty of the ACVP technology is its capacity to profile these sediment fluxes across both the bed load layer and the suspension load layer (see section 4.2 for more details on the ACVP). Recently, the ACVP has been successfully applied under waves

[*Hurther and Thorne,* 2011; *Chassagneux and Hurther,* 2014] and in flume experiments above migrating sand dunes, where the distribution and contribution of both bed load and suspended load to dune migration were investigated [*Naqshband et al.,* 2014b]. By deploying the ACVP in the present study, we are able to measure – for the first time – the contribution of the turbulent sediment flux to the total sediment flux along the dune profile and over the entire water column. Beyond a better understanding of the physical interaction processes between the flow and the transported sediments, these insights can be used for validation of complex numerical models that predict the turbulent flow and sediment concentration above bed forms [e.g., *Nabi et al.,* 2013]. Moreover, such unique high-resolution data are useful for the improvement – via calibration – of engineering codes modeling sediment transport.

4.2 FLUME EXPERIMENTS AND INSTRUMENTATION

The flume experiments were conducted in the Hydraulics Laboratory of the Leichtweiss institute of the Technical University of Braunschweig (LWI), Germany. Below the experimental set-up and experimental conditions are outlined briefly followed by a description of the deployed instruments. For a more detailed description of the experimental work reference is made to chapter 3.

The flume has a width of 0.5 m and a length of 30 m, where the effective measuring length for dune morphology was approximately 8 m. The flume slope and the weir at the end of the flume were adjustable, which made it possible to achieve equilibrium flow conditions. A sand layer approximately 25 cm thick was installed over the entire length of the flume and flattened at the beginning of each experiment. For each experiment, the water discharge and water depth were predefined. The flume was slowly filled with water from both the downstream and upstream end of the flume to make sure the bed was not disturbed. Subsequently, the predefined discharge was set and the required water depth was obtained by adjusting the flume slope and the weir level at the downstream end of the flume. Starting from plane beds, ripples appeared instantaneously as the flow was introduced in the flume. Dunes subsequently developed and finally a steady-state condition was obtained where the dunes migrated through the flume with a constant speed and without significantly changing their shape. This dynamic equilibrium was verified by analyzing dune height and length statistics from the measured bed profiles using the bedform tracking tool of *Van der Mark et al.* [2008]. The dynamic dune equilibrium was reached after approximately 150 minutes with an equilibrium dune height Δ_e of 0.082 and equilibrium dune length λ_e of 2.25 m.

Table 3.1 in chapter 3 gives an overview of the flow, sediment and bed conditions for the conducted experiment (EXP1).

To study the contributions of the turbulent sediment fluxes to the total sediment fluxes along dunes, profiles of flow velocity and sediment concentration were measured using the ACVP. Measurements with the ACVP started as soon as equilibrium flow condition was obtained and the dunes were in dynamic equilibrium. The carriage with the ACVP was placed at a fixed position along the flume and the dunes migrated underneath the carriage at a constant speed. One dune length was typically covered within 1 h of ACVP measurement. An averaging period of 10 s was chosen for the ACVP measurements so that bed displacement within this period was negligibly small compared to the dune length. This results in a maximum bed displacement of 0.7 cm for a dune length of 2.25 m. In addition, this averaging period of 10 s was chosen to encompass both the short-term turbulent events (small burst and sweeps) and relatively long-term turbulent events (larger energy-carrying structures: vortices and eddies).

For a proper functioning of the ACVP, the set of ACVP sensors must be submerged totally in the flow. As the water depth in the experiments was limited (25 cm), this necessity would reduce the measurement height above the bed significantly. In addition, due to its dimensions, the ACVP would induce flow and bed shape perturbations. To avoid this, a partly enclosed PVC box was constructed and filled with water to produce negative pressure in the box. The ACVP was fixed in this box and located just below the water surface enabling the measurement of flow velocity and sediment concentration over nearly the entire flow depth.

The ACVP technology combines an Acoustic Doppler Velocity Profiler (ADVP) [*Hurther and Lemmin,* 2001, Mignot et al. 2009] with a multi-frequency Acoustic Backscatter System (ABS) [e.g., *Thorne and Hanes,* 2002] into a single measuring tool enabling the direct measurement of sediment fluxes in the suspension layer and in the bed load layer. The major advantage of this single system is that it provides bed referenced, simultaneous, co-located profile measurements of two-component flow velocity and sediment concentration at high temporal (25 Hz) and spatial resolution (±1.5 mm). Sediment concentration profiles are determined by applying the dual-frequency inversion method proposed by [Hurther et al. 2011]. Compared to the well-known implicit iterative [*Thorne et al*., 1993] and the explicit inversions [*Lee and Hanes*, 1995], this method offers the unique advantage of being unaffected by the non-linear sediment attenuation effect induced by the high sediment concentration in the

nearbed region. The Acoustic Bed Interface Tracking (ABIT) method of [Hurther and Thorne 2011] is applied to determine the vertical positions of the flow bed and the interface between the suspended load and the bed load. This technique relies on the distinction, in the backscattered intensity profile, of the non-moving bed echo characterized by its immobility from the echo of the moving sediments. The suspension interface corresponds to the position of maximal suspension concentration. These two near-bed echoes can be separated when the acoustic intensity profile is derived from the demodulated Doppler signals instead of using the frequency modulated acoustic signal in the MHz range with standard ABS technologies. This results in the time evolution of the non-moving sand bed, the overlaying high sediment concentration layer (the bed load layer) and the suspended load layer. Combining the interface detection method with the sediment flux profiling ability, the bed load and the suspension load sediment transport can be evaluated along the dune profile.

The ACVP data presented in the following section correspond to the period of time needed for the migration of at least one entire dune length beneath the ACVP. As the dune migration speed in equilibrium C_e is nearly constant, multiplying the measured time by the migration speed converts time into streamwise distance x along the dune. Furthermore, the horizontal x and vertical z axes are made dimensionless using the measured dune length and height, respectively.

4.3 RESULTS

4.3.1 MEAN STREAMWISE SEDIMENT FLUXES

Contour maps and selected profiles of the total mean streamwise sediment flux $\overline{cu}$, mean advective flux $\overline{c}\,\overline{u}$ and mean turbulent flux $\overline{c'u'}$ along the dune bed are shown in Figure 4.1 and Figure 4.2. The mean position of the dune bed is the solid black line and the mean flow direction is from left to right. The flow reattachment points on the dune bed are indicated with open circles. Irregularities in the dune topography are due to the presence of small, mobile secondary bedforms that migrate on the stoss side of the main dune towards its crest. The black, dotted line represents the interface between the suspended load and the bed load layer obtained with the ABIT method explained in section 4.2. This interface represents a concentration threshold that varies between 40 to 60 kg m^{-3} [for details see *Naqshband et al.*, 2014b].

The total mean sediment flux $\overline{cu}$ (Figure 4.1a and Figure 4.2a) is largest close to the bed and decreases with distance towards the water surface. On the stoss side of the dune in the bed load layer, $\overline{cu}$ is positive and increases towards the dune crest due to flow acceleration and the associated increase in the bed shear stresses. At a further distance from the bed and above the dune trough, $\overline{cu}$ displays local peaks that decay towards the dune stoss side. On the lee side of the dune and mainly in the flow separation region close to the bed, sediment is transported in the opposite direction towards the dune crest while at higher distance from the bed a positive sediment flux is observed (see the selected profiles in the dune trough shown in Figure 4.2a). Although most of the sediment that is transported over the stoss side of the dune remains in the same dune by deposition on the lee side and in the trough of the dune thus contributing to dune migration, a significant amount of sediment is advected towards the following dune. This is reflected in the positive flux rates just downstream of the flow reattachment points.

The mean advective sediment flux $\bar{c}\bar{u}$ (Figure 4.1b and Figure 4.2b) displays very similar behavior as observed for the total mean sediment flux $\overline{cu}$. However, along the entire dune profile (both dune stoss and dune lee side) and mainly in the bed load layer, the absolute magnitudes of the advective fluxes are much larger than the total sediment fluxes. This can be clearly observed from the peaks in the selected profiles of $\bar{c}\bar{u}$ (Figure 4.2b), which are more pronounced near-bed than the peaks in the selected profiles of $\overline{cu}$ (Figure 4.2a). This overestimation of the total mean flux by the mean advective flux should be compensated by the contribution of the mean turbulent flux $\overline{c'u'}$ (see Figure 4.1c and Figure 4.2c). The contour map and selected profiles of $\overline{c'u'}$ show negative values over the stoss side of the dune with pronounced peaks in the bed load layer, that reaches up to 40% of the total mean sediment flux over the stoss side of the dune. Negative but much smaller values of $\overline{c'u'}$ were also observed over a flat bed in an open channel [see *Nikora and Goring,* 2002]. Over the lee side of the dune and in the dune trough, where turbulent intensities are the highest [see *Naqshband et al.*, 2014b], the contribution of $\overline{c'u'}$ to the total sediment flux is even larger and reaches up to 50%.

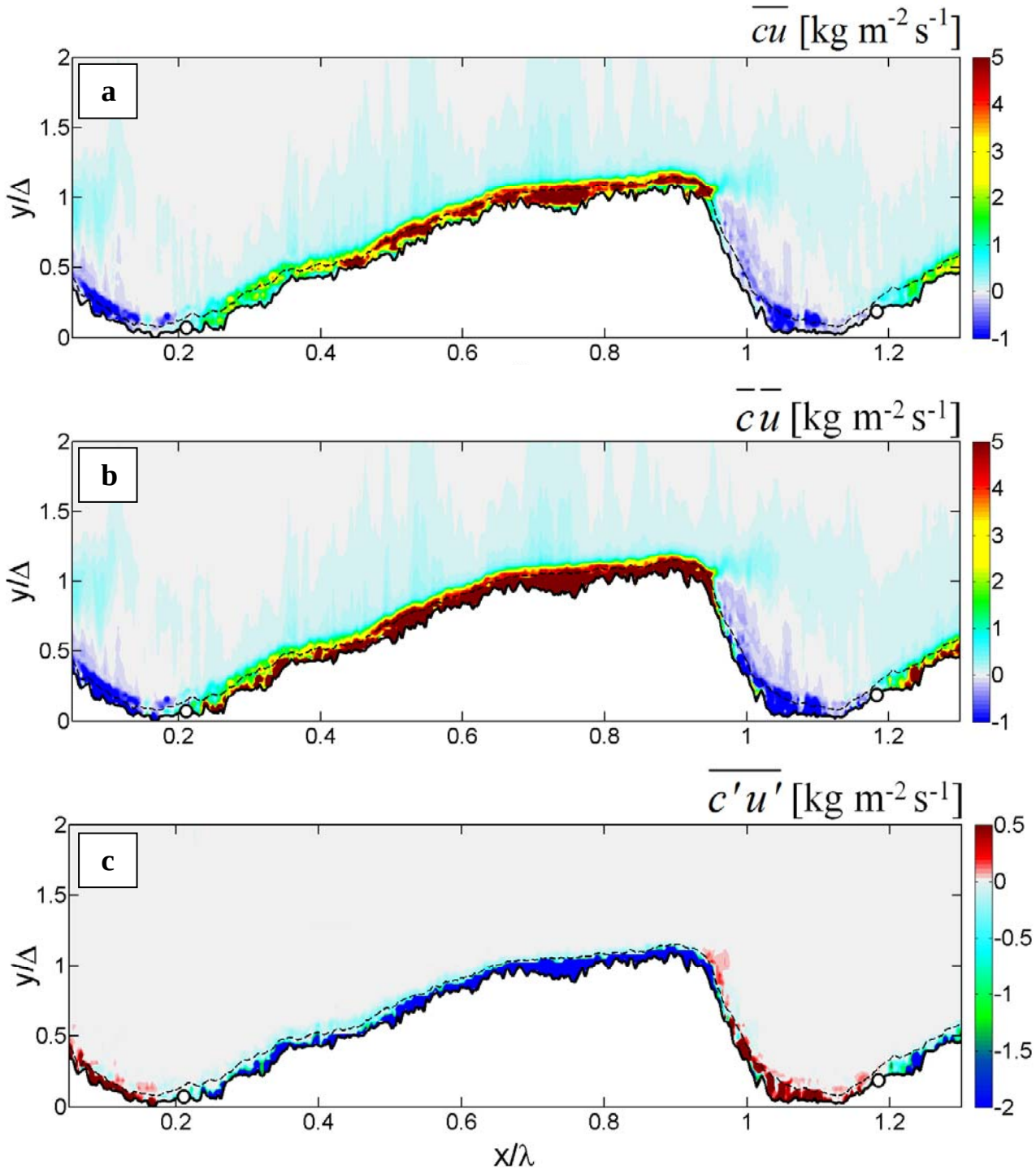

Figure 4.1 – Contour maps of the total mean streamwise flux $\overline{cu}$ (a), mean advective streamwise flux $\overline{c}\,\overline{u}$ (b) and mean turbulent streamwise flux $\overline{c'u'}$ (c). The black, solid line indicates the dune profile and the black, dotted line is the interface between the suspended load and the bed load layer determined by acoustic interface detection method. The open circles at the dune bed are the flow reattachment points and the flow direction is from left to right.

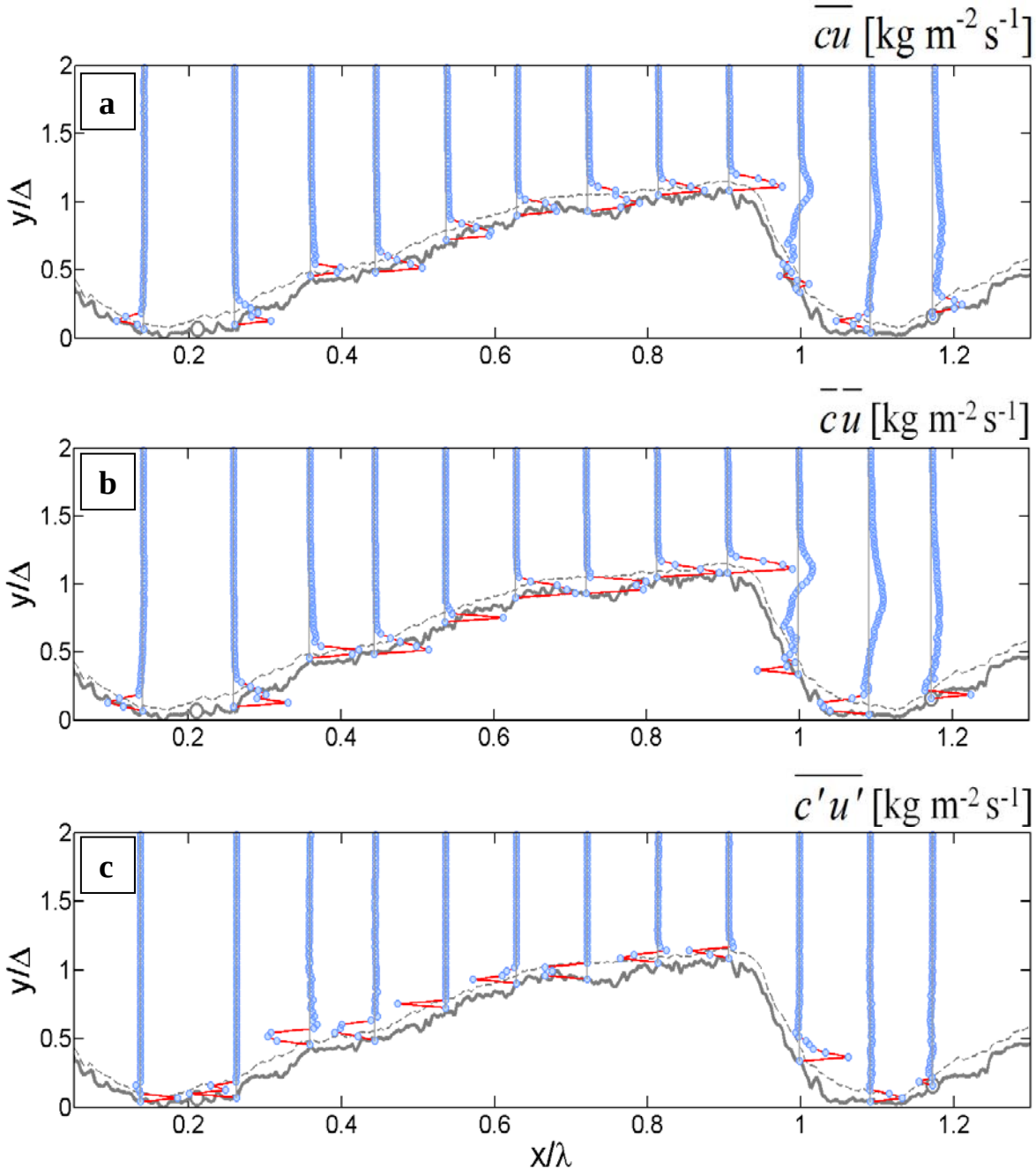

Figure 4.2 – Selected profiles along the dune bed of the total mean streamwise flux $\overline{cu}$ (a), mean advective streamwise flux $\overline{\bar{c}\bar{u}}$ (b) and mean turbulent streamwise flux $\overline{c'u'}$ (c). Vertical, solid lines along the dune bed indicate the location of the profiles origin with positive flux to the right and negative to the left. For (a) and (b), the distance between two vertical lines scales with $\overline{cu}$ = 8 [kg m^{-2} s^{-1}]. For (c), the distance between two vertical lines scales with $\overline{cu}$ = 2 [kg m^{-2} s^{-1}].

4.3.2 MEAN VERTICAL SEDIMENT FLUXES

Contour maps and selected profiles of the total mean vertical sediment flux $\overline{cw}$, mean advective flux $\bar{c}\bar{w}$ and mean turbulent flux $\overline{c'w'}$ along the dune bed are shown in Figure 4.3 and Figure 4.4. The total mean vertical flux $\overline{cw}$ (Figure 4.3a and Figure 4.4a) is largest close to the bed and decreases strongly with increasing distance from the bed. Positive (upward) sediment fluxes are observed over the entire dune with large peaks on the stoss side of the dune downstream of the flow reattachment point, reflecting the pick-up of sediment. These peaks may be the result of the shear layer vortices that impact the dune bed, generating turbulent sediment bursts that are absent elsewhere. Negative (downward) sediment fluxes are observed above the upper flat part of the dune and after the dune crest in the dune lee side, with the largest values over the dune crest and dune lee side reflecting sediment deposition in these locations. In addition, in the dune trough close to the bed, upward vertical fluxes are coupled with small downward fluxes further from the bed, illustrating the turbulent behavior of the flow in the flow separation zone.

Figure 4.3b and Figure 4.4b show the mean advective sediment flux $\bar{c}\bar{w}$. Although $\bar{c}\bar{w}$ roughly follows the same trend as observed for the total mean sediment flux $\overline{cw}$, the peaks observed at the stoss side of the dune in the suspended load layer (Figure 4.3a) are not encountered in the contour map of $\bar{c}\bar{w}$ (Figure 4.3b). In addition, along the entire dune profile (both dune stoss and dune lee side) and mainly in the bed load layer, the absolute magnitudes of the advective fluxes are generally larger than the total sediment fluxes. This is reflected in the selected profiles of $\bar{c}\bar{w}$ (Figure 4.4b), that show more pronounced peaks in the near-bed region compared to the selected profiles of $\overline{cw}$ (Figure 4.4a). These differences observed between $\overline{cw}$ and $\bar{c}\bar{w}$ are compensated by the contribution of the mean turbulent flux $\overline{c'w'}$ (see Figure 4.3c and Figure 4.4c). The contour map of $\overline{c'w'}$ (Figure 4.3c) shows the peaks in the suspended load layer that were not present in the contour map of $\bar{c}\bar{w}$ (Figure 4.3b) but were observed in the contour map of the total mean sediment flux $\overline{cw}$ (Figure 4.3a). These peaks are thus clearly related to the turbulent burst/generation resulting from the shear layer vortices hitting the dune bed. Furthermore, in the bed load layer and almost along the entire dune bed, the magnitude of the $\overline{c'w'}$ reaches up to 30% of the total mean sediment flux.

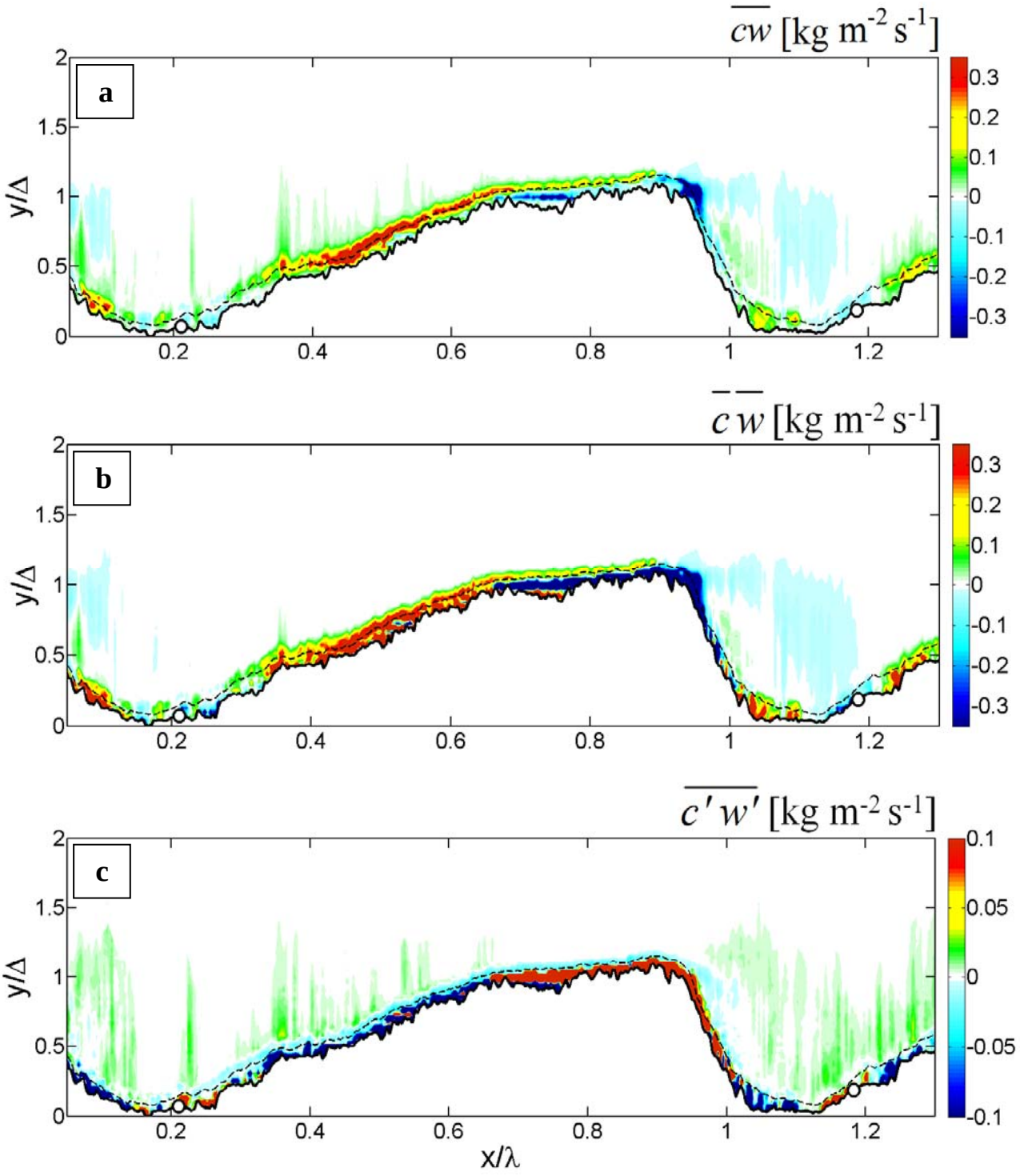

Figure 4.3 – Contour maps of the total mean vertical flux $\overline{cw}$ (a), mean advective vertical flux $\overline{c}\,\overline{w}$ (b) and mean turbulent vertical flux $\overline{c'w'}$ (c).

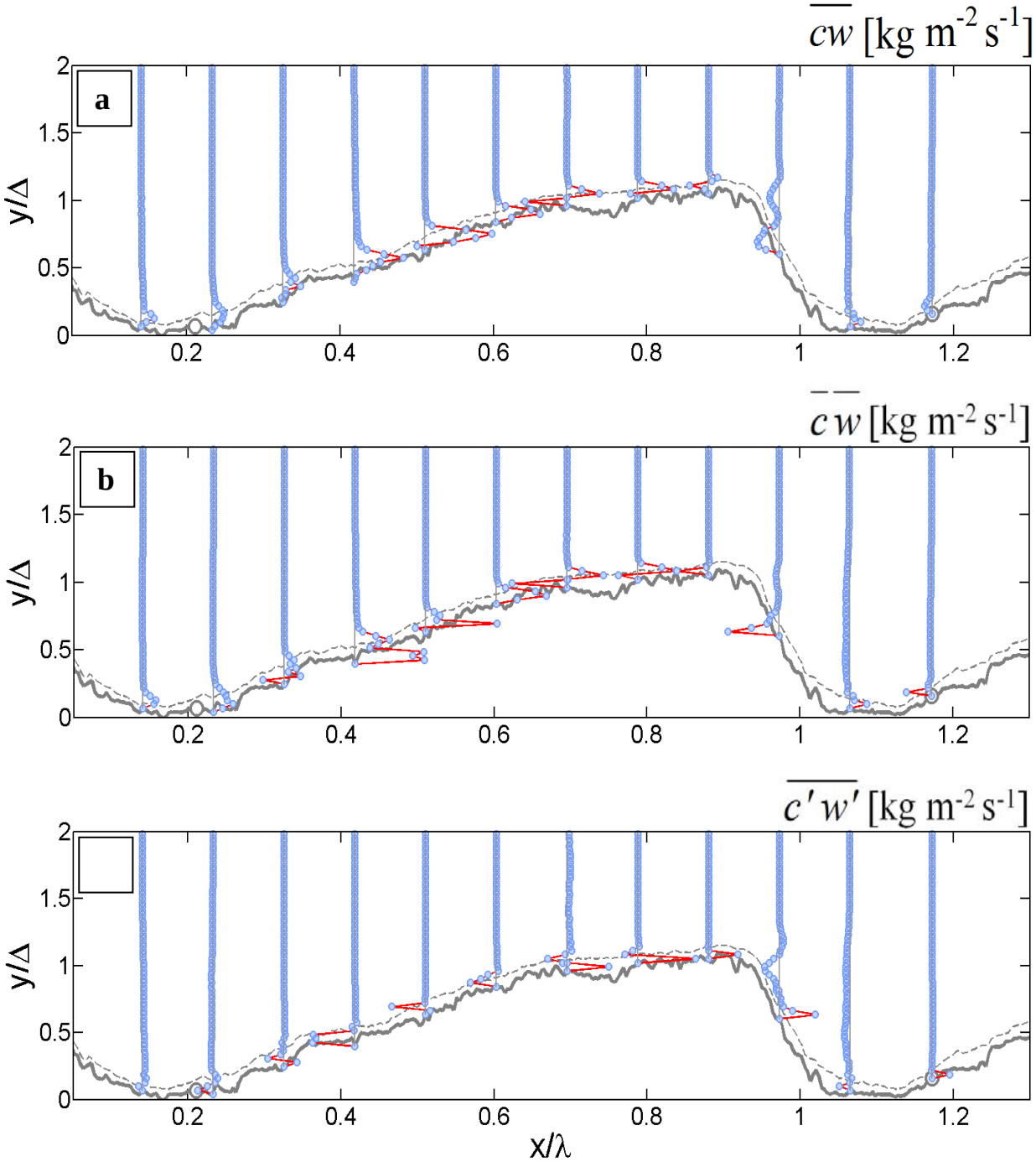

Figure 4.4 – Selected profiles along the dune bed of the total mean vertical flux $\overline{cw}$ (a), mean advective vertical flux $\overline{\bar{c}\bar{w}}$ (b) and mean turbulent vertical flux $\overline{c'w'}$ (c). For (a) and (b), the distance between two vertical lines scales with $\overline{cw} = 0.35$ [kg m^{-2} s^{-1}]. For (c), the distance between two vertical lines scales with $\overline{cw} = 0.15$ [kg m^{-2} s^{-1}].

4.4 DISCUSSION AND RECOMMENDATIONS

The present study has focused on the details of sediment flux dynamics along mobile, migrating sand dunes in equilibrium. In particular, the contribution of turbulent sediment fluxes – in both streamwise and vertical directions – to the total sediment fluxes were investigated. Direct sediment flux measurements were carried out using the ACVP during a series of mobile bed experiments. For the investigated experimental condition, we showed that the turbulent flux forms 30-50% of the total mean sediment flux measured along the dune bed. Therefore, indirect measurements of sediment fluxes along mobile dunes could significantly deviate from the actual net sediment fluxes. However, it should be noticed that the results of this study are strongly related to 2D dune topography in a laboratory flume. Future research is needed to investigate whether these findings are consistent for field conditions with a strong 3D dune topography and for a wider range of flow conditions.

Other important direction for future research is linking the results of this study to complex numerical models that describe the turbulent flow and sediment concentration above dunes [e.g., *Nabi et al.,* 2013]. In particular, under same flow and bed conditions, the complex numerical models should be able to reproduce the contribution of the turbulent fluxes to the total fluxes observed in this study. In addition, the new insights obtained in our research may improve the current engineering methods in modeling sediment transport.

Furthermore, because the ACVP provides co-located, simultaneous profiles of both two-component flow velocity and sediment concentration, we are now able to make direct computations of the turbulent Prandtl-Schmidt number β along the dunes and over the entire flow depth. The turbulent Prandtl-Schmidt number is the ratio of the turbulent diffusivity of momentum ε_v to the turbulent diffusivity of suspended sediment ε_s and is an important parameter within sediment transport models. To date, the exact behavior of this parameter is not quantified due to the limitations of the available instruments [see *Sassi et al.,* 2013 and references therein].

4.5 CONCLUSIONS

Our flume experiments on the measurements of sediment fluxes along migrating dunes have provided new insights into the dynamics of turbulent fluxes. The main findings of our study can be summarized as follows:

1. The behavior of the total mean streamwise sediment flux $\overline{cu}$ and the mean advective flux $\bar{c}\bar{u}$ is very similar along the dune profile. However, along the entire dune profile and mainly in the bed load layer, the absolute magnitudes of $\bar{c}\bar{u}$ are much larger compared to $\overline{cu}$. This overestimation is caused by the negative contribution of the mean turbulent flux $\overline{c'u'}$. Over the stoss side of the dune, $\overline{c'u'}$ reaches up to 40% of the total mean sediment flux, and over the lee side of the dune the contribution of $\overline{c'u'}$ to the total sediment flux is larger and reaches up to 50%. Therefore, indirect measurements of sediment fluxes along dunes (limited to $\bar{c}\bar{u}$) may overestimate the actual sediment fluxes ($\overline{cu}$) up to a factor 2.

2. Contour maps of the total mean vertical flux $\overline{cw}$ showed peaks on the stoss side of the dune. These peaks were found to be the result of turbulent bursts emanating from the flow detachment zone subject to strong shear instabilities and hitting the dune bed downstream of the flow reattachment point.

3. The mean vertical turbulent flux $\overline{c'w'}$, along the entire dune bed and in the bed load layer, reaches nearly 30% of the total mean vertical flux $\overline{cw}$.

CHAPTER 5 – MODELING RIVER DUNE DEVELOPMENT AND DUNE TRANSITION TO UPPER STAGE PLANE BED*

ABSTRACT

Large asymmetric bedforms known as dunes commonly dominate the bed of sand rivers. Due to the turbulence generation over their lee sides, dunes are of central importance in predicting hydraulic roughness and water levels. During floods in several rivers, dunes are observed to grow rapidly as flow strength increases, undergoing an unstable transition regime, after which they are washed out in what is called upper stage plane bed. This transition of dunes to upper stage plane bed is associated with high transport of bed sediment in suspension. In the present study, we aim to improve the prediction of dune development and dune transition to upper stage plane bed by introducing the transport of suspended sediment in an existing dune evolution model. In addition, flume experiments are carried out to investigate dune development under bed load and suspended load dominated transport regimes, and to get insight in the time scales related to the transition of dunes to upper stage plane bed. Simulations with the extended model including the transport of suspended sediment show significant improvement in the prediction of equilibrium dune parameters (e.g. dune height, dune length, dune steepness, dune migration rate, dune lee side slope) both under bed load dominant and suspended load dominant transport regimes. The chosen modeling approach also allows us to model the transition of dunes to upper stage plane bed which was not possible with the original dune evolution model. The extended model predicts the change in the dune shapes as was observed in the flume experiments with decreasing dune heights and dune lee side slopes. Furthermore, the time scale of dune transition to upper stage plane bed was quite well predicted by the extended model.

* This chapter is based on a paper that is currently under review as: Naqshband, S., van Duin, O.J.M., Ribberink & S.J.M.H. Hulscher (under review). Modeling river dune development and their transition to upper stage plane beds.

5.1 INTRODUCTION

Bedforms arise from the interaction of flow and sediment at a wide variety of spatial and temporal scales. Dunes are the most common bedforms observed in sandy rivers having an asymmetric shape with a gentle upstream stoss side slope and a steep downstream lee face slope. Due to associated flow separation and energy dissipation, dunes form the main source of hydraulic roughness of the river bed. During floods in several rivers (e.g. Elkhorn, Missouri, Niobrara, Rio Grande), dunes are observed to grow rapidly as flow strength increases, undergoing an unstable transition regime after which they are washed out in what is termed as upper stage plane beds (USPB). This morphological evolution of dunes to upper stage plane bed is the strongest bedform adjustment during time-varying flows and is associated with a significant change in hydraulic roughness and water levels [*Nelson et al*., 2011].

Hydraulic roughness due to the presence of dunes is directly related to the dune height Δ and the dune length λ [*Yalin*, 1964; *Van Rijn*, 1984; *Karim*, 1999; *Van der Mark*, 2009]. Therefore, during time-varying flow, reliable predictions of bed-form regimes (e.g. dune regime, dune transitional regime and USPB) and bedform dimensions are of great importance in determining hydraulic roughness and water levels for flood management purposes [*Best*, 2005a].

Many approaches have been taken to describe dune dimensions, ranging from simple, empirically derived equilibrium dune height and dune length predictors [e.g. *Yalin*, 1964; *Allen*, 1978; *Ranga Ruju and Soni*, 1976; *Van Rijn*, 1984; *Julien and Klaassen*, 1995; *Karim*, 1995] to various forms of stability analyses [e.g. *Kennedy*, 1963; *Reynolds*, 1965; *Engelund*, 1970; *Fredsøe*, 1974; *Yamaguchi and Izumi*, 2002; *Colombini and Stocchino*, 2008]. On the other hand, numerical models exist that try to capture hydrodynamics and sediment transport dynamics in great detail [e.g. *Nabi et al.*, 2010]. Such computationally expensive models are valuable for studying detailed flow and sediment processes, but are unable to predict the time evolution of dune dimensions – in a river reach – at operational time scales for flood management purposes. This is mainly caused by the complexity related to the solving of the turbulent flow along the dunes. Simpler, more efficient dune evolution models exist that calculate the turbulent flow field over dunes or use a parameterization for the flow separation zone in combination with morphodynamic calculations [e.g. *Shimizu et al*., 2001; *Jerolmack and Mohrig*, 2005; *Nelson et al*., 2005; *Tjerry and Fredsøe*, 2005; *Giri and Shimizu*, 2006; *Paarlberg et al*., 2007, 2009; *Shimizu et al*., 2009; *Niemann et al*., 2011].

However, there is a trade-off between the accuracy and the efficiency (required computational cost) of the models mentioned. One important aspect of this is the accurate prediction of different bedform regimes, in particular the evolution of dunes to upper stage plane bed with increasing flow strength. The reason for this is that the transport mode within the majority of the existing, simpler dune evolution models is assumed bed load and the transport of bed sediment in suspension is neglected. This is shown to be appropriate for dune development in the lower flow regime (bed load dominant transport regime) but insufficient for the transition of dunes to upper stage plane bed in the higher flow regime where suspended sediment transport becomes dominant and plays an important role in changing dune shapes [e.g. *Kostaschuk et al*., 2009, and references therein]. In addition, several numerical and experimental studies have illustrated the link between increasing bed sediment transport in suspension and the transition from dunes to upper stage plane bed [see *Best*, 2005a and references therein]. In a recent study, *Naqshband et al*. [2014a] – by analyzing 414 flume and field bedform experiments – illustrated that the transition from dunes to upper stage plane bed occurs if sufficient bed sediment is transported in suspension depending on the magnitude of the Froude number. By defining the suspension number u_*/w_s – which represents the relative importance of suspended load to bed load – they showed that dune heights increase for $u_*/w_s < 1$ (bed load dominant transport regime) while dune heights decrease for $u_*/w_s > 1.25$ (suspended load dominant transport regime). Furthermore, detailed acoustic measurements of the sediment transport along migrating dunes by *Naqshband et al.* [2014b] showed that, for the flow conditions measured, bed load fully contributes to dune migration by avalanching on the dune lee side and in the dune trough. However, a significant part of the suspended sediment transport was observed to bypass the flow reattachment point of the dune and therefore did not contribute to the migration of the dune front. This fraction of the suspended sediment transport (the bypass fraction) was observed to increase significantly with increasing flow strength and is therefore appointed as a key process for the transition of dunes to upper stage plane bed.

For flood management purposes and in particular for Flood Early-Warning Systems (FEWS), there is need for a bedform evolution model that can efficiently predict (low computational time) the river bed regime and the exact bedform dimensions over the course of a full flood wave including the transition of dunes to upper stage plane bed. *Paarlberg et al.* [2009] successfully developed a dune evolution model that is able to predict dune development from small initial disturbances towards fully developed dunes in the lower flow regime (bed load dominated regime). The model's computational time

was drastically reduced by using a parameterization of the flow separation zone instead of solving the full hydrodynamic and sediment equations in this turbulent region [see *Paarlberg et al.,* 2007]. Although the dune evolution model is shown to give good predictions of both the dune dimensions in the dune regime [*Paarlberg et al.,* 2009] and the water levels in the River Rhine when coupled to a depth-averaged hydraulic model (SOBEK) [see *Paarlberg et al.,* 2010], the dune evolution model is not able to predict the transition of dunes to upper stage plane bed in the higher flow regime (suspended load dominant regime). The main reason for this is the use of an equilibrium bed load transport model and not including the transport of the bed sediment in suspension. In addition, in case of flow separation at the dune lee side, the total sediment transport at the dune crest is forced to avalanche down the dune lee side at a fixed angle of 30° (angle of repose, for more details see section 5.2.4). By doing this, the dune lee side slope maintains this fixed angle of repose independent of the flow condition.

The main objective of the present study is to investigate to what extent suspended sediment transport contributes to the transition of dunes to upper stage plane bed. In addition, the effect of suspended sediment transport on equilibrium dune parameters (e.g. dune height, dune length, dune steepness, dune migration rate, dune lee side slope) is investigated. To this end, we use the dune evolution model of *Paarlberg et al.* [2009] as a basis and we include in this model the transport of bed sediment in suspension by a sediment relaxation model. In addition, the sediment transport at the dune crest is no longer forced to avalanche at a fixed angle which enables the dune lee side slope to adapt to changing flow conditions during the transition of dunes to upper stage plane bed. Furthermore, new laboratory experiments have been carried out to understand the morphological behavior of dunes under bed load and suspended load dominant transport regimes, and to investigate the time scales related to the transition of dunes to upper stage plane bed. Although several researchers have studied the transition of dunes to upper stage plane beds in both flume and field, the exact morphological evolution of dunes and the corresponding time scales during their transition to upper stage plane beds are not well documented [e.g. *Guy et al.,*1966; *Van Rijn*, 1984; *Julien and Klaassen*, 1995; *Karim*, 1995].

The dune evolution model is presented in section 5.2 followed by the experimental work in 5.3. The model results and a comparison with the experimental data are presented in section 5.4. Future work is discussed in 5.5 followed by an overview of the main findings of this study in 5.6.

5.2 DUNE EVOLUTION MODEL

5.2.1 GENERAL DESCRIPTION

Paarlberg et al. [2009] developed a dune evolution model for application in operational flood forecasting (FEWS). To predict the evolution of dune dimensions over the time scale of a flood wave (several days), computation time was highly reduced by modeling the flow and sediment transport at the flow separation zone in a parameterized way. This dune evolution model by *Paarlberg et al.* [2009] is based on the numerical model of *Hulscher* [1996]; different versions of the *Hulscher* [1996] model were developed to predict the time evolution of offshore sand waves [*Németh et al*., 2006; 2007; V*an den Berg et al.,* 2012]. *Paarlberg et al*. [2009] extended the process-based morphodynamic model of *Németh et al*. [2006] with a parameterization of flow separation in order to enable simulation of finite-amplitude river dunes. The dune evolution model is able to predict the evolution of river dunes from small initial disturbances up to equilibrium dimensions with limited computational time and can be applied to model the bed form evolution during discharge waves [see *Paarlberg et al.* 2010]. Recently, the *Paarlberg et al.* [2009] model was also successfully applied by *Warmink et al.* [2014] in investigating the process of dune splitting. The dune evolution model operates with a domain length equal to the wave length of the fastest growing mode determined from a linear stability analysis [see *Paarlberg et al*., 2009]. Effectively, the dimensions of a single dune that is representative for the current flow conditions are modeled.

The *Paarlberg et al.* [2009] model consists of a flow module, a sediment transport module and a bed evolution module which are concisely described in the following sections. For additional details reference is made to *Paarlberg et al.* [2007; 2009; 2010].

5.2.2 FLOW MODULE

5.2.2.1 GOVERNING EQUATIONS

The flow is described by the two-dimensional shallow water equations in a vertical plane (2-DV), assuming hydrostatic pressure conditions. Using a scaling analysis on 2-DV Navier-Stokes equations, *Paarlberg* [2008, Appendix A] showed that the momentum equation in the vertical direction reduces to the hydrostatic pressure condition, and that the time variations in the horizontal momentum equation can be dropped. The resulting model equations are shown in equations (5.1) and (5.2).

$$u\frac{\partial u}{\partial x}+w\frac{\partial u}{\partial z}=-g\frac{\partial \zeta}{\partial x}+A_v\frac{\partial^2 u}{\partial z^2}+gi \tag{5.1}$$

$$\frac{\partial u}{\partial x}+\frac{\partial w}{\partial z}=0 \tag{5.2}$$

The velocities in the x and z directions are u and w, respectively. The water surface elevation is denoted by ζ, i is the average channel slope, and g and A_v indicate the acceleration due to gravity and the vertical eddy viscosity, respectively.

5.2.2.2 BOUNDARY CONDITIONS

The boundary conditions are defined at the water surface ($z=h+\zeta$) and at the bed ($z=z_b$). The boundary conditions at the water surface, equation (5.3) represents no flow through the surface and equation (5.4) means no shear stress at the surface. The kinematic boundary condition at the bed, equation (5.5) yields that there is no flow through the bed.

$$\left.\frac{\partial u}{\partial z}\right|_{z=h+\zeta} = w \tag{5.3}$$

$$u\left.\frac{\partial \zeta}{\partial x}\right|_{z=h+\zeta} = w \tag{5.4}$$

$$u\left.\frac{\partial z_b}{\partial x}\right|_{z=z_b} = w \tag{5.5}$$

As basic turbulence closure, an eddy viscosity is assumed that is independent of time and depth, which leads to a parabolic velocity profile. In order to represent the bed shear stress correctly for a constant eddy viscosity, a partial slip condition at the bed is necessary (equation 5.6).

$$\tau_b = A_v\left.\frac{\partial u}{\partial z}\right|_{z=z_b} = Su_b \tag{5.6}$$

In equation (5.6), τ_b m^2 s^{-2} is the volumetric bed shear stress and the resistance parameter S m s^{-1} controls the resistance at the bed. Furthermore, *Paarlberg et al.* [2009] used periodic boundary conditions to simulate river dunes.

5.2.2.3 PARAMETERIZATION OF THE FLOW SEPARATION ZONE

Flow separation occurs as the amplitude of the dunes grows and the dunes become asymmetrically shaped. The lee side slopes increase and eventually, the flow separates resulting in a recirculation zone behind the crests of the dunes. This process is included in the dune evolution model of *Paarlberg et al*. [2009] in a parameterized way using

experimental data of turbulent flow over two-dimensional subaqueous bed forms [see *Paarlberg et al.,* 2007]. The flow separation is modeled when the dune lee side slope exceeds a critical value of 10°.

5.2.3 SEDIMENT TRANSPORT MODULE

The sediment transport module of the *Paarlberg et al.* [2009] dune evolution model only considers the bed load transport. To be able to predict the evolution and transition of dunes to USPB in the suspended load dominant regime, the sediment transport module is extended with a relaxation model for the calculation of suspended sediment transport.

5.2.3.1 EQUILIBRIUM BED LOAD MODEL

The bed load transport q_b m^2 s^{-1} is calculated using the formula of *Meyer-Peter and Müller* [1948], including gravitational bed slope effects (equation 5.7). This formula is based on an equilibrium approach, meaning that there is no spatial and/or temporal lag between the maximum bed shear stress and the maximum sediment transport.

$$q_b = \begin{cases} \beta\left(\tau(x)-\tau_c(x)\right)^n \left(1+\eta\dfrac{\partial z_b}{\partial x}\right)^{-1} & \text{if} \quad \tau > \tau_c \\ 0 & \text{if} \quad \tau \le \tau_c \end{cases} \tag{5.7}$$

Here, $\tau(x)$ is the local, turbulence-averaged bed shear stress and $\tau_c(x)$ the local, critical bed shear stress. The proportionality constant β s^2 m^{-1} describes how efficiently the sand particles are transported by the bed shear stress [*Van Rijn*, 1993] and its value is found from the following equation.

$$\beta = \frac{m}{\left(\rho_s / \rho\right) g} \tag{5.8}$$

Here, ρ_s / ρ is the specific grain density, and m is an empirical coefficient which was set to 4 by *Paarlberg et al.* [2009]. The bed slope parameter η reflects the downhill preference of moving sediment and is inversely related to the tangent of the angle of repose φ=30°. The local, critical bed shear stress $\tau_c(x)$, corrected for bed slope effects, is given by the following equation.

$$\tau_c(x) = \tau_{c0} \frac{1 + \frac{\partial z_b}{\partial x}}{\sqrt{1 + \frac{\partial z_b}{\partial x}^2}} \tag{5.9}$$

Equation (5.10) defines τ_{c0}, the critical bed shear stress for a flat bed. In this equation, $\theta_{c0} = 0.05$ is the critical Shields parameter and D_{50} is the median grain size.

$$\tau_{c0} = \theta_{c0} g \left(\rho_s / \rho - 1 \right) D_{50} \tag{5.10}$$

5.2.3.2 RELAXATION MODEL FOR SUSPENDED LOAD

The suspended sediment transport in turbulent flows can be described by a first-order relaxation model shown in equation (5.11). This model concept for suspended sediment transport has been applied in a similar way for studying trench evolution [*Galappatti and Vreugdenhil*, 1985; *Davy and Crave*, 2000; *Lague et al.,* 2003; *Seminara*, 2006], soil erosion problems [*Hairsine and Rose*, 2002], aeolian transport [*Kroy et al.,* 2002], and flume experiments [*Charru*, 2006].

$$\frac{dq_s}{dx} = \frac{q_{se} - q_s}{L_{sat}} \tag{5.11}$$

In contrast to the bed sediment transport, the suspended sediment transport q_s needs more time and distance to respond to the changing flow conditions (thus changing bed shear stress) and to reach its equilibrium value q_{se}. The time and length over which the suspended sediment transport relaxes towards saturation are the relaxation time T_{sat} and relaxation length L_{sat}, respectively. This saturation or equilibrium value corresponds to the homogenous and steady state for which the suspended sediment transport is constant in both space and time for given flow conditions. Several approaches are available in literature for the calculation of the equilibrium suspended sediment transport. In this study, the empirical equation of *Van Rijn* [1993] is applied because of its validity in a variety of environments [*Kostaschuk*, 2006]. The equilibrium suspended sediment transport q_{se} m^2 s^{-1} at each grid point along the bed is calculated from equation (5.12) with U the mean depth-averaged flow velocity, H the mean flow depth, U_{cr} the critical depth-averaged entrainment velocity given by equation (5.13) and D_* the dimensionless grain diameter calculated from equation (5.14) where v is the kinematic viscosity.

$$q_{se} = 0.012UH\left[\frac{U - U_{cr}}{\left\{\left(\rho_s/\rho - 1\right)gD_{50}\right\}^{1/2}}\right]^{2.4}\left(\frac{D_{50}}{H}\right)D_*^{-0.6} \tag{5.12}$$

$$U_{cr} = \begin{cases} 0.19\left(D_{50}\right)^{0.1}\log\left(\dfrac{4H}{D_{90}}\right) & \text{for} \quad 0.1 \le D_{50} \le 0.5\,\text{mm} \\ 8.50\left(D_{50}\right)^{0.6}\log\left(\dfrac{4H}{D_{90}}\right) & \text{for} \quad 0.5 < D_{50} \le 2.0\,\text{mm} \end{cases} \tag{5.13}$$

$$D_* = D_{50}\left[\frac{\left(\rho_s/\rho - 1\right)g}{\nu^2}\right]^{1/3} \tag{5.14}$$

For the calculation of the suspended sediment relaxation length L_{sat} in the suspended sediment relaxation model, a relationship as proposed by *Galappatti and Vreugdenhil* [1985] is used (equation 5.15). More recently, from a mode analysis of the advection-diffusion equation for the particle concentration, *Claudin et al.* [2011] derived a similar relationship for the relaxation length.

$$L_{sat} = \frac{u_*}{w_s}\exp\left(-\alpha\frac{w_s}{u_*}\right)\frac{C}{\sqrt{g}}H \tag{5.15}$$

This equation shows that – for a given Chézy coefficient C $\text{m}^{1/2}\,\text{s}^{-1}$ and water depth H – the relaxation length increases with increasing flow strength or decreasing sediment diameter which is reflected in the decreasing of the particle fall velocity w_s defined in equation (5.16) after *Soulsby* [1997]. The bed shear velocity u_* is calculated from equation (5.17).

$$w_s = \frac{\nu}{D_{50}}\left[\left(10.36^2 + 1.049D_*^3\right)^{1/2} - 10.36\right] \tag{5.16}$$

$$u_* = \sqrt{gHi} \tag{5.17}$$

The parameter α in equation (5.15) is a distribution factor representing the influence of the sediment diffusion coefficient ε_s and is set to 2.0 which is in the range of what is proposed in literature [see e.g. *Galappatti and Vreugdenhil*, 1985; *Davy and Lague*, 2009; *Claudin et al.,* 2011]. The influence of parameter α on the model results is studied in section 5.5. The behavior of the relaxation length equation – for different Chézy coefficients – is illustrated in Figure 5.1 for a range of suspension numbers. It can be observed that, in the bed load dominant transport regime ($u_*/w_s < 1$), the relaxation length is in the order of millimeters to centimeters where in the suspended load dominant transport regime ($u_*/w_s > 1.25$), the relaxation length increases exponentially and reaches up to several meters.

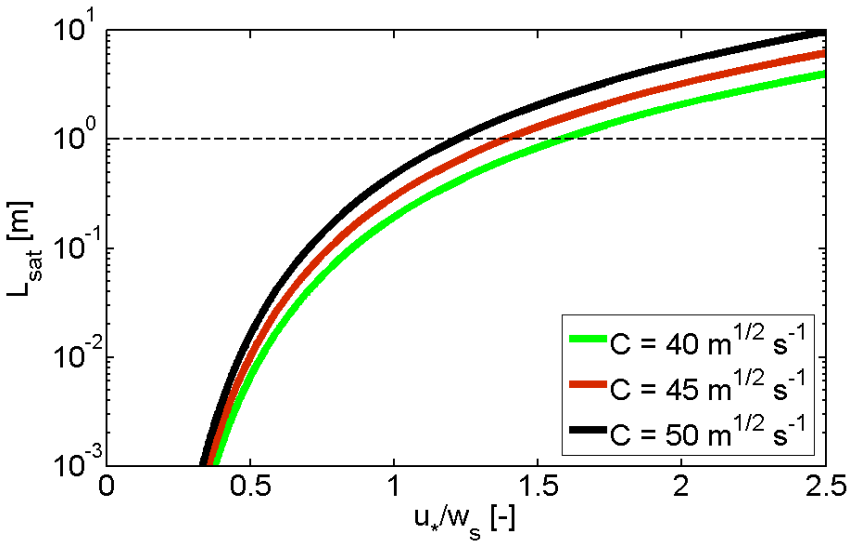

Figure 5.1 – The behavior of the relaxation length L_{sat} for different Chézy coefficients C $m^{1/2}$ s^{-1} for a range of suspension numbers. The water depth H and sediment diameter D_{50} are kept constant (H=0.25 m, D_{50}=0.29 mm).

5.2.4 BED EVOLUTION

The topographic changes are modeled using the Exner equation shown below where ε_p=0.4 is the bed porosity.

$$\left(1-\varepsilon_p\right)\frac{\partial z_b}{\partial t} = -\frac{\partial q_T}{\partial x} \tag{5.18}$$

In the original *Paarlberg et al.* [2009] dune evolution model, the bed evolution is calculated only by considering the bed load transport rate ($q_T=q_b$) and equation (5.18) is applied over the entire model domain if there is no flow separation. In case of flow separation, equation (5.18) is only applied outside the flow separation zone. In the flow separation zone, all sediment that is passing the flow separation point is assumed to settle in the flow separation zone and avalanche down the lee face where it distributes evenly at an angle of 30° (angle of repose).

In the extended dune evolution model, both the bed load and the suspended load transport rates are used to calculate topographic changes ($q_T=q_b+q_s$). In addition, equation (5.18) is applied to the entire domain length under all circumstances. This means that the dune lee side slope is no longer fixed at 30° and that the dune shape is entirely determined from the sediment transport gradients along the bed. This approach makes it possible to model low-angle dunes and the transition of dunes to USPB in the higher flow regimes (see section 5.4).

5.3 FLUME EXPERIMENTS

The flume experiments were conducted in the Hydraulics Laboratory of the Leichtweiss institute of the Technical University of Braunschweig (LWI), Germany. Below the experimental set-up and procedure are outlined briefly followed by the experimental conditions. For more details on the experimental work reference is made to *Naqshband et al.* [2014b].

Three experiments were carried out to understand the morphological behavior of dunes under bed load (EXP1) and suspended load dominant transport regimes (EXP2), and to investigate the time scales related to the transition of dunes to upper stage plane bed (EXP3). EXP1 and EXP2 focused on the development of equilibrium dunes starting from plane bed where EXP3 aimed on the transition from steady-state dune bed to upper stage plane bed. The flow strength for EXP3 was chosen such that dunes were washed out after reaching their equilibrium dimensions.

5.3.1 EXPERIMENTAL SET-UP AND PROCEDURE

The flume has a width of 0.5 m and a length of 30 m, where the effective measuring length for dune morphology was 8 m. A sand layer of approximately 25 cm thick was installed over the entire length of the flume and the sand bed was flattened at the beginning of each experiment. Applying the bedform stability diagram of *Van den Berg*

and Van Gelder [1993], uniform sand with D_{50} of 0.29 mm was used to obtain 2D dunes in the flume. The flume slope and the weir at the end of the flume are adjustable, which made it possible to realize equilibrium flow conditions at a predefined discharge and water depth. In this way, the water depth was kept constant for different flow conditions through the entire experiment. The sand bed and water levels were measured continuously over the entire effective measurement section of the flume using echo sensors fixed on a semi-automatic measurement carriage. Every 2 to 3 minutes, the carriage made a scan of the entire flume at three parallel transects across the flume width.

Starting from a flat bed, ripples appeared instantaneously as the flow was introduced in the flume. The ripples merged into dunes and finally a steady-state condition was obtained where the dunes migrated through the flume without changing their shapes (EXP1 and EXP2). This dynamic equilibrium was found by analyzing dune height and length statistics from the measured bed profiles using the bedform tracking tool of *Van der Mark et al.* [2008]. Average and standard deviations of dune height and length were determined over the effective measurement section of the flume. For EXP3, after reaching a dynamic dune-equilibrium for a predefined flow condition, the discharge was increased until the dunes were completely washed out and the upper stage plane bed regime was reached. After the completion of the measurement program of one experimental condition, the discharge through the flume was stopped and the sediment accumulated at the end of the flume was transported back to the upstream end of the flume. The bed was flattened and the same procedure outlined above was repeated.

5.3.2 FLOW, SEDIMENT AND BED CONDITIONS

Table 5.1 gives an overview of the flow, sediment and bed conditions for the three experiments. The experiments EXP1 and EPX2 were carried out with two different and predefined flow strengths while the water depths were kept constant by adjusting the flume slope and the flume tail gate. A discharge of 0.08 m^3 s^{-1} was used for EXP1 where a discharge of 0.10 m^3 s^{-1} was used for EXP2. Details on dune height and dune length evolution during experiments EXP1 and EXP2 can be found in Chapter 3 (see Figures 3.5 and 3.6).

Parameter	EXP1	EXP2	EXP3
Discharge Q, $m^3 s^{-1}$	0.080	0.100	0.080 - 0.160
Flume slope $S \times 10^{-3}$	1.0	2.20	1.0 - 3.36
Water depth H, m	0.25	0.25	0.25
Mean bulk velocity U, m s^{-1}	0.64	0.80	0.64 - 1.28
Froude number Fr	0.41	0.51	0.41 - 0.82
Hydraulic radius R_b , m	0.14	0.15	0.14 - 0.17
Bed shear stress τ_b, Pa	1.47	3.24	1.47 - 5.96
Bed shear velocity u_*, m s^{-1}	0.038	0.057	0.038 - 0.077
Suspension number u_*/w_s	0.90	1.59	0.90-1.91
$D_{10} \times 10^{-3}$, m	0.21	0.21	0.21
$D_{50} \times 10^{-3}$, m	0.29	0.29	0.29
$D_{90} \times 10^{-3}$, m	0.40	0.40	0.40
Equilibrium dune height Δ_e, m	0.082	0.072	0.018
Equilibrium dune length λ_e, m	2.25	4.35	-
Equilibrium dune steepness Δ_e/λ_e	0.036	0.018	-
Time to equilibrium T_e, min	150	90	-
Equilibrium migration speed $C_e \times 10^{-4}$, m s^{-1}	7.0	13.0	-

Table 5.1 – Flow, sediment and bed conditions for the experiments conducted.

For EXP3 – the transition from steady-state dune bed to upper stage plane bed – initially the discharge was set equal to the discharge under EXP1 of 0.08 $m^3 s^{-1}$. After 250 minutes, as the dunes where fully developed, the discharge was increased to 0.16 $m^3 s^{-1}$. The development of steady-state dunes from a flat bed and the transition of dunes to upper stage plane bed are shown in Figure 5.2 with the green dotted lines indicating the increase in the flow discharge from 0.08 to 0.16 $m^3 s^{-1}$. Dunes immediately responded to the changing flow conditions with a large increase in the migration speeds (Figure 5.2a). Initially, dune heights (Figure 5.2b) decreased slowly (250-300 minutes) and eventually within 40 minutes (300-340 minutes) the dunes were totally washed out. Dune lengths (Figure 5.2c) increased rapidly and responded more quickly to the changing flow conditions. Figure 5.3 shows several snapshots of the flume and the dunes during EXP3 in time with the initial flat bed (Figure 5.3a), occurrence of well-organized ripples (Figure 5.3b), fully developed dunes in equilibrium (Figure 5.3c), dune transitional regime (Figure 5.3d and Figure 5.3e) and upper stage plane bed (Figure 5.3f).

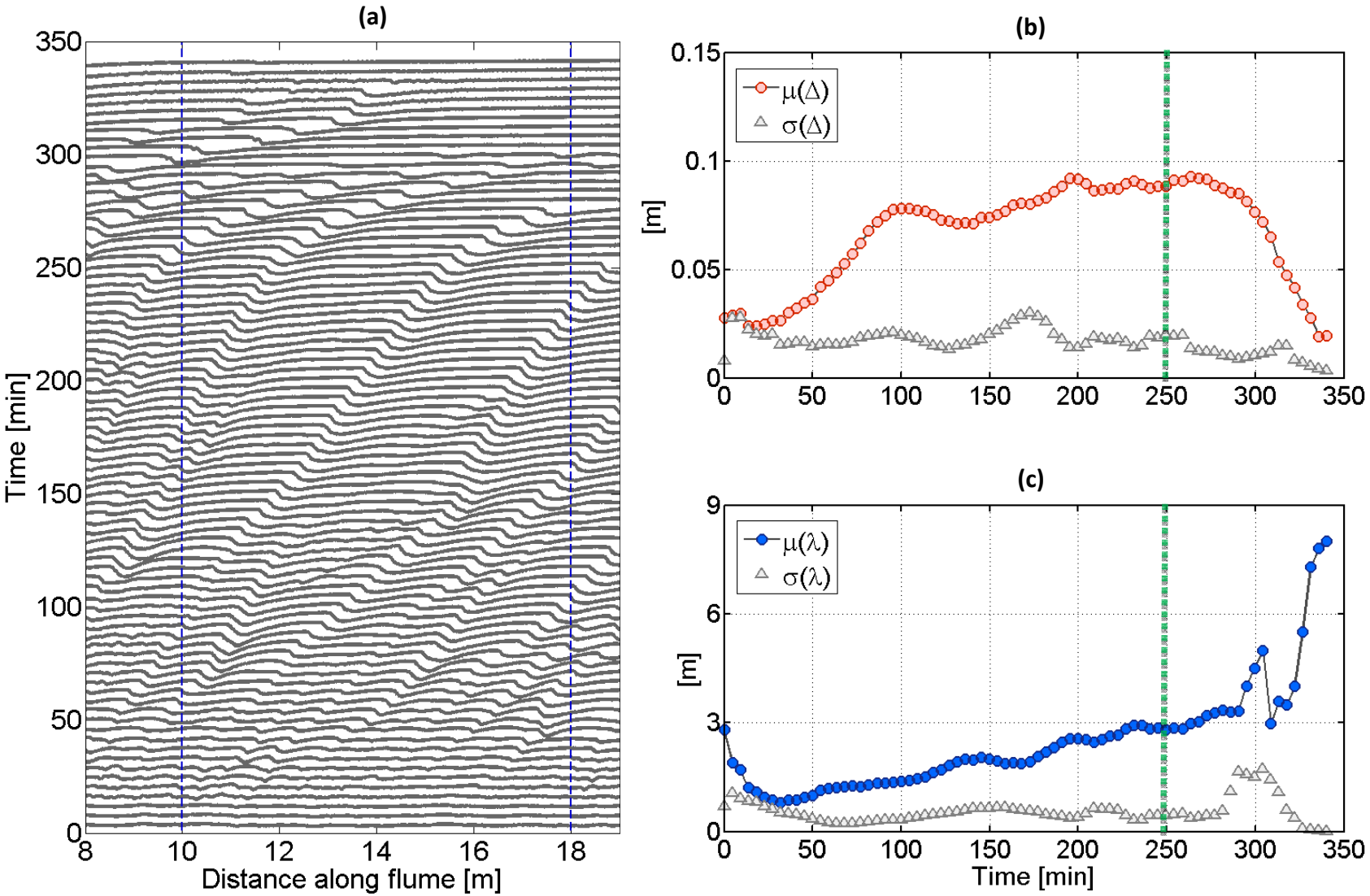

Figure 5.2 – Bed evolution in time along the effective measuring section of the flume for EXP3 (a). Average μ and standard deviation σ for the dune height Δ (b) and dune length λ (c) of EXP3. The green dotted lines indicate the increase in discharge leading to the transition of dunes to USPB.

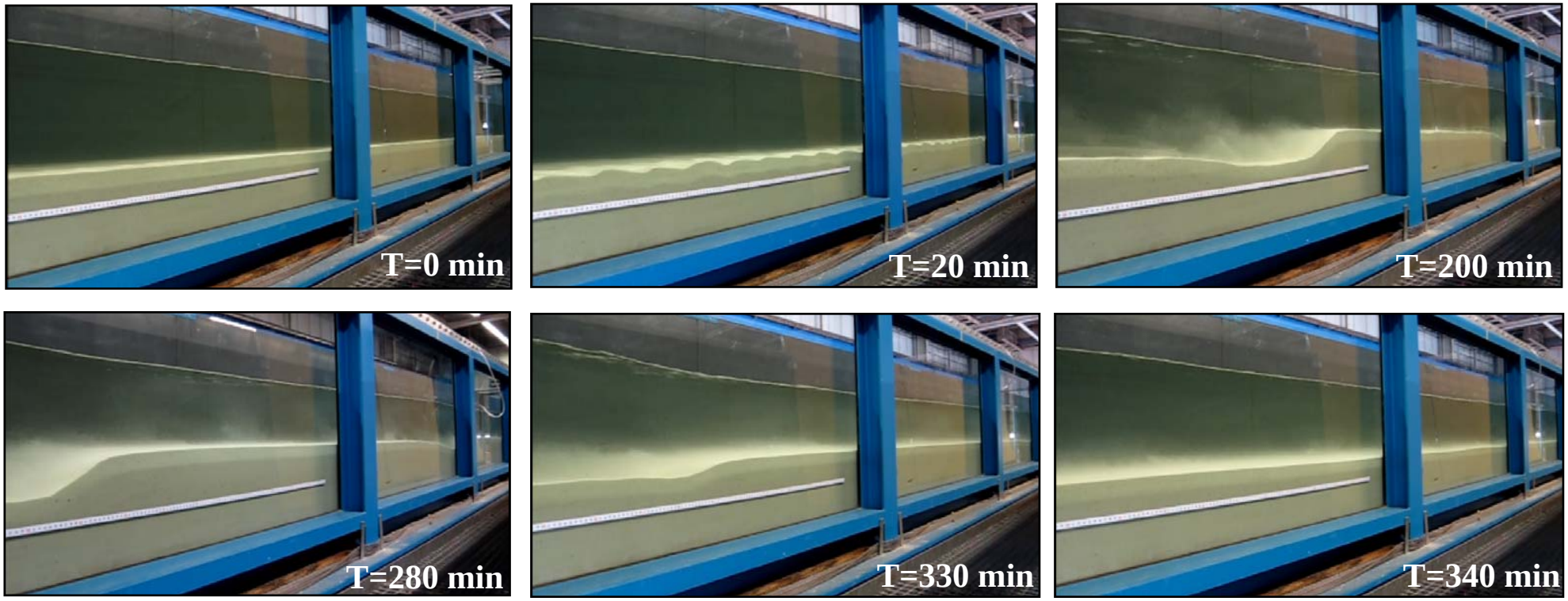

Figure 5.3 – Snapshots of EXP3 in time with the initial flat bed (a), well-organized ripples (b), fully developed dunes in equilibrium (c), transitional dune stage (d & e) and upper stage flat bed (f). Flow is from right to left and each flume window has a width of about 1.5 meters (the horizontal distance between two vertical bars). A dynamic content video is associated with this figure.

5.4 MODEL RESULTS AND COMPARISON WITH EXPERIMENTAL DATA

In this section, the model results are discussed and compared to the experimental data. In section 5.4.1, for the experimental conditions of EXP1 and EXP2 in Table 5.1, the development of dunes are presented from small initial disturbances up to equilibrium dimensions both with the original *Paarlberg et al.* [2009] model (hereafter referred to as 'the bed load model (BL-model)' for brevity) as well as with the extended dune evolution model that includes both bed load and suspended load (hereafter referred to as 'the bed load + suspended load model (BL+SL-model)' for brevity). Next, in section 5.4.2, model results are discussed for the conditions of EXP3 showing the transition of fully developed dunes in equilibrium to upper stage plane bed.

5.4.1 EQUILIBRIUM DUNE DEVELOPMENT

5.4.1.1 BED LOAD DOMINANT TRANSPORT REGIME

Figure 5.4a and Figure 5.4b show the temporal dune evolution for the bed load dominant experimental condition EXP1 ($u_*/w_s = 0.90$, see Table 5.1) with the BL-model and the BL+SL-model, respectively. The dune evolution from small initial disturbances up to steady-state dunes is quite similar for both models. Where the lee side angle of dunes in the BL-model are forced to and remain at the angle of repose (30°) after exceeding a critical angle of 10° (see Figure 5.4a: after 100 minutes), lee side angles of the dunes with the BL+SL-model develop more gradually and reach up to 26° in equilibrium. The equilibrium dune migration speed C_e with the BL-model is slightly lower than with the BL+SL-model (see also Table 5.2).

The corresponding dune height evolution for both models are shown in Figure 5.5a together with the measured dune heights of EXP1. The BL-model overestimates the measured dune height over the entire course of dune development towards equilibrium where the BL+SL-model follows the course of the measured dune heights more closely. The equilibrium dune height Δ_e is also predicted more accurately by the BL+SL-model compared to the original BL-model. Dune heights predicted by the BL-model grow much faster than the BL+SL-model, and therefore reach the steady-state condition earlier (see T_e in Table 5.2, with T_e corresponding to the time when the deviation of the dune height from the final dune height is no more than 2%). Despite the simple approach of the dune evolution model, both models give a reasonable prediction of the measured equilibrium dune lengths λ_e for this experimental condition (see Table 5.2).

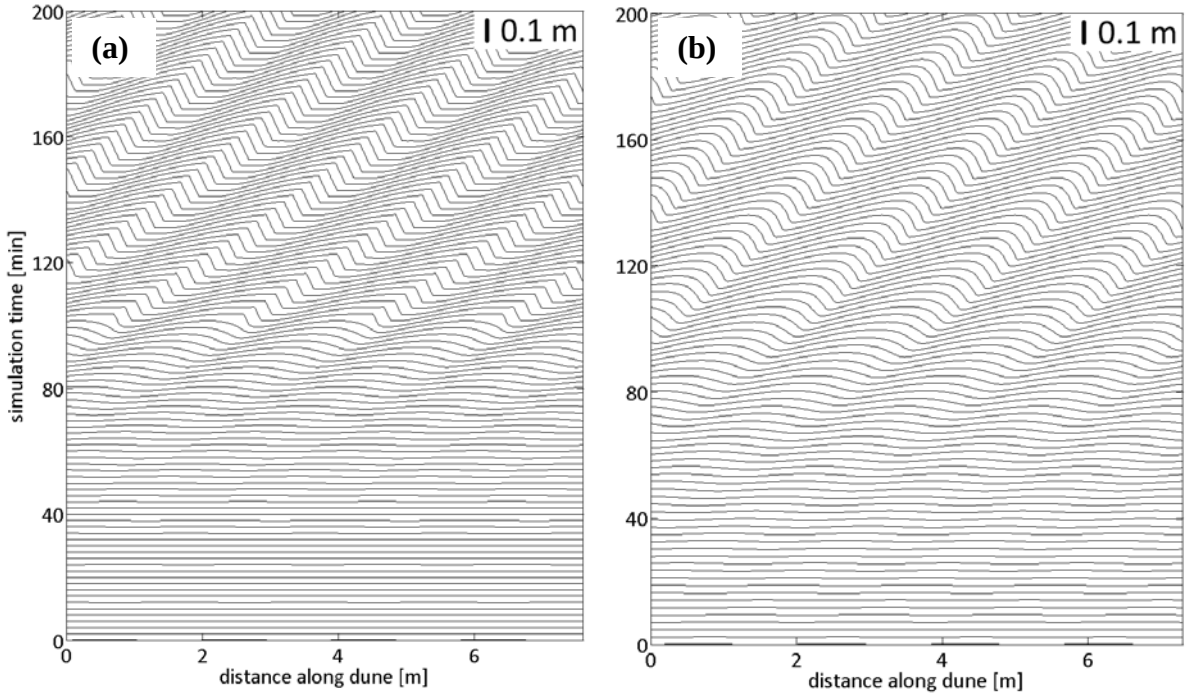

Figure 5.4 – Model results of the temporal dune evolution for the bed load dominant experimental condition EXP1. Results with the BL-model (a) and with the BL+SL-model (b).

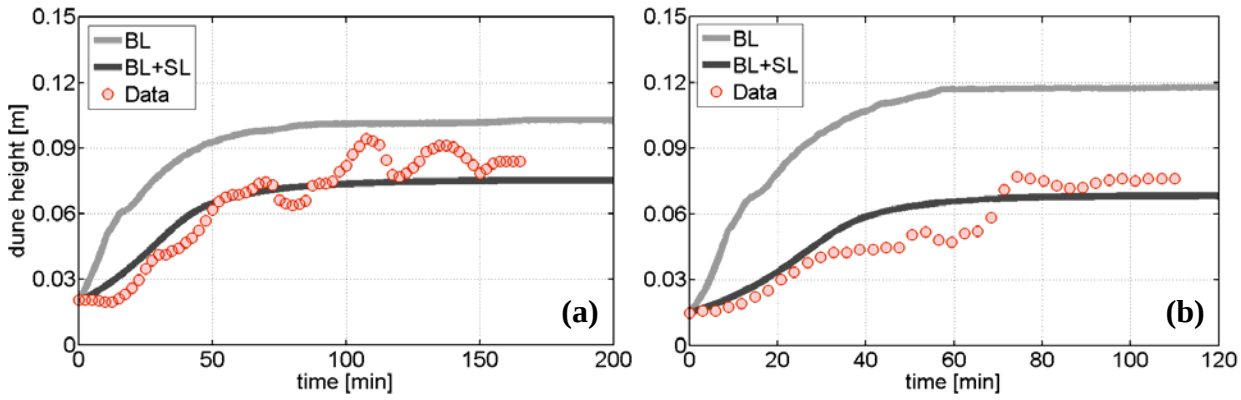

Figure 5.5 – Comparison of model results and experimental data for the dune height evolution corresponding to the bed load dominant experiment EXP1 (a) and the suspended load dominant experiment EXP2 (b).

5.4.1.2 SUSPENDED LOAD DOMINANT TRANSPORT REGIME

Figure 5.5b shows the dune height evolution for the suspended load dominant experimental condition EXP2 ($u_*/w_s = 1.59$, see Table 5.1). The measured equilibrium dune height for this experiment is slightly lower than the equilibrium dune height of EXP1 where bed load transport was dominant. Also, for this experimental condition, the BL-model overestimates the measured dune height over the entire course of dune development towards equilibrium where the BL+SL-model follows the course of the measured dune heights more closely. The equilibrium dune height predicted by BL+SL-model is surprisingly close to the measured value while the BL-model gives a significant overestimation of more than 50%.

Figure 5.6 shows the equilibrium values of the bed load (equation 5.7) and the suspended load (equation 5.12) for a range of suspension numbers. Both bed load and suspended load increase with increasing suspension number. For suspension numbers smaller than about 1.3, bed load is larger than suspended load while for suspension numbers greater than 1.3, suspended load becomes more dominant over bed load [see also *Van Rijn*, 1993]. For the experimental condition of EXP2 ($u_*/w_s = 1.59$), both the bed load and the suspended load are significantly greater than the bed load and the suspended load of EXP1 ($u_*/w_s = 0.90$). As the BL-model only considers the transport of bed material as bed load, higher bed load for EXP2 leads to larger dunes due to the sediment avalanching process (see section 5.2.4). The BL+SL-model on the other hand, by also modeling the transport of bed sediment in suspension and not explicitly avalanching bed load on the dune lee side, allows a part of the sediment transport arriving at the dune crest to be transported more downstream acting as the bypass fraction. Consequently, not all sediment transport arriving at the dune crest contributes to the growth and propagation of the dunes. This "loss of sediment" (the bypass fraction) contributes to the lowering of the dune heights as also observed in the flume experiments [e.g. *Naqshband et al.,* 2014a; 2014b]. Furthermore, for dunes in equilibrium under both experimental conditions (EXP1 and EXP2), the BL-model gives same lee side angles of 30° while the BL+SL-model predicts a lower lee side angle for the suspended load dominant condition (23°) compared to the bed load dominant condition (26°) [see also *Smith and McLean*, 1977; *Bridge and Best*, 1988; *Amsler and Schreider*, 1999; *Best*, 2005a and references therein]. However, both models strongly underestimate the equilibrium dune lengths for the suspended load dominant experiment (see EXP2 in Table 5.2).

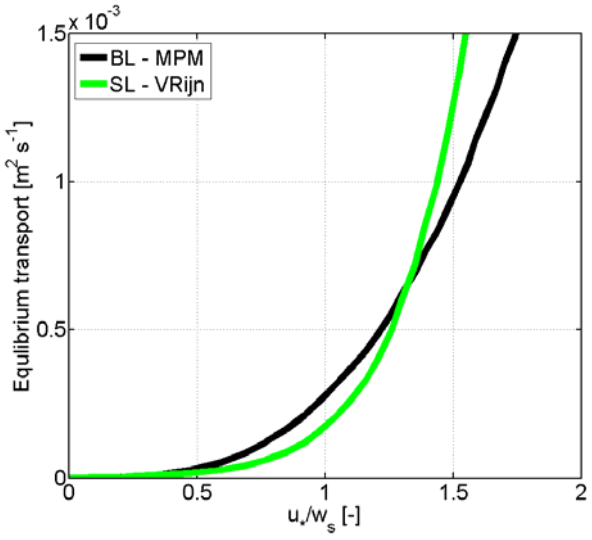

Figure 5.6 – Equilibrium values of the bed load (equation 5.7) and the suspended load (equation 5.12) for a range of suspension numbers with H=0.25 m, D_{50}=0.29 mm and D_{90}=0.40.

5.4.2 DUNE TRANSITION TO UPPER STAGE PLANE BED

Figure 5.7a and Figure 5.7b show the temporal dune evolution with the BL-model and the BL+SL-model for the experimental condition of EXP3 (see Table 5.1). The bold dune profile at 250 minutes in both figures indicate the time of the increase in discharge (from 0.08 to 0.16 m^3 s^{-1}) after reaching the steady-state dune bed corresponding to a discharge of 0.08 m^3 s^{-1}. The initial development of dunes from small disturbances, for a discharge of 0.08 m^3 s^{-1}, is not shown here and can be found in Figure 5.4a. As observed in the flume experiments, dune profiles in both models immediately respond to the changing flow conditions with a large increase in the migration speeds. The BL-model shows an increase in the dune heights with an increase in the flow discharge and the dune lee slopes remain unchanged. However, the BL+SL-model predicts the measured result much better (Figure 5.7b); dune heights decrease in time and eventually dunes are totally washed out. In addition, the dune shapes change with the lee side slopes becoming progressively flatter as observed in the experiments [see also *Best,* 2005a and references therein].

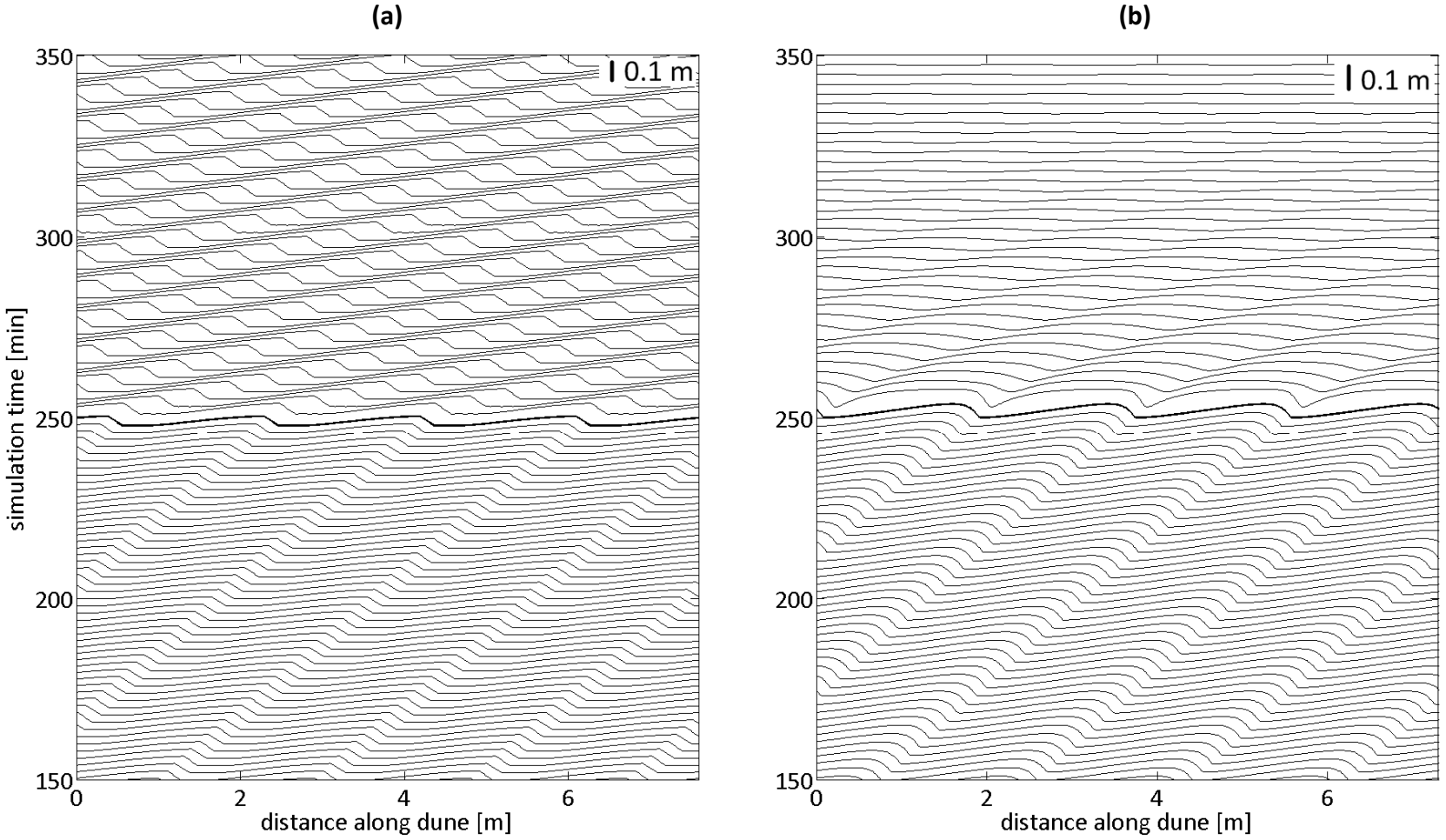

Figure 5.7 – Model results of the temporal dune evolution for the experimental condition EXP3. Results with the BL-model (a) and with the BL+SL-model (b). The bold dune profile after about 250 minutes indicate the time of the increase in the flow discharge from 0.08 to 0.16 $m^3 s^{-1}$.

The corresponding dune height evolution for both models are shown in Figure 5.8 together with the measured dune heights of EXP3. The green dotted line indicates the increase in the flow discharge. The BL-model overestimates the measured dune height over the entire course of dune transition towards upper stage plane bed. The results with the BL+SL-model are much closer to the observed dune heights during the experiments. However, the BL+SL-model responds immediately to the changing flow conditions with a fast decrease in the dune heights whereas the measured dune heights show a temporal lag before decreasing. Furthermore, the time needed to reach upper stage plane bed after increasing the flow discharge is quite well predicted by the BL+SL-model (90 minutes in the flume experiments and 80 minutes with the BL+SL-model, see Table 5.2). Although due to its complexity, the exact behavior of dune heights during the dune-USPB transition is not very well captured by the BL+SL-model, the dimensions and the time scales of dune transition to upper stage plane bed are well predicted.

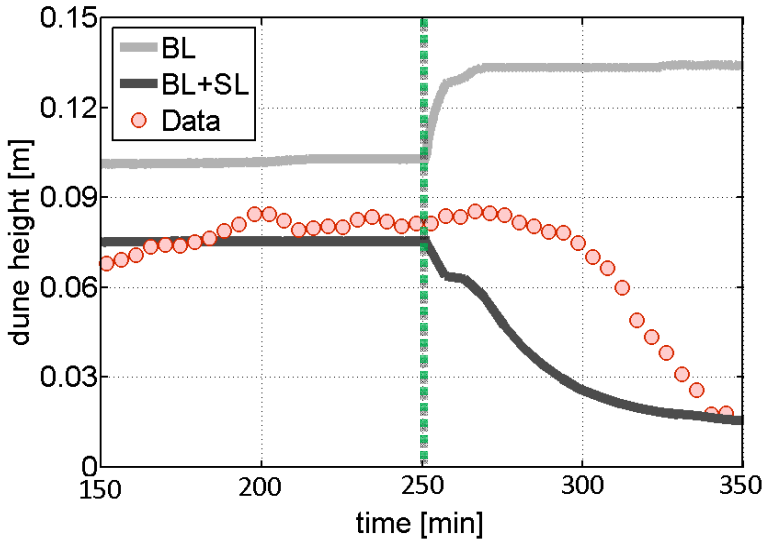

Figure 5.8 – Comparison of model results and experimental data for the dune height evolution corresponding to experiment EXP3. The green dotted line indicates the increase in the flow discharge after reaching equilibrium.

An overview of the measured and predicted dune equilibrium parameters, for the three experimental conditions discussed, is shown in Table 5.2.

Table 5.2 – An overview of the measured and predicted dune evolution parameters in equilibrium for the three experimental conditions (EXP1, EXP2 and EXP3). EXP represents the measured parameter values where BL and BL+SL are the model predicted parameter values.

	EXP1: BL dominant			EXP2: SL dominant			EXP3: D-USPB transition		
Parameter	EXP	BL	BL+SL	EXP	BL	BL+SL	EXP	BL	BL+SL
Equilibrium dune height Δ_e, m	0.082	0.103	0.075	0.072	0.117	0.068	0.018	0.127	0.016
Equilibrium dune length λ_e, m	2.25	1.90	2.49	4.35	2.28	2.51	-	2.34	3.07
Equilibrium dune steepness Δ_e/λ_e	0.036	0.054	0.030	0.017	0.051	0.027	-	0.054	0.0052
Time to equilibrium T_e, min	150	100	130	90	60	80	90[a]	40	80[a]
Equilibrium migration speed $C_e \times 10^{-4}$, m s^{-1}	7.0	4.4	5.4	13.0	6.6	10.0	-	23.4	40.5

[a]Time needed for the transition of dunes to USPB.

Table 5.3 – Model sensitivity to the relaxation length parameter α of the suspended sediment transport module. An overview is given of the predicted dune evolution parameters in equilibrium for the three experimental conditions (EXP1, EXP2 and EXP3].

Parameter	EXP1: BL dominant			EXP2: SL dominant			EXP3: D-USPB transition		
Relaxation parameter α	1.0	2.0	3.0	1.0	2.0	3.0	1.0	2.0	3.0
Relaxation length L_{sat}, m	1.46	0.54	0.20	2.63	1.4	0.75	4.69	2.78	1.65
Equilibrium dune height Δ_e, m	0.073	0.075	0.079	0.056	0.068	0.075	0.01	0.016	0.02
Equilibrium dune length λ_e, m	2.51	2.49	2.49	2.56	2.51	2.51	3.09	3.07	3.07
Equilibrium dune steepness Δ_e/λ_e	0.029	0.030	0.032	0.022	0.027	0.030	0.003	0.0052	0.007
Time to equilibrium T_e, min	180	200	220	70	80	135	25[a]	80[a]	100[a]
Equilibrium migration speed $C_e \times 10^{-4}$, m s^{-1}	5.5	5.4	5.2	11.1	10.0	9.7	50.1	40.5	38.5

[a]Time needed for the transition of dunes to USPB.

5.5 DISCUSSION AND RECOMMENDATIONS

In this study, we presented the development of dunes and their transition to upper stage plane bed by including the transport of bed sediment in suspension in the dune evolution model of *Paarlberg et al.* [2009]. We showed that, in the suspended load dominant transport regime, the equilibrium dune parameters and the dune transition to upper stage plane bed are well predicted by the extended model. For the calculation of the suspended sediment transport, the sediment relaxation length L_{sat} (equation 5.15) was determined where the parameter α was 2.0 (see section 5.2.3.2). We performed a sensitivity analysis to study the influence of this parameter on the model results. For the three experimental conditions (EXP1, EXP2 and EXP3), model predictions of the dune evolution parameters are shown in Table 5.3 corresponding to different values of α (α = 1, 2 and 3). The parameter α and the relaxation length L_{sat} are inversely related. For the bed load dominant experimental condition EXP1, a decrease in the value of α and thus an increase in the relaxation length results in a slight decrease of the equilibrium dune height. This effect is stronger for the suspended load dominant experimental condition EXP2. Furthermore, dune migration speeds increase with increasing relaxation lengths and dune equilibrium dimensions are reached much faster. Equilibrium dune lengths are much less affected by the parameter α. This is because the dune length is determined from a linear stability analysis and the result of this analysis is almost linearly related to the water depth which remained unchanged. For the transition of dune to upper stage plane bed (EXP3), Table 5.3 shows that parameter α strongly determines the time scale of dune transition. For α = 3, dunes are washed out within 25 minutes whereas for α = 1, this time scale is four times larger. The results of this sensitivity analysis clearly indicate that α – and therefore the relaxation length – is an important parameter in the dune evolution model that should be carefully dealt with. For the current data set, the chosen value of α = 2 seems to give the best results in terms of the predicted equilibrium dune heights and the time scale of dune transition. Further research is required for the quantification of the suspended sediment relaxation lengths for a range of suspension numbers.

As discussed in the present study, dune lengths are poorly predicted by the current dune evolution model [see also *Warmink et al.,* 2014]. The main reason for this is that dune length is generally assumed to depend only on the water depth [e.g. λ/h = 7.3, see *Van Rijn*, 1984]. However, *Naqshband et al.* [2014a] showed that the relative dune length (λ/h) is not constant but linearly increases with increasing suspension number. The proposed dune length by *Naqshband et al.* [2014a] can be imposed on the dune evolution model. In this way, the dune evolution model's predictability will increase

while the computational time will be kept to a minimum. This aspect will be investigated in future work.

5.6 CONCLUSIONS

The present study has focused on the modeling of dune development and dune transition to upper stage plane beds. New laboratory experiments were carried out to understand the morphological behavior of dunes under different flow conditions, and to find the flow and sediment conditions for which the dunes were totally washed out. Insights from literature and the laboratory experiments were used to extend the dune evolution model of *Paarlberg et al*. [2009] by including in the model the transport of bed sediment in suspension. The main findings of this study can be summarized as follows:

1. The extended dune evolution model showed significant improvement in the prediction of equilibrium dune parameters (e.g. dune height, dune length, dune steepness, dune migration rate, dune lee side slope) both under bed load dominant and suspended load dominant transport regimes.

2. Where simulations with the original dune evolution model always results in a fixed dune lee side slope of 30° after a critical angle of 10° is exceeded, the dune lee side slope predicted with the extended dune evolution model entirely depends on the sediment transport rates. For the suspended load dominant experimental condition a lower lee side slope was predicted (23°) compared to the bed load dominant condition (26°).

3. The chosen modeling approach allowed us to model the transition of dunes to upper stage plane bed which was not possible with the original dune evolution model. The extended model predicted the change in the dune shapes as was observed in the flume experiments with decreasing dune heights and dune lee side slopes. Furthermore, the time needed to reach upper stage plane bed after increasing the flow discharge is quite well predicted by the extended model (90 minutes in the flume experiments and 80 minutes with the extended model).

CHAPTER 6 – DISCUSSION

The new insights presented in this thesis are strongly based on the results of new detailed flume experiments combined with numerical studies of dune morphodynamics. Although this thesis substantially extends our understanding of dune morphodynamics and dune evolution to upper stage plane bed, important assumptions and limitations of the applied research methods need some reflection. Both experimental work and numerical modelling have focused on bedform dynamics under laboratory conditions and consequently the current study was focused on flow and sediment processes associated with small-scale dune geometry that may not be representative for dunes generally observed in sand bed rivers (see section 6.1). What the study results may mean for bedforms under field conditions – particularly for the Dutch rivers – is discussed in section 6.2. Additionally, some implications of this study for bedforms in other environments are highlighted (section 6.3).

6.1 DUNE GEOMETRY: LOW-ANGLE DUNES

Fluid and sediment dynamics over dunes are controlled by dune geometry and in particular the dune lee side angle [*Kostaschuk and Villard*, 1996; *Best and Kostaschuk*, 2002; *Best*, 2005a; *Venditti*, 2013]. In flumes, interaction between flow and sediment transport gives rise to high-angle dunes with long, gentle upstream stoss side slopes and short lee sides with steep angles often reaching the angle of repose (~30°). The advantage of utilizing dunes in flumes is that it allows controlled flow and sediment measurements associated with desired predefined flow conditions without difficulties of measuring bedforms over large water depths. However, observations from field studies suggest that high-angle dunes may be rather uncommon in large sand bed rivers where most sand is transported in suspension. In such rivers dunes with much smaller lee side angles (usually < 10°) are repeatedly observed [*Roden*, 1998; *Kostaschuk*, 2000; *Best and Kostaschuk*, 2002; *Bradley et al*., 2013 and references therein]. Although the geometries of dunes in flumes (high-angle) and in the field (low-angle) may be quite different, several studies have revealed similar mean flow patterns over both types of dune geometries [e.g., *Nelson et al*., 1993; *McLean et al*., 1994; *Bennett and Best*, 1995; *Venditti and Bennett*, 2000; *Best*, 2005a; *Venditti and Bauer*, 2005], except that the well-known separation zone and counter-rotating eddy observed in the lee trough of high-angle dunes are notably weak (intermittent) or absent in the lee trough of low-angle dunes [*Best and Kostaschuk*, 2002; *Bradley et al*., 2013]. The presence of a well-developed flow separation zone in the lee trough of high-angle dunes in the flume may result in a higher contribution of turbulent sediment fluxes to the total sediment fluxes along high-angle dunes compared to low-angle dunes (see chapter 4). Furthermore, high-angle dunes are observed when significant sand transport occurs as bed load, whereas low-angle dunes develop when most sand transport is in suspension [*Best and Kostaschuk*, 2002 and references therein]. *Kostaschuk and Villard* [1996] suggested that the steep lee sides of high-angle dunes are maintained by avalanching of bed load down the lee slope, whereas the much lower angle lee sides of low-angle dunes result from deposition of sand from suspension in the lee side and trough of dunes. The fact that different dune geometries are observed in the flume (high-angle) and in the field (low-angle) may further be described by scale differences. In particular, sediment excursion (step) length relative to dune length may be a key parameter in explaining the observed dune geometries.

6.2 FLOOD MANAGEMENT IN THE NETHERLANDS: DUNE – USPB TRANSITION?

In the present study we have shown that the transition of dunes to upper stage plane bed depends on the magnitude of the free surface effect (Froude number, *Fr*) and the amount of bed sediment that is transported in suspension (suspension number, u_* / w_s). Here, we apply this method to investigate whether upper stage plane bed may occur in the river Rhine during extreme discharges. For this, we use 2 extreme events: (1) the maximum discharge during the flood wave of 1995 reaching 12,000 [$m^3 s^{-1}$] and (2) the design discharge of 16,000 [$m^3 s^{-1}$] that is determined from statistical analysis of historical discharge data. Detailed data for both cases are presented in *Wilbers*, [2004, Chapter 8 and Appendix A] where a hypothetical flood wave is defined for the design discharge of 16,000 [$m^3 s^{-1}$] based on the flood wave of 1995.

Applying the method discussed in Chapter 2 to the maximum discharge during the flood wave of 1995 (12,000 $m^3 s^{-1}$) results in suspension number range u_* / w_s of 0.59 – 0.72 with Froude number of $Fr = 0.23$. From Figures 2.1 and 2.2, this suggests the presence of well-developed dunes in the bed load regime as also confirmed from bedform measurements of *Wilbers and Ten Brinke* [2003] shown in Figure 1.3. For the design discharge of 16,000 [$m^3 s^{-1}$], the suspension number range is 0.63 – 0.77 with Froude number of $Fr = 0.21$. This also still indicates the presence of dunes in the bed load regime. However, it should be noticed that for these calculations, the sediment is assumed to be highly uniform with $D_{50} = 3.34 * 10^{-3}$ [m] (see *Wilbers*, 2004). A finer D_{50} may significantly increase the range of the suspension numbers. When considering $D_{50} = 0.73 * 10^{-3}$ [m] as observed in the river Waal (see *Wilbers*, 2004), for the design discharge of 16,000 [$m^3 s^{-1}$], the suspension number range becomes 1.4 – 1.5 with $Fr = 0.21$. Despite the significant increase in the suspension number range due to finer sand, the Froude number remains relatively low. According to the study results of Chapter 2, for dunes to evolve to upper stage plane beds under relatively low Froude numbers ($Fr < 0.32$), the suspension number must exceed 4.0 (see Chapter 2, Figure 2.1). Therefore, dunes may still be expected to occur in the river Rhine and the dune transition to upper stage plane bed can still not be expected for the design discharge of 16,000 [$m^3 s^{-1}$].

6.3 IMPLICATIONS FOR DUNES IN A BROAD ENVIRONMENT

Dunes exist at a variety of spatial-temporal scales and display a wide range of morphologies in environments ranging from large deserts to deep oceans [*Parsons and Best*, 2013]. Mobile dunes have also been recently observed on the surface of Mars showing unexpectedly high morphodynamic similarities with aeolian dunes observed on Earth (Figure 6.1). For example, calculated dune migration rates in the Nili Patera dune field, Mars are very close to dune migration rates observed in Victoria Valley, Antarctica, implying that rates of landscape modifications on Mars and Earth are similar [*Bridges et al*., 2012]. Furthermore, bedform superimposition – particularly ripples on dunes – is also observed on dunes of Mars [*Parsons and Best*, 2013].

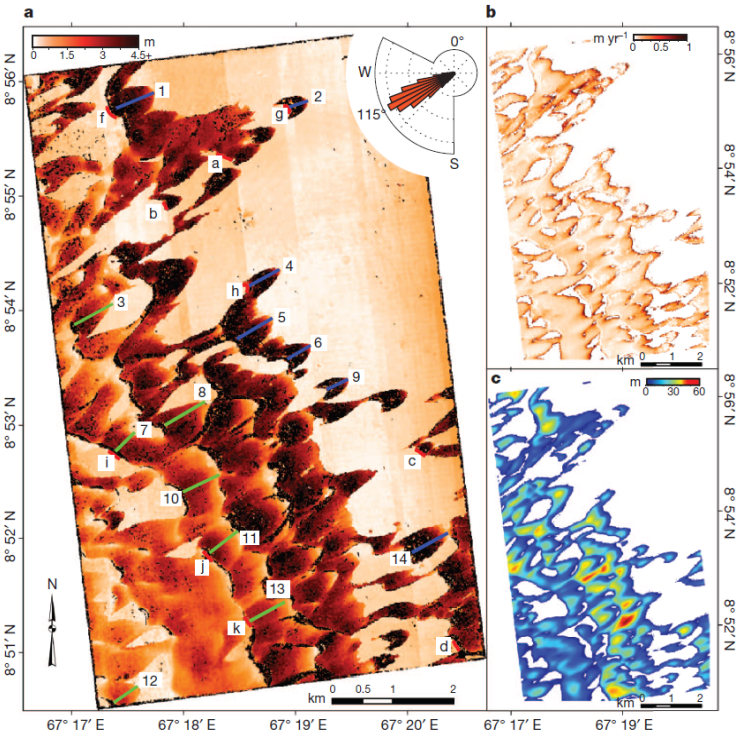

Figure 6.1 – Dune displacements in the Nili Patera dune field, Mars, between June 30, 2007 and October 13, 2007 (after Bridges et al., 2012 and reproduced by Parsons and Best, 2013). The green and blue numbered lines show where profiles of dune displacement were measured, with the red lines with letters showing where dune leeside displacements were measured. Inset rose diagram shows distribution of ripple migration azimuth, (b) dune migration rates and (c) dune elevation relative to bedrock base.

Like river dunes, aeolian dunes are formed by predominantly unidirectional currents and have slip faces with a region of flow separation in the dune lee [e.g., *Sauermann et al*., 2000; *Paarlberg et al*., 2008 and references therein]. In fact, simulation models for aeolian dunes are generally based on linearized flow equations [e.g., *Kroy et al*., 2002].

Parsons et al. [2005] used computational fluid dynamics to describe the full process of aeolian dune formation, employing a k-epsilon turbulence model. A main difference between river dunes and aeolian dunes is that in the former case a free surface is present that limits the growth of river dunes relative to the water depth. Despite the differences, knowledge on river dunes and in particular new dune morphodynamic insights presented in this thesis may also substantially increase our understanding of the behaviour, formation and occurrence of aeolian dunes.

Hulscher and Dohmen-Janssen [2005] suggested that offshore sand waves and river dunes are similar features with respect to their dimensions and processes controlling their formation. Offshore sand wave dynamics occur at large spatial scales (~kilometres) and long temporal scales (~years). More recently, *Borsje et al*. [2014] showed, by studying the influence of suspended sediment transport on the formation of tidal sand waves, that occurrence of sand waves are related to the suspension number. They found that an increase in transport of suspended sediment causes damping of sand waves which is very similar to the diminishing of dunes when significant sediment is transported in suspension (see chapters 2 and 5).

CHAPTER 7 – SYNTHESIS

7.1 CONCLUSIONS

The work presented in this thesis aimed to obtain a better understanding and quantitative data of the flow and sediment transport mechanisms controlling the dune morphology and dune transition to upper stage plane beds. Four research questions were identified, focusing on: (1) the dominant flow and sediment transport processes that control dune morphology and dune transition to upper stage plane bed; (2) the relative contributions of bed load and suspended load sediment transport to dune morphology and dune transition to upper stage plane bed; (3) the relative contributions of the turbulent and the advective sediment fluxes to the total sediment fluxes along dunes; and (4) modelling of the transition of dune to upper stage plane bed with an idealized dune evolution model. The four research questions are addressed below.

Q1. What are the dominant flow and sediment transport processes that control dune morphology and dune transition to upper stage plane bed?

An extended literature study was carried out to identify the processes controlling the dune morphology and dune transition to upper stage plane beds (Chapter 2). A large number of dune dimension data sets was compiled and analyzed in this study – 414 experiments from flumes and the field – showing a significantly different evolution of dune height and dune length in flows with low Froude numbers (negligible free surface effects) and flows with high Froude numbers (large free surface effects). For high Froude numbers (0.32 – 0.84), relative dune heights are observed to grow only in the bed load dominant transport regime and start to decay for u_* / w_s (suspension number) exceeding 1. Dunes in this case are not observed for suspension numbers greater than 2.5. For low Froude numbers (0.05 – 0.32), relative dune heights continue to grow from the bed load to suspended load dominant transport regime. Dunes in this case are not observed for suspension numbers greater than 5. The study revealed that for reliable predictions of dune morphology and their evolution to upper stage plane beds, it is essential to address both free surface effects and sediment transport mode.

Q2. What are the relative contributions of bed load and suspended load sediment transport to dune morphology and dune transition to upper stage plane bed?

Detailed flume experiments were carried out at LWI of the Technical University of Braunschweig (Germany) to obtain quantitative knowledge on the behavior of the bed and the suspended load transport along mobile dunes (Chapter 3). Using the newly developed acoustic system (ACVP, developed by *Hurther et al*. [2011]), we were able – for the first time – to measure co-located, simultaneous, and high temporal and spatial resolution profiles of both two-component flow velocity and sediment concentration referenced to the exact position at dune bed. The data has illustrated that, due to the presence of a dense sediment layer close to the bed and migrating secondary bedforms over the stoss side of the dune towards the dune crest, the near-bed flow and sediment processes are significantly different from the near-bed flow and sediment dynamics measured over fixed dunes. The pattern of the total sediment transport distribution along dunes is dominated by the bed load transport. This implies that bed load transport is mainly responsible for the continuous erosion and deposition of sediment along the stoss side of the migrating dunes. The bed load distribution at the lee side of the dunes decays rapidly because of sediment avalanching on the dune slip face. The suspended load transport, on the other hand, is advected further downstream and is more gradually deposited on the lee side and in the trough of the dune. Whereas the bed load is entirely captured in the dune with zero transport at the flow reattachment point, a significant part of the suspended load (the bypass fraction) is advected to the downstream dune depending on the flow conditions. For the two flow conditions measured, the bypass fraction was about 10% for flow with $Fr = 0.41$ and 27% for flow with $Fr = 0.51$. This means that respectively 90% (for the $Fr = 0.41$ flow) and 73% (for the $Fr = 0.51$ flow) of the total sediment load that arrived at the dune crests contributed to the morphology and migration of the dunes. Based on the insights obtained from these flume experiments, the part of the suspended load acting as the bypass fraction is expected to play an important role during the transition of dunes to upper stage plane bed where dunes are flattened and eventually washed out.

Q3. What are the relative contributions of the turbulent and the advective sediment fluxes to the total sediment fluxes along dunes?

The total sediment fluxes along mobile dunes were – for the first time – quantified by deploying the ACVP (Chapter 4). The data revealed a similar behavior of the total mean streamwise sediment flux $\overline{cu}$ and the mean advective flux $\bar{c}\bar{u}$ along the dune profile. However, along the entire dune profile and mainly in the bed load layer, the absolute magnitudes of $\bar{c}\bar{u}$ are much larger compared to $\overline{cu}$. This overestimation is caused by the negative contribution of the mean turbulent flux $\overline{c'u'}$. Over the stoss side of the dune, $\overline{c'u'}$ reaches up to 40% of the total mean sediment flux, and over the lee side of the dune the contribution of $\overline{c'u'}$ to the total sediment flux is larger and reaches up to 50%. Therefore, indirect measurements of sediment fluxes along dunes (limited to $\bar{c}\bar{u}$) may overestimate the actual sediment fluxes ($\overline{cu}$) up to a factor 2.

Contour maps of the total mean vertical flux $\overline{cw}$ showed peaks on the stoss side of the dune. These peaks were found to be the result of turbulent bursts emanating from the flow detachment zone subject to strong shear instabilities and hitting the dune bed downstream of the flow reattachment point. The mean vertical turbulent flux $\overline{c'w'}$, along the entire dune bed and in the bed load layer, reaches nearly 30% of the total mean vertical flux $\overline{cw}$.

Q4. To what extent can the transition of dune to upper stage plane bed be reproduced with an idealized dune evolution model?

The dune evolution model of *Paarlberg et al.* [2009] was used to study the transition of dunes to upper stage plane bed (Chapter 5). This model was extended by including in the model the transport of bed sediment in suspension. The extended dune evolution model showed significant improvement in the prediction of equilibrium dune parameters (dune height, dune steepness, dune migration rate, dune lee side slope) both under bed load dominant and suspended load dominant transport regimes. However, the equilibrium dune length is still poorly predicted by the dune evolution model.
Where simulations with the original dune evolution model always resulted in a fixed dune lee side slope of 30° after a critical angle of 10° is exceeded, the dune lee side slope predicted with the extended dune evolution model entirely depends on the

sediment transport rates. For the suspended load dominant experimental condition a lower lee side slope was predicted (23°) compared to the bed load dominant condition (26°). The chosen modeling approach allowed us to model the transition of dunes to upper stage plane bed which was not possible with the original dune evolution model. The extended model predicted the change in the dune shapes as was observed in the flume experiments with decreasing dune heights and dune lee side slopes. Furthermore, the time needed to reach upper stage plane bed after increasing the flow discharge is quite well predicted by the extended model (90 minutes in the flume experiments and 80 minutes with the extended model).

7.2 RECOMMENDATIONS

The work presented in this thesis has led to a number of challenges and directions for further research that are summarized below. These recommendations focus on the experimental work as well as on numerical modeling and its applications for flood management.

Deploying the Acoustic Concentration and Velocity Profiler (ACVP) during the experimental work revealed the distribution of the bed load and the suspended load transport along migrating dunes. It was observed that the bed load was entirely captured in the dune with zero transport at the flow reattachment point, while a significant part of the suspended load (the bypass fraction) was advected to the downstream dune depending on the flow conditions. The bypassed suspended sediment probably plays an important role during the transition of dunes to upper stage plane beds where dunes are flattened and eventually washed out [e.g., *Naqshband et al.,* 2014a]. Therefore, further research is needed on the quantification of this fraction during the dune transitional stages under non-equilibrium flow conditions.

Another important direction for future research is linking the results of this study to complex numerical models that describe the development and migration of dunes [e.g., *Nabi et al.*, 2010]. In particular, the near-bed flow behavior above migrating dunes observed in this study should be well reproduced by numerical models. In addition, the new insights obtained in this research on the distribution of bed load and suspended load can be used as reference for modeling sediment transport. However, it should be noticed that the results of this study are strongly related to 2D dune topography in a laboratory flume. Future research is needed to investigate whether these findings are consistent for field conditions with a strong 3D dune topography. This topographic

aspect is also relevant for the quantification of turbulent sediment fluxes. Using the ACVP, we showed that the turbulent flux may form 30-50% of the total mean sediment flux measured along the 2D dune bed. Future research should point out whether these findings are consistent for field conditions with a strong 3D dune topography and for a wider range of flow conditions.
Because the ACVP provides co-located, simultaneous profiles of both two-component flow velocity and sediment concentration, we are now able to make direct computations of the turbulent Prandtl-Schmidt number β along the dunes and over the entire flow depth. The turbulent Prandtl-Schmidt number is the ratio of the turbulent diffusivity of momentum ε_v to the turbulent diffusivity of suspended sediment ε_s and is an important parameter within sediment transport models. To date, the exact behavior of this parameter is not quantified due to the limitations of the available instruments [see Sassi et al., 2013 and references therein].

Modeling dune morphology and dune transition to upper stage plane bed with an extended dune evolution model including the transport of bed sediment in suspension showed significant improvement in the prediction of equilibrium dune parameters (dune height, dune steepness, dune migration rate, dune lee side slope) both under bed load dominant and suspended load dominant transport regimes (Chapter 5). However, the equilibrium dune length is still poorly predicted by the extended dune evolution model. The main reason for this is that dune length is generally assumed to depend only on the water depth (e.g. λ/h = 7.3, see *Van Rijn*, 1984). However, *Naqshband et al.* [2014a] showed that the relative dune length (λ/h) is not constant but linearly increases with increasing suspension number. The proposed dune length by *Naqshband et al.* [2014a] could therefore be included in the dune evolution model. In this way, the dune evolution model's predictability will increase while the computational time will be kept to a minimum. Additional research is required to address this aspect.

Furthermore, in this study, the extended dune evolution model is applied under flume conditions. Applying this model under field conditions – for a flood wave – may be an interesting next challenge.

REFERENCES

Allen, J. R. L. (1978), Computational methods for dune time-lag: Calculations using Stein's rule for dune height, Sedimentary Geology, 20(3), 165–216.

Amsler, M. L., H. H. Prendes, M. D. Montagnini, R. Szupiany, and M. H. Garca (2003), Prediction of dune height in sand-bed rivers: The case of the Parana River, Argentina, in Proceedings of the 3rd IAHR Symposium on River, Coastal and Estuarine Morphodynamics, pp. 1104–1113, IAHR Secret., Madrid.

Amsler, M. L., and M. I. Schreider (1999), Dune height prediction at floods in the Parana River, Argentina. River Sedimentation: Theory and Applications, edited by A. W. Jayewardena, J. H. W. Lee, and Z. Y. Wang, 615– 620, A. A. Balkema, Brookfield, Vt.

Ashworth, P. J., J. L. Best, J. E. Roden, C. S. Bristow, and G. J. Klaassen (2000), Morphological evolution and dynamics of a large, sand braid-bar, Jamuna River, Bangladesh. Sedimentology, 47, pp. 533–555.

Bagnold, R. A. (1966), An approach to the sediment transport problem from general physics, Geol. Survey Prof. Paper 422-I, Washington, D.C.

Bennett, S. J., and J. L. Best (1995), Mean flow and turbulence structure over fixed, two-dimensional dunes: Implications for sediment transport and bedform stability, Sedimentology, 42, 491– 513, DOI: 10.1111/j.1365-3091.1995.tb00386.x.

Best, J. L. (1996), The fluid dynamics of small-scale alluvial bedforms, Advances in Fluvial Dynamics and Stratigraphy, edited by P. A. Carling and M. R. Dawson, pp. 67–125, John Wiley, Hoboken, N. J.

Best, J. (2005a), The fluid dynamics of river dunes, a review and some future research directions, Journal of Geophysical Research, 110, F04S02, DOI:10.1029/2004JF000218.

Best, J. L. (2005b), The kinematics, topology and significance of dune-related macro-turbulence: Some observations from the laboratory and field, in Fluvial Sedimentology VII, edited by M. D. Blum, S. B. Marriott, and S. Leclair, Special Publications of International Association of Sedimentologists, 35, 41– 60.

Best, J. L., and R. A. Kostaschuk (2002), An experimental study of turbulent flow over a low-angle dune, Journal of Geophysical Research, 107(C9), 3135, DOI:10.1029/2000JC000294.

Borsje, B. W., W. M. Kranenburg, P. C. Roos, J. Matthieu, and S. J. M. H. Hulscher (2014), The role of suspended load transport in the occurrence of tidal sand waves, Journal of Geophysical Research – Earth Surface, 119, 701–716, Doi:10.1002/2013JF002828.

Bradley, R. W., J. G. Venditti, R. A. Kostaschuk, M. Church, M. Hendershot, and M. A. Allison (2013), Flow and sediment suspension events over low-angle dunes: Fraser Estuary, Canada, Journal of Geophysical Research-Earth Surface, 118, DOI:10.1002/jgrf.20118.

Bridge, J. S., and J. L. Best (1988), Flow, sediment transport and bedform dynamics over the transition from dunes to upper stage plane beds, Sedimentology, 35, 753–764.

Bridges, N. T., F. Ayoub, J-P., Avouac, S., Leprince, A., Lucas, and S. Mattson (2012), Earth-like sand fluxes on Mars, Nature, 485, pp. 339–342, http://dx.doi.org/10.1038/nature11022.

Brownlie, W. (1982), Prediction of flow depth and sediment transport in open channels, PhD dissertation, California Inst. of Technol., Pasadena, California., 410.

Camenen, B., A. Bayram, and M. Larson (2006), Equivalent roughness height for plane bed under steady flow, Journal of Hydraulic Engineering, 132(11), 1146–1158, DOI:10.1061/(ASCE)0733-9429(2006)132:11(1146).

Carling, P. A., J. J. Williams, E. Gölz, and A. D. Kelsey (2000), The morphodynamics of fluvial sand dunes in the River Rhine near Mainz, Germany, part II: Hydrodynamics and sediment transport, Sedimentology, 47, 253–278.

Cellino, M., and W. H. Graf (2000), Experiments on suspension flow in open channels with bedforms, Journal of Hydraulic Research, 38, 289– 298.

Charru, F., (2006), Selection of the ripple length on a granular bed sheared by a liquid flow, Physics of fluids 18(12), 121508.1–121508.9, DOI:10.1063/1.2397005.

Chassagneux, F. X., and D. Hurther (2014), Wave bottom boundary layer processes below irregular surfzone breaking waves with light-weight sheet flow particle transport, Journal of Geophysical Research - Oceans, 119, DOI: 10.1002/2013JC009338.

Claudin, P., F., Charru, and B. Andreotti (2011), Transport relaxation time and length scales in turbulent suspensions, Journal of Fluid Mechanics, 671: 491–506, DOI:10.1017/S0022112010005823.

Coleman, S. E., and J. D. Fenton (2000), Potential-flow instability theory and alluvial stream bed forms, Journal of Fluid Mechanics, 418, 101–117.

Coleman, S.E., and V. I. Nikora (2011), Fluvial dunes: initiation, characterization, flow structure, Earth Surface Processes and Landforms 36: 39–57. DOI: 10.1002/esp.2096.

Coleman, S. E., V. I. Nikora, B. W. Melville, D. G. Goring, T. M. Clunie, and H. Friedrich (2008), SWAT.nz: New-Zealand-based ‘Sand waves and turbulence’ experimental programme, Acta Geophysica 56: 417– 439.

Colombini, M. and A. Stocchino (2008), Finite-amplitude river dunes, Journal of Fluid Mechanics, 611, 283–306.

Colombini, M. and A. Stocchino (2012), Three-dimensional river bed forms, Journal of Fluid Mechanics, 695, 63–80

Davy, P., and A. Crave (2000), Upscaling local-scale transport processes in large-scale relief dynamics, Physics and Chemistry of the Earth 25(6–7), 533–541, DOI:10.1016/S1464-1895(00)00082-X.

Davy, P., and D. Lague (2009), Fluvial erosion/transport equation of landscape evolution models revisited, Journal of Geophysical Research 114: F03007, DOI:10.1029/2008JF001146.

Delft Hydraulics Lab, (1979), Verification of flume tests and accuracy of flow parameters, TOW Report R 657-VI, Delft hydraulics, Delft, The Netherlands.

Ditchfield, R., and J. Best (1992), Development of bed features: Discussion, Journal of Hydraulic Engineering, 118, 647–650.

Dohmen-Janssen, C. M., W. N. Hassan, and J. S. Ribberink (2001), Mobile-bed effects in oscillatory sheet flow, Journal of Geophysical Research, 106, 27,103–27,115.

Driegen, J. (1986), Flume experiments on dunes under steady flow conditions. Description of bed forms, TOW Report R 657, WL Delft Hydraulics, Delft, Netherlands.

Engelund, F. (1970), Instability of erodible beds, Journal of Fluid Mechanics, 42 (2), 225-244.

Fredsøe, J. (1974a), On the development of dunes in erodible channels, Journal of Fluid Mechanics, 64 (1), 1-16.

Fredsøe, J. (1974b), Rotational channel flow over small 3-dimensional bottom irregularities, Journal of Fluid Mechanics, 66, 49–66.

Fredsøe, J. (1979), Unsteady flow in straight alluvial streams: modification of individual dunes, Journal of Fluid Mechanics, 91 Ž3, 497–512.

Fredsøe, J. (1981), Unsteady flow in straight alluvial streams, Part 2: Transition from dunes to plane bed, Journal of Fluid Mechanics, 102, 431-453.

French, R. H. (1985), Open-Channel Hydraulics, McGraw-Hill, New York.

Galappatti, G., and C. B. Vreugdenhil (1985), A depth-integrated model for suspended sediment transport, Journal of Hydraulic Research 23, 359–377, DOI: 10.1080/00221688509499345.

Giri, S., and Y. Shimizu (2006), Computation of sand dune migration with free surface flow, Water Resources Research, 42, W10422, DOI. 10.1029/ 2005WR004588.

Grigoriadis, D. G. E., E. Balaras, A. A. Dimas (2009), Large-eddy simulations of unidirectional water flow over dunes, Journal of Geophysics Research 114, F02022, DOI:10.1029/2008JF001014.

Guy, H. P., Simons, D. B., and E. V. Richardson (1966), Summary of alluvial channel data from flume experiments, U.S. Geology Survey, 462-1, 1956-61.

Hairsine, P. B., and C. W. Rose (1992), Modeling water erosion due to overland-flow using physical principles: 1. Sheet flow, Water Resource Research, 28(1), 237– 243, DOI:10.1029/91WR02380.

Hulscher, S. J. M. H. (1996), Tidal-induced large-scale regular bedform patterns in a three-dimensional shallow water model, Journal of Geophysical Research, 101, 20727–20744.

Hulscher, S. J. M. H. and C. M. Dohmen-Janssen (2005), Introduction to special section on Marine Sand Wave and River Dune Dynamics, Journal of Geophysical Research, 110 (F04S01), DOI:10.1029/2005JF000404.

Hurther, D., and U. Lemmin (2001), A correction method for turbulence measurements with a 3D acoustic Doppler velocity profiler, Journal of Atmospheric and Oceanic Technology, 18(3), 446–458.

Hurther, D., and P. D. Thorne (2011), Suspension and near-bed load sediment transport processes above a migrating, sand-rippled bed under shoaling waves, Journal of Geophysical Research: Oceans, 116, 07001.

Hurther, D., P. D. Thorne, M. Bricault, U. Lemmin, and J. M. Barnoud (2011), A multi-frequency Acoustic Concentration and Velocity Profiler (ACVP) for boundary layer measurements of fine-scale flow and sediment transport processes, Coastal Engineering, 58, 594–605.

Jerolmack, D. J., and D. Mohrig (2005), A unified model for subaqueous bedform dynamics, Water Resources Research, 41, W12421, DOI. 10.1029/2005WR004329.

Johns, B., R. L. Soulsby, and T. J. Chesher (1990), The modeling of sand wave evolution resulting from suspended and bed load transport of sediment, Journal of Hydraulic Research, 28, 355–374.

Julien, P.Y. (1992), Study of bedform geometry in large rivers, Report Q1389, Delft Hydraulics, Emmeloord, Netherlands.

Julien, P. Y., and G. J. Klaassen (1995), Sand-dune geometry of large rivers during floods, Journal of Hydraulic Engineering, ASCE, 121(9), 657–663.

Karim, F. (1995), Bed configuration and hydraulic resistance in alluvial channel flows, Journal of Hydraulic Engineering, ASCE, 121(1), 15–25.

Karim, F. (1999), Bed-form geometry in sand-bed flows, Journal of Hydraulic Engineering 125 (12), 1253–1261. DOI: 10.1061/(ASCE)0733–9429(1999)125:12(1253).

Kennedy, J. F. (1963), The mechanics of dunes and anti-dunes in erodible-bed channels, Journal of Fluid Mechanics, 16, 521-544.

Kleinhans, M. G. (2004), Sorting in grain flows at the lee side of dunes, Earth-Science Reviews, 65, 75–102.

Kostaschuk, R. A. (2000), A field study of turbulence and sediment dynamics over subaqueous dunes with flow separation, Sedimentology, 47, 519– 531.

Kostaschuk, R. A. (2005), Sediment transport mechanics and dune morphology, In River, Coastal and Estuarine Morphodynamics: RCEM 2005, Parker G and Garcia M (eds). Taylor & Francis: London; 795–803.

Kostaschuk, R. (2006), In Proceedings of the 4th IAHR Symposium on River, Coastal and Estuarine Morphodynamics, Vol. 2, Urbana IL, Parker G, Garcia MH (Eds), Taylor & Francis Group, London, 795–801.

Kostaschuk, R., and J. Best (2005), Response of sand dunes to variations in tidal flow: Fraser Estuary, Canada, Journal of Geophysical Research, 110, F04S04, DOI:10.1029/2004JF000176.

Kostaschuk, R., D., Shugar, D., J., Best, D., Parsons, S., Lane, R., Hardy, and O. Orfeo (2009), Suspended sediment transport and deposition over a dune: Río Paraná, Argentina, Earth Surface Processes and Landforms, 34, 1605–1611, DOI: 10.1002/esp.1847.

Kostaschuk, R.A. and P. V. Villard (1996), Flow and sediment transport over large subaqueous dunes: Fraser River, Canada, Sedimentology, 43, 849-863.

Kostaschuk, R. A., and P. V. Villard (1999), Turbulent sand suspension over dunes, in Fluvial Sedimentology VI, edited by N. D. Smith and J. Rogers, Special Publications of International Association of Sedimentologists, 28, 3–14.

Knighton, D. (1998), Fluvial Forms and Processes: A New Perspective, Arnold, UK, 383 pages, ISBN 0-340-66313-8.

Kroy, K., G., Sauermann, and H. J. Herrmann (2002), Minimal model for sand dunes, Physical Review Letters, 88(5), 054301.1– 054301.4, DOI:10.1103/PhysRevLett.88.054301.

Lague, D., A., Crave, and P. Davy (2003), Laboratory experiments simulating the geomorphic response to tectonic uplift, Journal of Geophysical Research, 108(B1), DOI:10.1029/ 2002JB001785.

Lee, T. H., and D. M. Hanes (1995), Direct inversion method to measure the concentration profile of suspended particles using backscattered sound, Journal of Geophysical Research, 100, 2649–2657, DOI:10.1029/94JC03068.

Liu, H. K. (1957), Mechanics of sediment-ripple formation, Journal of Hydraulics Division, ASCE, 83, HY2, 1-21.

Lyn, D. A. (1993), Turbulence measurements in open-channels flows over artificial bedforms, Journal of Hydraulic Engineering, ASCE 119, 306–326.

Maddux, T. B., S. R. McLean, and J.M. Nelson (2003), Turbulent flow over three-dimensional dunes: 2. Fluid and bed stresses, Journal of Geophysical Research 108, F1, DOI:10.1029/2003/JF000018.

McLean, S. R., J. M. Nelson, and L. Gary (2008), Suspended sediment in the presence of dunes, In River, Coastal and Estuarine Morphodynamics: RCEM 2007, Dohmen-Janssen CM, Hulscher SJMH (eds), Taylor & Francis Group, London, 611–618.

McLean, S. R., J. M. Nelson, and S. R. Wolfe (1994), Turbulence structure over two-dimensional bedforms: Implications for sediment transport, Journal of Geophysical Research, 99, 12,729–12,747.

McLean, S. R., S. R. Wolfe, and J. M. Nelson (1999), Spatially averaged flow over a wavy boundary revisited, Journal of Geophysical Research, 104, 15743–15753.

Meyer-Peter, E., and R. Müller (1948), Formulas for bed-load transport, In Proceedings of the 2nd IAHR Congress, Vol. 2, Stockholm, Sweden, IAHR, Madrid, 39–64.

Middelkoop, H., and H. Buitenveld (1999), Implications of climate change for landscape planning alternatives for the river Rhine floodplains, NRP project 952210, RIZA report 99.065, ISBN: 9036952913.

Mignot, E., E. Barthélemy, and D. Hurther (2009), Double-averaging analysis and local flow characterization of near bed turbulence in gravel-bed channel flows, Journal of Fluid Mechanics 618, 279-303.

Ministry of Transportation, Public Works and Water Management (2007), Hydraulische Randvoorwaarden 2006: voor het toetsen van primaire waterkeringen (in Ducth), Ministerie van Verkeer en Waterstaat, Directoraat-Generaal Water, Den-Haag, the Netherlands, ISBN: 978-90-369-5761-8.

Mohrig, D., and J. D. Smith (1996), Predicting the migration rates of subaqueous dunes, Water Resource Research, 32, 3207–3217.

Nabi, M., H. J., De Vriend, E., Mosselman, C. J., Sloff, and Y. Shimizu (2013), Detailed simulation of morphodynamics: 3. Ripples and dunes, Water Resources Research, 49(9), 5930–5943, DOI. 10.1002/wrcr.20457.

Naqshband, S., J. S., Ribberink, and S. J. M. H. Hulscher (2014a), Using both free surface effect and sediment transport mode parameters in defining the morphology of river dunes and their evolution to

upper stage plane beds, Journal of Hydraulic Engineering, 140(6), 06014010, DOI: 10.1061/(ASCE)HY.0733-9429.0000873.

Naqshband, S., J. S., Ribberink, D., Hurther, and S. J. M. H. Hulscher (2014b), Bed load and suspended load contributions to migrating sand dunes in equilibrium, Journal of Geophysical research, 119, 1043–1063, DOI: 10.1002/2013JF003043.

Neill, C.R. (1969), Bed Forms in the Lower Red Deer River, Alberta, Canada, Journal of Hydrology, Vol. 7, 58 -85.

Nelson, J. M., A. R., Burman, Y., Shimizu, S. R., McLean, R. L., Shreve, and M. Schmeeckle (2005), Computing flow and sediment transport over bedforms, In Proceedings of the 4th IAHR Symposium on River, Coastal and Estuarine Morphodynamics, Vol. 2, Urbana IL, Parker G, Garcia MH (Eds), Taylor & Francis Group, London, 861–872.

Nelson, J.M., B. L., Logan, P. J., Kinzel, Y., Shimizu, S., Giri, R. L., Shreve, and S. R. McLean (2011), Bedform response to flow variability, Proc. Earth. Surf. Landforms, 36.

Nelson, J. M., S. R. McLean, and S. R. Wolfe (1993), Mean flow and turbulence fields over two-dimensional bed forms, Water Resources Research, 29, 3935–3953.

Németh, A. A., S. J. M. H., Hulscher, and R. M. J. Van Damme (2006), Simulating offshore sand waves, Coastal Engineering, 53, 265–275, DOI. 10.1016/j.coastaleng.2005.10.014.

Németh, A. A., S. J. M. H., Hulscher, and R. M. J. Van Damme (2007), Modeling offshore sand wave evolution, Continental Shelf Research, 27(5), 713–728, DOI. 10.1016/j.csr.2006.11.010.

Niemann, S.L., J., Fredsoe, and N. G. Jacobsen (2011), Sand dunes in steady flow at low Froude numbers: Dune height evolution and flow resistance, Journal of Hydraulic Engineering, 137(1), 5-14.

Nikora, V. I., and D. G. Goring (2002), Fluctuations of suspended sediment concentration and turbulent sediment fluxes in an open-channel flow, Journal of Hydraulic Engineering, 128(2), 214–224.

Nittrouer, J. A., M. A. Allison, and R. Campanella (2008), Bedform transport rates for the lowermost Mississippi River, Journal of Geophysical Research, 113, F03004, DOI:10.1029/2007JF000795.

Nnadi, F. N., and K. C.Wilson (1995), Bed-load motion at high shear stress: Dune washout and plane-bed flow, Journal of Hydraulic Engineering, 121, 267–273.

Omidyeganeh, M., and U. Piomelli (2011), Large-eddy simulation of two dimensional dunes in a steady, unidirectional flow, Journal of Turbulence, 12(42), 1-31.

Paarlberg, A. J. (2008), Modeling dune evolution and dynamic roughness in rivers, PhD Thesis, University of Twente, Enschede, The Netherlands.

Paarlberg, A. J., C. M., Dohmen-Janssen, S. J. M. H., Hulscher, and P. Termes (2007), A parameterization of flow separation over subaqueous dunes, Water Resources Research, 43, W12417, DOI. 10.1029/2006WR005425.

Paarlberg, A. J., C. M., Dohmen-Janssen, S. J. M. H., Hulscher, and P. Termes (2009), Modeling river dune development using a parameterization of flow separation, Journal of Geophysical Research, 114, F01014, DOI. 10.1029/2007JF000910.

Paarlberg, A. J., C. M., Dohmen-Janssen, S. J. M. H., Hulscher, P., Termes, and R. Schielen (2010), Modeling the effect of time-dependent river dune evolution on bed roughness and stage, Earth Surface Processes and Landforms, 35, 1854–1866, DOI. 10.1002/esp.2074.

Parsons, D. R., and J. L. Best (2013), Bedforms: views and new perspectives from the third international workshop on Marine and River Dune Dynamics (MARID3), Earth Surface Processes and Landforms. Published online. DOI: 10.1002/esp.3360.

Parsons, D. R., J. L. Best, O. Orfeo, R. J. Hardy, R. Kostaschuk, and S. N. Lane (2005), Morphology and flow fields of three-dimensional dunes, Rio Parana, Argentina: Results from simultaneous multi-beam echo sounding and acoustic Doppler current profiling, Journal of Geophysical Research, 110, F04S03, DOI:10.1029/2004JF000231.

Prent, M. T. H. and E. J. Hickin (2001), Annual regime of bedforms, roughness and flow resistance, Lillooet River, British Columbia, BC, Geomorphology, 41, 369-390, DOI:10.1016/S0169-555X(01)00068-X.

Ranga Raju, K. G., and J. P. Soni (1976), Geometry of ripples and dunes in alluvial channels, Journal of Hydraulic Research, Delft, The Netherlands, 14(3).

Raslan, Y. (1994), Resistance to flow in the upper-regime plane bed, PhD dissertation, Department of Civil Engineering, Colorado State University, Fort Collins, Colo., 135.

Raudkivi, A. J. (1966), Bedforms in alluvial channels, Journal of Fluid Mechanics, 26, 507–514.

Reynolds, A. J. (1965), Waves on the erodible bed of an open channel, Journal of Fluid Mechanics, 22, 113-133.

Roden, J. E. (1998), The sedimentology and dynamics of mega-dunes, Jamuna River, Bangladesh, Ph.D. thesis, 310 pp., Department of Earth Sciences, University of Leeds, Leeds, U. K.

Ruessink, B.G., H. Michallet, T. Abreu, F. Sancho, D. A, J. J. van der Werf, and P. A. Silva (2011), Observations of velocities, sand concentrations, and fluxes under velocity-asymmetric oscillatory flows, Journal of Geophysical Research, 116, C03004, DOI:10.1029/2010JC006443.

Sassi, M. G., A. J. F. Hoitink, and B. Vermeulen (2013), Quantified turbulent diffusion of suspended sediment using acoustic Doppler current profilers, Geophysical Research Letters, 40, 5757-5763, DOI:10.1002/2013GL058299.

Sauermann, G., P. Rognon, A. Poliakov, and H. J. Herrmann (2000), The shape of the barchan dunes of southern morocco, Geomorphology, 36, pp. 47–62.

Seminara, G. (2006), Meanders. Journal of Fluid Mechanics, 554, 271–297, DOI:10.1017/S0022112006008925.

Shimizu, Y., M. W., Schmeeckle, and J. M. Nelson (2001), Direct numerical simulations of turbulence over two-dimensional dunes using CIP methods, Journal of Hydroscience and Hydraulic Engineering, 19(2), 85–92.

Shimizu, Y., S., Giri, I., Yamaguchi, and J. Nelson (2009), Numerical simulation of dune-flat bed transition and stage-discharge relationship with hysteresis effect, Water Resources Research, 45, W04429, DOI. 1029/2008WR006830.

Shugar, D. H., R. A. Kostaschuk, J. L. Best, D. R. Parsons, S. N. Lane, O. Orfeo, and R. J. Hardy (2010), On the relationship between flow and suspended sediment transport over the crest of a sand dune, Río Paraná, Argentina, Sedimentology, 57, 252–272, DOI:10.1111/j.1365- 3091.2009.01110.x.

Simons, D. B. and E. V. Richardson (1966), Resistance to flow in alluvial channels, Geological survey professional paper 422-J, U.S. Department of the Interior, Washington, D.C., 61.

Smith, J. D., and S. R. McLean (1977), Spatially-averaged flow over a wavy surface, Journal of Geophysical Research, 82, 1735–1746.

Soulsby, R. (1997), Dynamics of marine sands, Thomas Telford, London.

Southard, J.B., and L. A. Boguchwal (1990), Bed configuration in steady unidirectional water flows; Part 2, Synthesis of flume data, Journal of Sedimentary Petrology, 60(5), 658-679.

Stein, R. A. (1965), Laboratory studies of total load and apparent bed load, Journal of Geophysical Research, 70, 1831-1842, DOI:10.1029/JZ070i008p01831.

Sumer, B.M., A. Kozakiewicz, J. Fredsøe and R. Deigaard (1996), Velocity and Concentration Profiles in Sheet-Flow Layer of Movable Bed, Journal of Hydraulic Engineering, vol. 122, 10, pp. 549-558.

Termes, A. P. P. (1986), Dimensies van beddingvormen onder permanente stromings-omstandigheden bij hoog sedimenttransport, Rapport M2130/Q232, Delft Hydraulics, Emmeloord, the Netherlands (in Dutch).

Thorne, P. D., and D. M. Hanes (2002), A review of acoustic measurement of small scale sediment processes, Continental Shelf Research, 22, 603– 632, DOI: 10.1016/S0278-4343(01)00101-7.

Thorne, P. D., P. J. Hardcastle, and R. L. Soulsby (1993), Analysis of acoustic measurements of suspended sediments, Journal of Geophysical Research, 98, 899–910, DOI:10.1029/92JC01855.

Tjerry, S., and J. Fredsoe (2005), Calculation of dune morphology, Journal of Geophysical Research - Earth Surface, 110(F4), Art. No. F04013, DOI. 10.1029/2004JF000171.

Tuijnder, A. P. (2009), Sand in short supply; modeling of bedforms, roughness and sediment transport in rivers under supply-limited conditions, Ph.D. thesis, University of Twente, Enschede, the Netherlands.

Tuijnder, A. P., J. S. Ribberink, and S. J. M. H. Hulscher (2009), An experimental study into the geometry of supply-limited dunes, Sedimentology, 56, 1713–1727, DOI: 10.1111/j.1365-3091.2009.01054.x

Van den Berg, J., F., Sterlini, S. J. M. H., Hulscher, and R. M. J. Van Damme (2012), Non-linear process based modeling of offshore sand waves, Continental Shelf Research, 37(1-4), 26-35, ISSN 0278-4343.

Van den Berg, J., and R. Van Damme (2005), Sand wave simulation on large domains, In Proceedings of the 4th IAHR symposium on River, Coastal and Estuarine Morphodynamics, Vol. 2, Urbana IL, Parker G, Garcia MH (eds.), Taylor & Francis Group, London, 991–997.

Van den Berg, J. H. and A. Van Gelder (1989), Scour and fill sequences in flows over very fine sand and silt, Proc. of 4th Int. Conf. on Fluvial Sedimentology, Barcelona, Spain.

Van den Berg, J. H. and A. Van Gelder (1993), A new bedform stability diagram, with emphasis on the transition of ripples to plane bed in flows over fine sand and silt, In Alluvial Sedimentation, Special Publications International Sediment Association 17, International Association of Sedimentologists, Gent, 11–21.

Van der Mark, C. F. (2009), A semi-analytical model for form drag of river bedforms, Ph.D. thesis, University of Twente, Enschede, the Netherlands.

Van der Mark, C. F., A., Blom, and S. J. M. H. Hulscher (2008), Quantification of variability in bedform geometry, Journal of Geophysical Research, 113, F03020, DOI. 10.1029/2007JF000940.

Van Mierlo, M. C. L. M., and J. C. C. de Ruiter (1988), Turbulence measurements above artificial dunes, Report Q789, Delft Hydraulics, the Netherlands.

Vanoni, V. A., and N. H. Brooks (1957), Laboratory studies of the roughness and suspended load of alluvial streams, Sedimentation Laboratory, California Institute of Technology, Pasadena, California, U. S. A.

van Rijn, L. C. (1984a), Sediment transport. Part II: Suspended load transport, Journal of Hydraulic Engineering, 110(11), 1613–1641.

Van Rijn, L. C. (1984b), Sediment transport, part III: bed forms and alluvial roughness, Journal of Hydraulic Engineering, 110 (12), 1733–1754. DOI: 10.1061/(ASCE)0733–9429(1984)110:12(1733).

Van Rijn, L. C. (1993), Principles of sediment transport in rivers, estuaries and coastal seas, AQUA Publications, Amsterdam, 335.

Venditti, J. G. (2007), Turbulent flow and drag over fixed two- and three dimensional dunes, Journal of Geophysical Research, 112, F04008, DOI:10.1029/2006JF000650.

Venditti, J. G. (2013), Bedforms in sand-bedded rivers, in Treatise on Geomorphology, Fluvial Geomorphology, vol. 9, edited by J. F. Shroder (Editor-in-chief), E. Wohl, pp. 137–162, (Volume Editor), Academic Press, San Diego.

Venditti, J. G., and B. O. Bauer (2005), Turbulent flow over a dune: Green River, Colorado, Earth Surface Processes and Landforms, 30, 289–304, DOI:10.1002/esp.1142.

Venditti, J. G., and S. J. Bennett (2000), Spectral analysis of turbulent flow and suspended sediment transport over fixed dunes, Journal of Geophysical Research, 105, 22,035–22,047.

Venditti, J. G., M., Church, and S. J. Bennett (2005), Morphodynamics of small-scale superimposed sand waves over migrating dune bed forms, Water Resources Research, 41, W10423, DOI:10.1029/2004WR003461.

Wan, Z., and Z. Wang (1994), Hyperconcentrated Flow, Balkema, A. A., Brookfield, Vt.

Warmink, J. J. (2011), Unraveling uncertainties: the effect of hydraulic roughness on desing water levels in river models, Ph.D. thesis, University of Twente, Enschede, the Netherlands.

Warmink, J. J., C. M., Dohmen-Janssen, J., Lansink, S., Naqshband, O. J. M., Van Duin, A. J., Paarlberg, P., Termes, and S. J. M. H. Hulscher (2014), Understanding river dune splitting through flume experiments and analysis of a dune evolution model, Earth Surface Processes and Landforms, DOI: 10.1002/esp.3529.

Wilbers, A. (2004), The development and hydraulic roughness of subaqueous dunes, Ph.D. thesis, University of Utrecht, Utrecht, the Netherlands.

Wilbers, A. W. E. and W. B. M. Ten Brinke (2003), The response of sub- aqueous dunes to floods in sand and gravel bed reaches of the Dutch Rhine, Sedimentology, 50, pp. 1013–1034, DOI:10.1046/j.1365-3091.2003.00585.x.

Wren, D. G., R. A. Kuhnle, and C. G. Wilson (2007), Measurements of the relationship between turbulence and sediment in suspension over mobile sand dunes in a laboratory flume, Journal of Geophysical Research-Earth Surface, 112, F03009, DOI:10.1029/2006JF000683.

Wren, D. G., and R. A. Kuhnle (2008), Measurements of coupled fluid and sediment motion over mobile sand dunes in a laboratory flume, International Journal of Sediment Research, Vol.23, No. 4, pp. 329–337.

Yalin, M. S. (1964), Geometrical properties of sand waves, Journal of the Hydraulics Division, HY5 (4055), 105–119.

Yalin, M. S. (1972), Mechanics of sediment transport, Pergamon Press, Braunschweig, Germany.

Yamaguchi, S., and N. Izumi (2002), Weakly nonlinear stability analysis of dune formation, In Proceedings of River Flow 2002, Bousmar, D, Zech, Y (Eds), Swets and Zeitlinger, Lisse, 843–850.

Zyserman, J.A. and J. Fredsøe (1994), Data analysis of bed concentration of suspended sediment, Journal of Hydraulic Engineering, ASCE, 120, 1021-1042.

PUBLICATIONS

PEER-REVIEWED JOURNAL PAPERS

Naqshband, S., Duin, O.J.M., Ribberink J.S. & Hulscher, S.J.M.H. (Under Review). Modeling river dune development and their transition to upper stage plane bed.

Naqshband, S., Ribberink, J., Hurther, D., Barraud, P.A. & S.J.M.H. Hulscher (in press). Experimental evidence for turbulent sediment flux constituting a large portion of total sediment flux along migrating sand dunes. Geophysical Research Letters, DOI: 10.1002/2014GL062322.

Naqshband, S., Ribberink, J.S. Hurther, D. & Hulscher, S.J.M.H. (2014). Bed load and suspended load contributions to migrating sand dunes in equilibrium. Journal of Geophysical research-Earth Surface. DOI: 10.1002/2013JF003043.

Naqshband S., Ribberink J. S. & Hulscher S. J. M. H. (2014). Using both free surface effect and sediment transport mode parameters in defining the morphology of river dunes and their evolution to upper stage plane beds. Journal of Hydraulic Engineering. 140(6), 06014010. 10.1061/(ASCE)HY.1943-7900.0000873.

Warmink, J.J., C.M. Dohmen-Janssen, J. Lansink, **S. Naqshband**, O.J.M. van Duin, A.J. Paarlberg, A.P.P. Termes & S.J.M.H. Hulscher (2014). Understanding river dune splitting through flume experiments and analysis of a dune evolution model. Earth Surface Processes and Landforms. DOI: 10.1002/esp.3529.

CONFERENCE PAPERS

Naqshband, S., Ribberink, J.S., Hulscher, S.J.M.H. & Hurther, D. (2014). Sediment transport distribution along developing sand dunes. In A.J. Schleiss, G. De Cesare, M.J. Franca and M. Pfister (Eds.), Proceedings of the International conference on fluvial hydraulics (River Flow), Lausanne, Switzerland, 3-5- September 2014 (pp. 156). London, UK: CRC Press Taylor & Francis Group.

Naqshband, S., Ribberink, J.S., Hurther, D. & Hulscher, S.J.M.H. (2014). Turbulent sediment fluxes along migrating sand dunes. In D.C.M. Augustijn and J.J. Warmink (Eds.), Book of abstracts NCR-days 2014, 2-3 October 2014, Enschede (pp. 21-22). Enschede: University of Twente.

Naqshband, S., Ribberink, J.S., Hurther, D. & Hulscher, S.J.M.H. (2013). Sediment transport distribution along equilibrium sand dunes. Van Lancker, V. and Garlan, T. (Eds), MARID 2013. Fourth International Conference on Marine and River Dune Dynamics. Bruges, Belgium, 15-17 April 2013. Royal Belgian Institute of Natural Sciences and SHOM. VLIZ Special Publication 65 – Flanders Marine Institute (VLIZ). Oostende, Belgium. 338p. ISSN 1377-0950. ISBN 978-2-11-128352-7.

Naqshband, S., Ribberink, J.S., Hurther, D. & Hulscher, S.J.M.H. (2013). Bed and suspended flux distribution along migrating dunes. In A. Crosato (Ed.), Book of abstracts NCR-days 2013, 3-4 October 2013, Delft (pp. 39-40). Delft: UNESCO-IHE.

Naqshband, S., Ribberink, J.S. & Hulscher, S.J.M.H. (2012). Free surface effect on dune morphology and evolution. In R.M.J. Schielen (Ed.), Book of abstracts NCR-days 2012, 4-5 October 2012, Arnhem (pp. 45-46). Arnhem: Rijkswaterstaat.

Naqshband, S., Ribberink, J.S., Hulscher, S.J.M.H. & Hurther, D. (2012). Simultaneous, co-located measurements of flow velocity and sediment concentration over mobile dunes. In R.M. Munoz (Ed.), Proceedings of the International conference on fluvial hydraulics (River Flow), San Jose, Costa Rica, 5-7- September 2012 (pp. 755-760). London, UK: CRC Press Taylor & Francis Group.

Naqshband, S., Sterlini, F., Dohmen-Janssen, C.M. & Hulscher, S.J.M.H. (2011). A model study on the influence of suspended sediment transport on river dune morphology and evolution. In Shao X. J., Wang, Z. Y., Wang G.Q. (Ed.). Abstracts of the 7th IAHR Symposium on River, Coastal and Estuarine Morphodynamics (RCEM), Tsinghua University Beijing, China, pp. 162.

Naqshband, S., Sterlini-van der Meer, F. M., Dohmen-Janssen, C.M. & Hulscher, S.J.M.H. (2010). On the influence of suspended sediment transport on dune evolution. In E. Stouthamer (Ed.), NCR-days 2010. Book of Abstracts, abstract no. 21 (pp.1). Delft: NCR.

ABOUT THE AUTHOR

Suleyman Naqshband was born on 15 September 1985 in Kabul, Afghanistan. At the age of 12, together with his family, he moved to the Netherlands where he received his pre-university education (VWO) at the "Scholengemeenschap Lelystad". Thereafter, Suleyman studied Civil Engineering & Management at the University of Twente. In September 2007, he obtained his BSc degree with a final project on Stakeholder expectations in the preparation-phase of the deepening of the Hanzerak-West waterway, carried out at Rijkswaterstaat IJsselmeergebied. In October 2009, Suleyman obtained his MSc degree *cum laude* with a graduation project on wave boundary layer streaming and its effect on bed shear stress.

After his studies, Suleyman started his PhD project on the effect of suspended load sediment transport on dune morphology and dune transition to upper stage plane bed. As part of this project, Suleyman worked for a period of six months at the Technical University Of Braunschweig where he conducted large scale flume experiments on dune morphodynamics. After this measuring campaign, Suleyman visited the University of Grenoble for a period of one month where he worked together with David Hurther on data processing. Suleyman published the results of his thesis in international peer-reviewed journals, such as 'Journal of Geophysical Research', 'Journal of Hydraulic Engineering' and 'Geophysical Research Letters'. In addition, he received two awards for the best paper presentation during the 4th International Conference on Marine and River Dune Dynamics (MARID 2013 Gent, Belgium) and during the 2014 NCR-days, Enschede.

Next to his research activities, Suleyman was involved in teaching a variety of courses within the Bachelor and Master programme of Civil Engineering & Management. He also supervised Bachelor students during their final BSc assignments and he was voluntarily involved in teaching and supervising high school students. Furthermore, during his PhD Suleyman was the general secretary of the UT-Muslims student association where he organised several workshops and lectures.